INFORMATION TO USERS

This manuscript has been reproduced from the microfilm master. UMI films the text directly from the original or copy submitted. Thus, some thesis and dissertation copies are in typewriter face, while others may be from any type of computer printer.

The quality of this reproduction is dependent upon the quality of the copy submitted. Broken or indistinct print, colored or poor quality illustrations and photographs, print bleedthrough, substandard margins, and improper alignment can adversely affect reproduction.

In the unlikely event that the author did not send UMI a complete manuscript and there are missing pages, these will be noted. Also, if unauthorized copyright material had to be removed, a note will indicate the deletion.

Oversize materials (e.g., maps, drawings, charts) are reproduced by sectioning the original, beginning at the upper left-hand corner and continuing from left to right in equal sections with small overlaps. Each original is also photographed in one exposure and is included in reduced form at the back of the book.

Photographs included in the original manuscript have been reproduced xerographically in this copy. Higher quality 6" x 9" black and white photographic prints are available for any photographs or illustrations appearing in this copy for an additional charge. Contact UMI directly to order.

UMI

A Bell & Howell Information Company
300 North Zeeb Road, Ann Arbor MI 48106-1346 USA
313/761-4700 800/521-0600

Liquid Chromatographic Separation and Sensing Principles with a Water Only Mobile Phase

by

Marc Douglas Foster

A dissertation submitted in partial fulfillment
of the requirements for the degree of

Doctor of Philosophy

University of Washington

1996

Approved by 

(Chairman of the Supervisory Committee)

Program Authorized to Offer Degree Chemistry

Date 6 Nov 96

Doctoral Dissertation

In presenting this dissertation in partial fulfillment of the requirements for the Doctoral degree at the University of Washington, I agree that the Library shall make its copies freely available for inspection. I further agree that extensive copying of this dissertation is allowable only for scholarly purposes, consistent with "fair use" as prescribed in the United States Copyright Law. Requests for copying or reproduction of the dissertation may be referred to University Microfilms, 1490 Eisenhower Place, P.O. Box 975, Ann Arbor, MI 48106, to whom the author has granted "the right to reproduce and sell (a) copies of the manuscript in microform and/or (b) printed copies of the manuscript made from microform."

Signature _____

Date 6 Nov 96

University of Washington

Abstract

Liquid Chromatographic Separation and Sensing Principles
with a Water Only Mobile Phase

by Marc Douglas Foster

Chairman of the Supervisory Committee:
Associate Professor Robert E. Synovec
Department of Chemistry

Two separate subjects will be developed in this work. The first subject is a novel chemical analyzer based on a polymer clad optical fiber inserted into a transparent capillary tube. This configuration is referred to as an annular column. A light source is directed into the end of the fiber optic. When a small sample volume is injected into a mobile phase flowing through the annular column, selective partitioning of an analyte into the fiber optic polymer cladding causes a local change in the cladding refractive index, and a consequent change in the amount of light emerging from the side of the optical fiber is detected. The result is a low volume chemical sensor that temporally separates, as well as detects, chemical species that partition into the fiber cladding. The sensor is both theoretically and experimentally characterized in terms of the sensitivity dependencies upon several parameters. The sensor can be used for the simultaneous separation and detection of organics in water and yields a detection limit of 500 parts-per-billion for cumene at 1 μL/min flow rate. This detection limit corresponds to an effective refractive index change in the mobile phase of 8×10^{-8} in a detection volume of 17 nL.

The second subject is the development of reversed phase high performance liquid chromatography columns for the separation of hydrophobic analytes such as aromatic hydrocarbons, using only water as the mobile phase. Achievement of reasonable capacity factors for hydrophobic species without organic modifier in the mobile phase is accomplished by substantially decreasing the phase volume ratio of stationary phase relative to the mobile phase volume, and also by increasing the polarity of the stationary phase relative to stationary phase materials commonly used for RP-HPLC. Using only water as the mobile phase results in the elimination of toxic organic solvent waste from HPLC analysis. Also, a water mobile phase provides an environment offering an improved signal-to-noise ratio for UV detection. Additionally, excellent prediction of the octanol/water partitioning coefficient (P_0) and aqueous solubility (X_0) for hydrophobic analytes are obtained from a single measurement of the capacity factor in the water mobile phase.

Table of Contents

List of Figures

List of Figures (continued)

List of Figures (continued)

List of Figures (continued)

List of Tables

Chapter 1. Introduction

1.1 Introduction to Chapter 1

The purpose of this text is to introduce two new analytical techniques which can be used for separation and quantitation of mixtures of non-polar species using only water as the solvent. Traditionally, analytical separation techniques for non-polar compounds, such as solvent extraction and high performance liquid chromatography (HPLC), have required the use of an organic solvent. While organic solvents are excellent solubilizers of hydrophobic species they are usually toxic and there is a great deal of impetus to eliminate or at least minimize the use of toxic organic solvents. The largest use for organic solvents is in industrial cleaning processes for the cleaning of metal parts, electronics components and paint stripping. The use of many of the more notorious organic solvents in industry has been dramatically reduced from the peak consumption period of the mid 1980's due largely to regulations by federal and state regarding the use of organic solvents. The use of organic solvents in analytical chemistry has also declined in recent years. Popular topics for publication regarding solvent extraction techniques in analytical chemistry are most often proposed alternatives to using solvent extraction at all. Supercritical fluid extraction has become an attractive alternative to traditional organic solvent extraction techniques. Solid phase extraction and miniaturized solvent extraction schemes have also been published with increasing frequency. The trend towards minimization of solvent use in HPLC has been accommodated primarily by reducing the bore of the columns. The trend towards minimization of solvent waste and pollution prevention in general is the observed result of a rich history of environmental catastrophe and reform. The next two sections will recount some of the more influential events and legislative acts contributing to pollution prevention.

1.2 Environmental Damage and Human Health Risks

The legislation of environmental laws are generally a consequence of a previously recognized or impending environmental problem. Consider the example set in 1948 in Donora, Pennsylvania. In the fall of 1948, an inversion layer trapped a layer loaded with pollutants from a steel mill, killing 19 people and leaving thousands of others ill.[1] In response to this and similar problems elsewhere, the Clean Air Act was first written by the department of Heath, Education & Welfare. Perhaps the most notorious environmental tragedy was the fiasco of building a school and a residential community on a hazardous waste dump at Love Canal, New York. The incident at Love Canal has been described by a number of texts on the subject including two good historical perspectives relating to industrial wastes.[1,2] In 1942, the Niagara Power and Development Company gave Hooker Chemical Company permission to begin dumping chemical wastes into the Love Canal and sold the property to Hooker in 1947. At that time and until the mid-1970's dumping of wastes required a permit from the local health department which was granted as long as the site would not endanger public health by attracting flies and other vermin. From 1942 to 1952 the site was used to dispose of over 21,000 tons of various chemicals. By 1953 the canal was full and was covered with dirt. Later in 1953 sixteen acres of land, including the Love Canal, were sold to the Niagara Falls school board for the construction of a new elementary school. In purchasing the property the school board also signed a disclaimer acknowledging the burial of chemical waste and transferal of all risk and liability to the school board. Initial construction of the school was begun in 1954 and halted when the contractor excavated a pit filled with chemicals. The architect of the school warned that the chemicals might harm the concrete foundation and the school board decided to move the foundation 85 feet to the north of the original location. The school was completed in 1955 with an enrollment of 400 children. Eventually, most of the land on and around the school was built into low cost residential housing. Over the next two decades there

were many sporadic reports of problems which were undoubtedly due to leaking wastes. Foul smells and oozing sludges leaking through basement walls were quite common. Holes opened in the ground exposing deteriorated chemical waste drums appeared from time to time and were covered over with dirt. Chemical burns and blisters were reported. Despite the seemingly obvious environmental tragedy which had occurred at Love Canal, no formal investigation of the site began until 1976. The extent of the problem slowly gained the attention of the public and public officials until finally in 1978 the New York state health commissioner issued an emergency health order recommending evacuation of homes in the area. The evacuation order was world wide news and finally brought the problem of disposal hazardous waste to the public's consciousness. In later review of the nationwide situation, the EPA estimated that there are as many as 30,000 hazardous waste sites across the country and that only 10% of all hazardous wastes were disposed of in environmentally sound ways.[2]

There are countless local incidents of human and environmental damage due to improper management of toxic wastes, but a relatively recent realization by the scientific community is that discharges of man made toxic pollutants are adversely affecting the environment on a global scale. An example of this is the destruction of a significant portion of the ozone layer due in large part to emissions of chlorinated hydrocarbons and chlorinated fluorocarbons (CFC's). The ozone layer shields the earth from low wavelength ultraviolet radiation. Without the protection of the ozone layer, scientists predict large increases in cancer rates, and deforestation problems on a global scale. Due to vocal statement of the problem by environmental scientists and public knowledge of the problem the "Montreal Protocol" was enacted which dictates a total elimination of the production of CFC's, halons, trichloroethane and carbon tetrachloride by 1996. The production of CFC's and chlorinated hydrocarbons peaked in the late 80's and has declined rapidly in recent years. Figure 1.1 shows the U.S. production of CFC's and the two most common chlorinated hydrocarbon solvents.[3]

Figure 1.1 A history of the U.S. production of five ozone depleting chemicals between the years of 1968 and 1996. Production peaks in the late 1980's due to pollution prevention policy established by the EPA. Data was obtained from the "Facts and Figures for the Chemical Industry" articles which appear annually in Chemistry and Engineering News. Symbols indicate: methylene chloride (▲), combined chlorofluorocarbons (□), and trichloroethane(■).

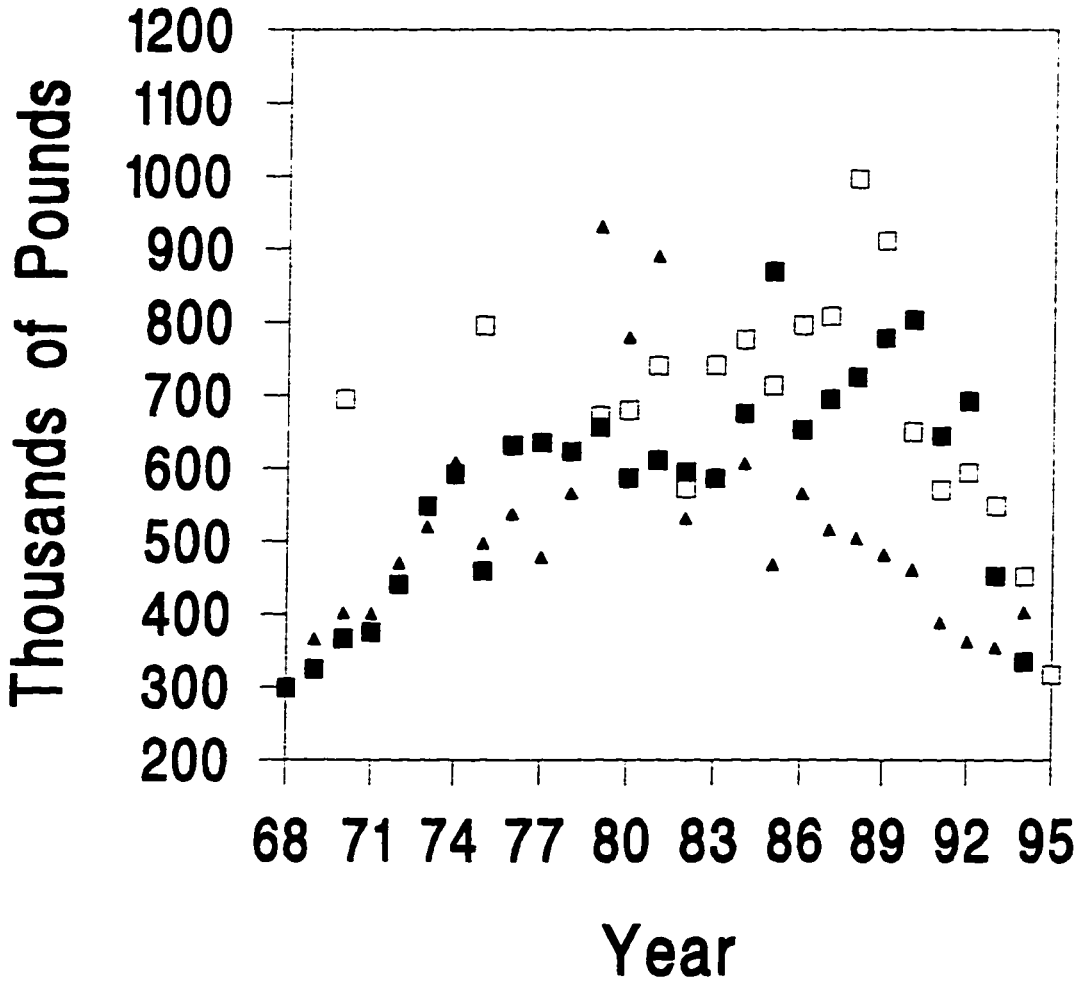
Thousands of Pounds
1200
1100
1000
900
800
700
600
500
400
300
200
68 71 74 77 80 83 86 89 92 95
Year

1.3 Environmental Regulations

Public awareness of environmental problems created political pressure for solutions to these problems and helped to promote change. One large historic development in the fight to control environmental degradation was the formation of a centralized federal agency devoted entirely to protection of the environment. In response to political pressure, president Richard Nixon created the Environmental Protection Agency in 1970. In the first two years of its creation, the EPA inherited the Clean Air Act and the Clean Water Act, both created in 1948 by the Department of Health, Education & Welfare. As stewardship of these acts are passed to the EPA, the EPA assumes the role of establishing emission standards, regulatory and enforcement programs and amendments to these acts. Compliance with the Clean Air and Water Acts is met by keeping air and water discharges below a set concentration level. One result of these acts was to dramatically increase the amounts of hazardous wastes which were containerized and put into disposal sites. While the mandated concentration levels have generally dropped around the board, the increase in industrial output has also increased and total discharge of pollutants continues to increase even as concentration limits decreased. A major part of this trend is indicated in the early 70's environmental revolution is the corporate slogan for pollution prevention strategy, "the solution to pollution is dilution." The idea behind this strategy is that if a regulated pollutant in an air or water waste stream tends to be above the regulated level, the problem can be remedied by increasing the amount of air or water introduced into that waste stream. Dilution of hazardous wastes is not a viable solution to environmental problems and the initial attempts at achieving compliance by this method resulted in measures to reduce introduction of pollutants into the environment. In response to the problem, the EPA has created three major acts which address reduction of total pollutants and has promulgated a true reduction of toxic pollutants into the environment for true pollution prevention. Four excellent texts which cover the history and regulation of waste reduction and explore methods for pollution prevention are available.[4-7]

The first of the pollution prevention acts was the Resource Conservation and Recovery Act (RCRA) of 1976 which was amended in 1984 to include the Hazardous and Solid Waste Amendments (HSWA). Subtitle 3 regulates hazardous solid wastes which governs all containerized wastes whether solid, liquid or gaseous in nature. RCRA established guidelines on how hazardous wastes would be dealt with in regards to storing on the site, shipping and disposal. RCRA also required all generators of hazardous wastes to implement programs to reduce the volume and toxicity of the hazardous wastes generated. Achievement of hazardous waste reduction has not yet been mandated by RCRA, but may come in the future. One of the most influential caveats of the RCRA legislation was the so called 'cradle to grave' liability of all parties associated with hazardous wasted dumping site. Cradle to grave is somewhat inappropriate as it implies that liability ceases once the waste is buried. In reality, liability for wastes once created is essentially infinite. Liability for a site applied to all potentially responsible parties (PRP's) of waste to the site which included all contributors of wastes, waste transporters and the site owners, whether the waste was deposited while they owned the property or not. The indefinite liability for hazardous wastes as much as an other factor frightened industry into taking a very tight control of how wastes were disposed of and created an environment which was very conducive to searching out methods to eliminate the generation of hazardous wastes or at least to minimize the toxicity and volume of wastes generated. Another of the most influential laws to date is the Comprehensive Environmental Response, Compensation and Liability Act (CERCLA) which is more commonly referred to as "Superfund". CERCLA was enacted in 1980 due, in large part, to the public outrage over the Love Canal disaster. The law was enacted so that the federal government could react to toxic spills or potential spills of toxics using moneys provided primarily by waste generators. More importantly, the law allowed the federal government to sue all PRP's for cleanup costs which made dumping of toxic wastes even more unpalatable to waste generators. In 1986 the Superfund was amended by the Superfund Amendments and Reauthorization Act (SARA). SARA has also had a profound impact on the use of

toxic substances in industry. One of the major impacts of SARA is the Emergency Planning and Community Right-To-Know Act (EPCRA) which requires that manufacturing facilities of 10 or more full time employees which manufacture or process 25,000 pounds or use 10,000 pounds or more of a list of 350 toxins must document and report their total usage of the monitored toxins and maintain an accounting of their discharge from the plant and the way in which they were discharged. The compilation of this list by the EPA is known as the Toxins Release Inventory and is available to the public by a number of methods. A CD-ROM containing data from 1987-1993 is available from the Government Printing Office for $38. In addition to the TRI data, the two disk set contains software for searching the database and chemical substance fact sheets. The TRI data can also be accessed via the internet at http//rtk.net. To use the on-line data base you must register and apply for an account which is free but takes about a week to be activated. An intended use for this data is for state and local fire departments and other emergency services to be able to establish contingencies for emergency response to release of toxic chemicals before they happen. Another use for this data is in tracking the actual progress in waste reduction by chemical or type of industry or individual manufacturer or by any of a number of other parameters.

1.4 Resulting Trends for Solvent Minimization in Industry

The reduction of solvent usage in industry is based primarily on economic considerations. The issue of liability is the largest contributor to the increasing total cost of solvent usage. The generator, the transporter, and the final site manager for hazardous wastes share liability for the indefinite safe containment of the waste. Naturally there is a premium price required for lifetime stewardship of hazardous wastes and for guaranteed safe transport of them. There has also been a large increase in the wage of the many people involved in packaging, documenting and shipping of hazardous wastes. Jobs which used to require a hard worker with a strong back now

also require training on legal regulations and procedures. Taxes on hazardous waste for generation of the Superfund budget and other projects have become a considerable portion of the cost of hazardous waste disposal. Simply requiring an accounting of toxins has done a lot to produce reductions of discharges. Public access to records of toxin releases has provided an incentive to reduce releases to maintain public favor.

The amount of work required to totally account for the fate of the target pollutant is a daunting task and industry has placed a priority on eliminating use of the target chemicals or to reducing consumption below the threshold reporting levels wherever possible. There is also an incentive to reduce solvent consumption by industry in order to attempt to reduce future regulation of hazardous waste generation. The EPA set voluntary goals for industry to achieve a 33% reduction of target compounds by 1992 and a 50% reduction of target compounds by 1995 relative to the first toxins release inventory data of 1988. Among the seventeen target compounds chosen were eleven common toxic solvents: benzene, toluene, xylene, methyl ethyl ketone, methyl isobutyl ketone, chloroform, methylene chloride, carbon tetrachloride, perchloroethylene, trichloroethylene and trichloroethane. The EPA indicated that the 33% reduction goal was surpassed with results of the TRI reports indicating a 40% reduction in waste and emissions of the seventeen targeted compounds. The TRI results of 1994 indicated that industry had already exceeded the 1995 goal of a 50% reduction of the targeted wastes and the 33/50 program was ended.[8]

1.5 Solvent Minimization in Analytical Chemistry

The prior sections of the introduction were introduced to provide an overview of the reasons that solvent reduction is an important issue. The next section will look at the steps that have been taken to reduce hazardous waste generation in the field of analytical chemistry. To save any significant amount of waste, the targeted analytical procedure should require a substantial amount of solvent for analysis and should also be a commonly used method. Two analytical techniques which apply are solvent

extraction and liquid chromatography. The most significant reduction in hazardous waste generation for analytical chemistry can be made in these two categories. There are three general approaches towards waste minimization for these techniques: miniaturize the equipment, replace the usual solvents with a non-hazardous solvent, or eliminate the method by use of an alternate technique.

Solvent extraction is a useful technique in analytical chemistry for many applications. With solvent extraction, specific analytes can be selectively separated from complex matrices, and if the solvent is considerably more volatile than the analytes, it can be reduced in volume to provide preconcentration of the analytes for improved detection limits. By reducing the scale of the process the advantages of solvent extraction can be maintained while reducing solvent consumption. The advantage of this technique is that procedures developed for larger scale extraction can simply be adapted to a smaller scale while leaving all other procedures intact. Solvent extraction techniques have been combined with flow injection analysis (FIA) techniques to drastically reduce the amount of solvent required and also to increase sample preparation throughput by using the FIA methodology.[9,10] Another solvent extraction method which has received a great deal of interest in recent years is supercritical fluid extraction using carbon dioxide. Carbon dioxide becomes a supercritical fluid at pressures in excess of 74 bars and temperatures above 31 Celsius. As a supercritical fluid, carbon dioxide performs well as an organic solvent and can be used for extraction purposes. The use of supercritical carbon dioxide as an extraction solvent has several unique advantages over traditional extraction solvents such as chloroform or ether. Most relevant to discussion at hand is the fact that carbon dioxide is non-toxic and is a gas at room temperature and pressure so that the use of carbon dioxide as an extraction solvent does not generate any solvent waste. Another unique advantage of supercritical carbon dioxide as an extraction solvent is that the solubility of a particular analyte in the supercritical carbon dioxide increases rapidly with the pressure and density of the supercritical fluid. Supercritical carbon dioxide is normally a gas so it is quite easy to preconcentrate analytes extracted into the carbon dioxide by allowing

some of the supercritical carbon dioxide to evaporate away from the solution. Another extraction technique which has gained a great deal of popularity is solid phase extraction. In solid phase extraction, the organic extraction solvent is replaced by a solid sorbent such as the stationary phase material from a chromatographic column. Immobilization of the solid phase extraction medium as the porous outlet of a sample container allows water samples which contain trace organic species to be selectively extracted into the solid phase extraction medium by filtering the water sample through it. Once preconcentrated into the solid phase material, the trace organics can be extracted with a small volume of organic solvent for further analysis.

Liquid chromatography (LC) is another analytical technique which uses a significant quantity of organic solvent and would benefit from solvent minimization techniques. There are a number of approaches which have been taken to reduce the amount of organic solvent waste generated by liquid chromatography. One approach is to replace the liquid chromatographic method with some other type of chromatographic method such as gas chromatography (GC) or supercritical fluid chromatography (SFC) methods which don't generate any hazardous solvent waste. GC is a well established method which is in wide use but it does not work for all types of samples. Some analytes, such as many types of pesticides, are thermally labile and will decompose at the temperatures required for GC analysis. Many other analytes are not very volatile so that it is difficult or impossible to analyze them by GC. Some examples are polyaromatic hydrocarbons, phenols, polymeric materials and surfactants which are commonly analyzed by LC methods. The use of HPLC also allows the use of some selective detectors that do not work with GC. SFC is generally better suited than GC for thermally labile or nonvolatile species, but SFC systems are not preferred by many analysts because special high pressure components are required which are more expensive than most LC and GC systems and are more difficult and costly to maintain. LC remains a popular technique for analytical separations because it can be the best way and sometimes the only way to analyze many mixtures which contain non-volatile or thermally labile components. In addition to performing well on mixtures not

achievable by GC and SFC, LC systems work well for the mixtures which can be analyzed by GC and SFC. Since the LC system works well for almost all mixtures, it is often called upon to perform all separations which might be required by a company. This is especially true for a company with limited resources which needs a single dedicated separation system and analyst to perform a variety of analytical separation tasks. Reducing the amount of waste generated by HPLC analysis has been by a an area of research pursued by a number of researchers and manufacturers of HPLC columns. Alltech provides a mobile phase recycling system which reduces the amount of waste generated by about two thirds. The drawbacks to this technique are that the unit is priced at $3000 dollars, there are concerns about the purity of the solvent with prolonged use, and the unit can only be used with isocratic elution. The most common way to reduce the amount of solvent used for HPLC is to reduce the bore of the chromatographic column.[11] Analytical HPLC columns have traditionally been supplied with a bore of 4.6 mm. As reduction of solvent consumption has become an important issue, manufacturers of HPLC columns have begun to offer analytical columns of increasingly small bore. The use of 2.1 mm and 1 mm bore columns has become increasingly common and columns with even smaller bores are beginning to be made available commercially. While reducing the bore of the chromatographic column provides dramatic reduction of the quantity of solvent used it is not without drawbacks. The primary drawback in reducing the bore of the column is that traditional chromatographic systems often will not work properly with small bore columns. As the bore of the column is reduced from 4.6 mm to 1 mm the volume of solvent used is reduced by a factor of about twenty, but in order to maintain good chromatographic efficiency, the injection volume and detection volume must be reduced accordingly.[11] Providing the appropriate injection and detection volumes usually requires buying equipment designed for these smaller bore columns. Even with the appropriate equipment the analyst must take extra care to eliminate any excess volumes in the connecting tubing and fittings and to avoid injecting any particulates which tend to clog the smaller bore columns more easily. Additionally, concentration-based detection

limits may decrease for the smaller bore columns since the appropriately designed detector flow cell will usually have a shorter pathlength than the detector flow cells designed for larger bore columns. Despite all these limitations, many analysts have switched over to smaller bore columns in order to reduce the amount of solvent used for chromatographic analysis. The object of this dissertation is to introduce a new concept in reversed phase separations which enables separations of organic species without the need of any organic solvent at all.

With the goal of eliminating the toxicity of the solvent, no better solvent could be chosen than water. In addition to being completely non-toxic, water is the least expensive solvent obtainable, it is non-flammable and it has a number of other unique qualities that make it an excellent solvent for chromatography. Two projects will be developed in the following sections of this dissertation, both of which will capitalize on the undeveloped concept of using pure water as the mobile phase for reversed phase chromatographic separation. First, the annular column chemical analyzer (ACCA) with mode filtered light detection (MFLD) will be discussed. The ACCA is a fiber optic based chemical sensor which physically separates and detects species partitioning into the polymeric cladding of an optical fiber. The ACCA will be shown to be a sensitive small volume sensor for separation and detection of trace organics in water. The ACCA is well suited for implementation of an on-line tool for quantifying trace organics in aqueous waste streams which not only eliminates the organic solvent waste generated by traditional off-line HPLC analysis but also eliminates the need for sample acquisition and preparation. Second, the development of columns for reversed phase high performance liquid chromatography (RP-HPLC) of organic analytes using only water as the mobile phase will be discussed.

1.6 Annular Column Chemical Analyzer

Optical fibers are often used in spectroscopic instrumentation as extrinsic detection elements of many detection schemes where the optical fiber is used as a path to provide the spectroscopic information to the detector.[12-17] Fiber optic chemical sensors (FOCS) have also been developed wherein the fiber optic itself is an intrinsic part of the sensing mechanism. FOCS provide chemical information based on a number of different mechanisms for analyte interaction with the light source along the fiber optic pathway. Evanescent field measurement with FOCS is an effective way to utilize fiber optics as intrinsic sensor. Additionally, sensing based on surface plasmon resonance can provide very sensitive refractive index responses.[18] Indicator chemistry in thin sol-gel coated fiber optic has also been used as a novel method of probing the evanescent field.[19] In recent reports,[20,21] fiber optics with polymer claddings were used for the purpose of solid phase microextraction of organics from aqueous solutions with direct injection into a GC, although the optical properties of the fiber optic were not exploited.

The annular column chemical analyzer (ACCA) is an intrinsic fiber optic chemical sensor that provides selective detection based upon an affinity for the polymeric coating of the fiber optic and accounts have been published in three articles.[22-24] The detection mechanism is called mode filtered light detection (MFLD) and will be discussed in detail both in regards to theoretically and observed dependence upon the refractive index (RI) and partitioning mechanisms in Chapter 2. The sensor incorporates a bare glass core section of fiber optic which is coated with a polymeric film which has a refractive index lower than the glass core, allowing for propagation of light in the fiber. By inserting this fiber optic with an appropriate coating into a section of capillary tubing which is just larger than the outside diameter of the fiber optic, an annular column sensor is produced. The annular gap between the outside of the fiber optic and the inside of the capillary tubing allows a mobile phase to be introduced. The polymeric coating of the fiber optic can then serve as the cladding for the fiber optic as well as a

chromatographic stationary phase for separation of species in the mobile phase. The term 'mode-filtered light' refers to the observation that light initially propagating down an optical fiber, can be decoupled from that fiber by an increase in the cladding RI at the core/clad interface by a permeating analyte, thus changing the allowable propagating modes within the fiber resulting in a continuous and nearly linear increase in mode filtered light with increasing clad RI. Traditionally, mode-filtered light is measured indirectly as the change in the transmitted beam intensity.[25-28] An alternative approach is discussed in Chapter 2 and 3 in which one measures the mode-filtered light emanating from a small area at a right angle to the fiber primary axis. This new approach has an advantage which is analogous to the increase in signal-to-noise ratio (S/N) one obtains in fluorescence detection relative to absorbance detection, that is, measuring essentially the same signal against a low background instead of a large background. Additionally, an annular column should perform favorably in terms of the chromatographic impedance function while easing constraints on the pump and sample injector. [29,30]

The work discussed in Chapter 3 is directed towards the developing of an improved annular column chemical sensor which could be used with a pure water mobile phase and with much better detectability than prior efforts. Initial work with the ACCA showed a linear increase in sensitivity with distribution constant which resulted in a exponential increase in sensitivity for a given analyte as the percentage of water in the mostly methanol mobile phase was increased. However, increasing the water content also caused broadening of peaks so that the detectability in terms of the injected concentration, for a typical analyte such as toluene, did not improve with increasing water content beyond about 30 percent water in methanol. Chapter 3 discusses improvements in the detectability for this sensor by decreasing the cladding thickness and thereby decreasing the phase volume ratio, i.e., the ratio of the volume of stationary phase to mobile phase. Peak broadening is proportional to the capacity factor, which is the product of the distribution constant and the phase volume ratio, so that a decrease in the phase volume ratio allows a proportional increase in distribution

constant while keeping the capacity factor, and peak broadening, constant. Thus, detectability for a given stationary phase and analyte is increased by reducing the phase volume ratio by using a thinner cladding and increasing the distribution constant by using a weaker mobile phase while maintaining the same capacity factor and peak broadening. Initial results were obtained with a commercially available, 15 μm thick poly[oxy(dimethylsilylene)] (PDMS) clad fiber optic which produced a phase volume ratio of 0.35 in the annular column. Chapter 3 covers the development of a 0.1 micron cladding on a bare glass core fiber, which should be about the thinnest layer that can guide a 633 nm He/Ne laser light source without a large increase in the background signal due to scattered light. The PDMS stationary phase was not used since extrapolations from our previous results indicated that capacity factors and peak broadening would be larger than desired for target analytes such as toluene in a pure water mobile phase. The PDMS would have likely produced better detection limits in pure water, but at the cost of wider peaks and longer analysis times. By consideration of solubility parameter theory,[31-34] which relates capacity factor to phase volume ratio and the polarity of the stationary phase, mobile phase and analyte, it was determined that a poly[oxy[methyl(3,3,3 trifluoropropyl)silylene]] (TFPS) cladding, which is more commonly called trifluoropropyl polysiloxane, would produce more satisfactory results. This particular material was chosen because it had a higher polarity as indicated by a solubility parameter value of 9.0 as compared to the PDMS value of 7.4.[35] The higher solubility parameter for TFPS should lead to slightly lower retention for the most hydrophobic analytes. Thus, the TFPS has good qualities for the development of a liquid chromatographic sensor for the analysis of trace organics in pure water, which should eliminate the generation of hazardous waste.

The purpose of Chapter 3 is to demonstrate that decreasing the phase volume ratio allows the use of weaker solvents and a consequent increase in the distribution coefficient, thus resulting in improved detectability for the annular column sensor. Additionally it is shown that a decreased phase volume ratio coupled with a moderate polarity stationary phase provides reasonable capacity factors for hydrophobic analytes

in a pure water mobile phase. A theory is developed which estimates the expected signal from the MFLD, and takes into account the hydrodynamic dilution of an analyte band as it travels down the annular column, in terms of the capacity factor of the analyte and the linear flow velocity of the mobile phase. Peak broadening of the analyte zone is approximated by the behavior expected for flow through parallel open plates.[36] The hydrodynamic aspects of the annular column sensor are characterized in terms of the sensor response throughout a wide range of flow rates in order to establish applicability with reasonably short analysis times. The utility of the annular column chemical sensor is demonstrated by showing chromatographic sensing of aromatic and chlorinated hydrocarbons on the annular column, using water as the mobile phase, with excellent sensitivity and good chemical selectivity by MFLD. Additionally, distribution coefficients, as derived from the analyte signal after eliminating the RI dependence, correlated well to octanol/water partition coefficients for a wide range of analyte species. Analyte sensitivity can be predicted by this correlation. The dynamic range of the MFLD is evaluated over a wide range of mobile phase compositions.

1.7 Hypotheses - MFLD

1. Off axis measurement of MFLD offers significant advantages over previous MFLD sensor schemes

The MFLD detection scheme is a unique method for obtaining sensitive and selective detection of target analytes. Other fiber optic based sensors have been developed which can sense analytes due to a change in the amount of mode filtered light propagating through the fiber. Previous sensors have measured a change in the transmitted light caused by analyte adsorbing to the surface of the fiber optic. The MFLD scheme developed here is unique because the mode filtered light is measured perpendicular to the primary axis of the fiber which offers two advantages to the traditional technique. One advantage is the increase in signal-to-noise ratio (S/N)

obtained by measuring essentially the same signal against a low background instead of a large background which is analogous to the increased S/N obtained in fluorescence detection relative to absorbance detection. Another advantage is that sensitive detection can be accomplished in a very small volume, on the order of nanoliters, while the traditional method requires a relatively long path length to achieve reasonable signal to noise ratios. The excellent sensitivity of the MFLD scheme and the small effective detection volume lend excellent potential for development of the MFLD as a new type of detector for liquid chromatography.

2. Use of a polymer clad fiber for MFLD introduces three different types of chemical selectivity

The annular column chemical analyzer offers three completely different ways to introduce selectivity into the MFLD detection scheme. The MFLD signal increases with both the chemical affinity of the analyte for the cladding, and the difference in RI between the analyte and the cladding. The selectivity due to the analyte affinity for the fiber cladding is somewhat analogous to mass sensitive sensors such as the quartz crystal microbalances (QCM's) where chemical selecitivity can be achieved by choosing a polymeric coating which has a large chemical affinity for the target analyte. The MFLD method also has selectivity based on the RI difference between the analyte and the cladding. For a given concentration of analyte in the stationary phase, the measured MFLD signal is directly proportional to the difference in refractive index between the analyte and the cladding. This permits the ability to enhance the signal of the target analyte class by selection of a cladding RI which is very different from the analyte RI and also the ability to tune out interfering species by choosing a cladding RI which is close to the RI of the interfering species. A completely different type of selectivity is achieved by using the polymeric cladding to achieve temporal separation of the species to be sensed which is observed as a difference in migration rates for different species partitioning between the fiber cladding material and the mobile phase

flowing through the annular column. The inclusion of three different ways to obtain selectivity for desired analytes into a very simple sensor design with excellent sensitivity makes the MFLD a very useful platform for future sensor designs.

3. The geometry of the annular column offers the potential for combining the chromatographic performance of open tubular columns with a relatively high volume per unit length like packed columns

Bristow and Knox introduced a quantity termed the separation impedance, E, for HPLC, which is a measure of the time of elution per theoretical plate multiplied by the pressure drop per theoretical plate and divided by the eluant viscosity. Since this parameter includes the number of plates, the retention time and the operating pressure, it offers a means of comparing the overall performance characteristics of different columns. Lower separation impedance means better performance. A good packed column, at optimum flow velocity, may have a separation impedance of 2000 while a good open tubular column might have a separation impedance of 20. Thus an open tubular column providing the same number of plates as a packed column could do so with a one hundred time reduction in operating pressure or analysis time. The annular column would provide a separation impedance of 14 , under the same conditions as the above and so offers a theoretical advantage to even open tubular columns.

From the preceding argument in favor of open tubular columns one might wonder why open tubular columns are so rarely used or reported in the literature. The problem with open tubular columns is that in order to limit peak broadening, the injection and detection volumes have to be extremely small. Efficient packed columns with diameters of 4.6 mm require injection and detection volumes on the order of microliters. An open tubular column with a diameter of 10 microns has a volume per length which is approximately 100,000 times less than a 4.6 mm I.D packed column, so injection and detection volumes would need to be on the order of picoliters. One of the major benefits of the annular column is that the performance of the annular column should be nearly equivalent to the open tubular column but has a volume per

length which is typically 1000 times larger than a comparable open tubular column so that open tubular column performance is feasible with available injector and detector technology.

1.8 Water Only Reversed Phase (WRP) Columns

Reversed phase HPLC separation of species with significant hydrophobicity has traditionally been performed on stationary phases that require a large fraction of an organic solvent in the mobile phase, such as 70% to 80% methanol or acetonitrile in water.[37] This current practice of RP-HPLC opposes the goals of pollution prevention because the high organic solvent content in the mobile phase is now considered a significant source of chemical waste. For example, last year over 6 billion liters of methanol were consumed in the United States, and a significant fraction of this consumption was associated with the current practice of RP-HPLC. Nonetheless, the scope of RP-HPLC applications is large, and a broad range of chemical species can be separated for either preparative or chemical analysis goals, such as neutral hydrocarbons containing aromatic and alkyl groups, and ionic surfactants containing hydrophobic groups. The stationary phase is generally a highly porous silica-based material derivatized with octadecylsilane (ODS), i.e., C18, resulting in a high surface area per gram of stationary phase.[38] The high surface area per gram of stationary phase provides a relatively high phase volume ratio (ratio of stationary phase volume to mobile phase volume), so the RP-HPLC separation is well-suited for the task of preparative chromatography, i.e., separating and purifying as much mass in a desired elution fraction as possible.[39] Unfortunately, the price paid for using a stationary phase resulting in a high phase volume ratio is the necessity for a large fraction of organic solvent in the mobile phase in order to achieve a good separation for chemical analysis in a reasonable time.[40,41] Even with the shortcoming of using organic solvents, RP-HPLC is currently a valuable tool in the chemical analysis of waste water and environmental samples. Chapter 4 addresses the need to rethink and develop RP-

HPLC methodology that is aimed toward pollution prevention, easy maintenance, and reduced cost as compared to current practice. A significant departure from current RP-HPLC methodology is proposed. This is accomplished by developing stationary phase materials that work well with only water as the mobile phase so little or no hazardous chemical waste will be generated, i.e., a non-polluting, water mobile phase. Furthermore, the proposed water-only RP-HPLC methodology should broaden the scope of current bench-top RP-HPLC analyses for adaptation to continuous monitoring, which is neither easy nor inexpensive to perform with current technology that requires organic solvents that are a significant source of pollution.

RP-HPLC is currently applied in a variety of waste water and environmental analyses. Polycyclic aromatic hydrocarbons (PAHs) are carcinogenic pollutants that commonly require chemical analysis and monitoring. RP-HPLC is often the method of choice, even though the separations require large amounts of either methanol or acetonitrile.[42-44] Thermally labile pesticides are also analyzed by RP-HPLC,[45-47] instead of by gas chromatography. While pesticides such as carbamates are generally more polar than PAHs, current RP-HPLC methodology with C18 stationary phases requires about 50% methanol. Chlorinated pollutants such as chlorobenzoic acids,[48] pentachlorophenol,[49] chlorolignins,[50] and chloracetic acids[51] have RP-HPLC methods reported for their analysis. The chlorolignin analysis[50] was developed for characterizing pulp mill effluents. The technology and methodology to be proposed, for example, should be applicable to continuous monitoring of the pulp mill effluent. Likewise, phenols, that are toxic to many life forms are often analyzed by RP-HPLC.[49,52] Many surfactants, although very soluble in water, exhibit an appreciable hydrophobic character during the RP-HPLC analysis, requiring a significant amount of organic solvent for the separation.[53,54] Other chemical substances that are becoming of interest for continuous monitoring in water systems based upon RP-HPLC studies are microcystins,[55] benzothiazoles,[56] and morpholine.[57] These examples using current RP-HPLC technology with organic solvents point toward the need to develop columns and

methods that eliminate mobile phase waste and pollution *from the analysis*, and make continuous monitoring a viable option, with minimum maintenance and cost.

The approach to meet this need is straightforward. Most applications of RP-HPLC as a chemical analysis tool, in contrast to preparative chromatography, usually require trace analysis. Therefore, it is not necessary to use stationary phases with a high surface area per mass, i.e., at a high phase volume ratio, because there is little worry that column overload will be approached. To obtain a separation in RP-HPLC, the correct balance of interactions must be achieved between the analytes, the mobile phase, and the stationary phase.[58] It is reasonable to anticipate that for any aqueous sample, such as an environmental water sample or a waste water stream, as long as the analytes are soluble in the original sample matrix, then the RP-HPLC of the sample should be achievable in pure water. Thus, it is necessary to develop stationary phases for RP-HPLC that function with a significantly lower phase volume ratio which will provide reasonable retention times for analytes exhibiting hydrophobic interactions with only water as the mobile phase. The new stationary phases to be proposed for water-based RP-HPLC will be referred to as WRP stationary phases, and packed to produce WRP columns, in order to emphasize the non-polluting, water mobile phase. Use of only water as the mobile phase will eliminate organic solvent use in many applications dealing with the direct analysis of aqueous systems. Furthermore, gradient elution can still be applied without organic solvents. Minimization of the organic solvent required for gradient analysis can be achieved by using a thermal gradient [59,60] or by using a gradient of non-polluting or non-hazardous surfactants, or buffering compound such as those used for biological systems.

In addition to saving the cost of buying and disposing of the minimal waste streams associated with traditional RP-HPLC, there are other compelling reasons to develop WRP columns that depend only upon water as the mobile phase. First, the water only mobile phase will be easier and less expensive to prepare than a mixed mobile phase. Second, the water-only mobile phase can be readily re-circulated and used over again by simply trapping any eluted analytes on a standard C18 column with

a higher phase volume ratio. Third, reduced phase volume ratio will also allow for analysis of extremely hydrophobic analytes which cannot be accomplished by traditional RP-HPLC columns at any mobile phase composition due to the excessive retention times. Along the same line of reasoning, cycle times will be drastically reduced for repetitive analyses since cleansing of the column of strongly retained components will require much less solvent. Fourth, reduced phase volume offers an inherent advantage of improved peak capacity as opposed to a higher phase volume column. Finally, water provides a low background for many detection methods, such as UV-Vis absorbance, fluorescence and conductivity, thus detection limits for many analytes will improve.[61]

An additional benefit of the proposed WRP columns will be improved correlation of analyte capacity factors to the octanol/water partition coefficient (P_0) and aqueous solubility values (X_0) of the analyte. These correlations are very useful in biological toxicity modeling and predictions. For instance, log P_0 and log X_0 values are often used for quantitative structure activity relationships (QSAR) for predicting the effects of nonspecific toxins in biological systems.[62-65] Capacity factor data for hydrophobic analytes in mixed organic/aqueous systems in RP-HPLC has long been used as a method for obtaining P_0 and X_0 and has been the topic of numerous publications. Two recent reviews [62,63] cover the topic and cite more than 100 references each. Accurate prediction of P_0 and X_0 values by RP-HPLC provides savings in solvent and time, in comparison to solvent extraction techniques, but has met with limited success due to the difficulty of extrapolating results from a mixed organic/aqueous phase to a pure aqueous phase. Application of WRP columns allows for very rapid and accurate predictions of P_0 and X_0 values from the determination of the capacity factor directly in water.

Use of only water as the mobile phase is a relatively underdeveloped concept. Most of the work has been directed toward ion exchange methodology [61] and hydrophobic interaction chromatography (HIC) for the separation of proteins.[66] Hamish Small discussed the merits of water-only ion exchange and obtained a patent on the technique for the separation of inorganic ions using a weak ion-exchange column.[61]

The use of a water mobile phase with a buffer gradient for the separation of proteins by HIC has been introduced to avoid protein denaturation that occurs with addition of organic modifier to the mobile phase.[66] The work developed in Chapter 4 complements the work on ion exchange chromatography and HIC, because the focus is on the overall control of phase volume ratio and stationary phase polarity to achieve separations of all types of organics in pure water with a reversed phase retention mechanism. To a limited extent, Jandera and Kubat[67] demonstrated RP-HPLC with pure water as the mobile phase during a study of the effect of high water percentage on reversed phase separations on commercial C18 materials. In order to elute test analytes under conditions of a large fraction of water in the mobile phase, very short columns were packed to compensate for the huge capacity factors observed due to the high phase volume ratio.[67] Several authors have explored the use of non-porous silica packing materials of low surface area with traditional bonded phases, e.g., C18 or similar materials for a number of special applications or purposes.[68-71] Work with nonporous silica based packing materials has demonstrated reduced requirements for addition of organic modifiers. Yet, the use of pure water mobile phase to obtain reasonable retention times for hydrophobic analytes with RP-HPLC has not previously been developed and reported.

1.9 Hypotheses - WRP-HPLC

1. Reversed Phase Separations of Hydrophobic Species Are Achievable Using Only Water as the Mobile Phase

The first hypothesis proposed is that the RP-HPLC separation of any hydrophobic species already present in a water matrix, such trace organics in an environmental water sample, can be achieved using only water as the mobile phase. Currently, RP-HPLC separations of such samples requires a significant fraction of organic solvent added to the mobile phase to achieve a reasonable separation, which

results in the generation of hazardous waste. The separation of equivalent species using only water as the mobile phase should be achievable by reducing the volume of stationary phase relative to the volume of the mobile phase in the column and/or selecting a stationary phase with a polarity which is significantly different from the species being separated. Additionally, it should be noted that all species have some solubility in water so that the separation of any mixture using only water as the mobile phase should be achievable so long as the species present in the mixture can dissolve within a small fraction of the length of the column.

2. Sample Loading Capacity Should be in the Linear Isotherm Region

A second hypothesis is that columns developed for use with water only as the mobile phase will provide more than adequate loading capacity for most RP-HPLC separations of environmental and industrial interest, in which chemical analysis is the goal. Since the distribution constant for organic species between a the stationary phase and the water mobile phase tend to be large for very hydrophobic species, it is conceivable that the stationary phase could become overloaded. However, the maximum concentration of the species in water is inversely related to the distribution constant so that the effect cancels out. As a quantitative example, the solubilities of benzene and isopropyl benzene in water are 0.04% and 0.0009%, respectively. The distribution constants for benzene and isopropyl benzene between octanol and water are 140 and 4600 respectively. If a water sample containing the maximum possible concentration of benzene and isopropyl benzene were injected into a column with octanol as the stationary phase, the maximum concentrations of the two components in the stationary phase would be 5.6% and 4.1% respectively. This represents the maximum loading likely to be encountered and is probably within the linear isotherm region.

3. Substantially Improved Detection Limits Using a Water Mobile Phase

A third hypothesis is that the use of a water-only mobile phase will provide substantially improved detection limits for most pollutants. Organic solvents limit the wavelength range and increase the noise in many detectors such as absorbance and fluorescence because they contribute significantly to the background absorbance or fluorescence. With absorbance detection, for example, the detection at 190 nm in water is easily achieved due to the near-zero absorbance of water. Furthermore, the molar absorptivities of typical organic compounds are generally 100-fold greater at 190 nm than at 254 nm, leading to 100-fold improvement in detectability. The implication of the 100-fold enhancement in detectability with a water mobile phase is either the improvement of existing detection limits for RP-HPLC analyses currently plagued by organic solvents, or the potential to simplify methods that currently require a preconcentration step.

4. Potentially Increased Resolution Due to Reduced Phase Volume

For any two columns which provide the same stationary phase and number of plates, the column which provides a larger difference in capacity factor between the two component will provide a large resolution for the two components. For two columns of different phase volume ratio, which provide the same capacity factor for one of two similar components, a larger capacity difference will be provided by the column which has a smaller phase volume ratio. The reason for this is that for any single component and stationary phase, the capacity factor is linearly proportional to the phase volume ratio while the logarithm of the capacity factor is linearly related to the water content of the mobile phase. Additionally, for any two components, the slope of the logarithm of capacity factor versus fraction of water in the mobile phase is large for the component having the higher capacity factor at a given mobile phase

composition. Consider the exponential increase in the capacity factor of both components achieved with a linear increase in the amount of water in the mobile. If the initial capacity factor is restored by a subsequent linear decrease in capacity factor by a linear reduction in phase volume ratio, then there will be a larger capacity factor difference between the two components. The rationale described above applies to any number of components so that the conclusion can be made that for two columns which have the same stationary phase and separative power, a larger peak capacity is achieved by the column with the smaller phase volume ratio.

1.10 Notes to Chapter 1

1. Colton, C. E., Skinner, P. N. in *The Road to Love Canal*, The University of Texas Press, Austin, TX, 1996.
2. Levine, A. G. in *Love Canal: Science, Politics and People*, D.C. Heath and Company, Lexington, MA, 1982.
3. *Chemical and Engineering News*, June 24, 1996, 40-46.
4. U. S. Environmental Protection Agency in *Solvent Waste Reduction*, Noyes Data Corporation, Park Ridge, NJ, 1990.
5. Selg, R. A. in *Hazardous Waste Control*, Marcel Dekker, Inc., New York, NY, 1993.
6. Thomas, S. T. in *Facility Manager's Guide to Pollution Prevention and Waste Minimization*, BNA Books, Washington, D.C., 1995.
7. Callahan, M. S., Green, B. in *Hazardous Solvent Source Reduction*, McGraw-Hill, New York, NY, 1995.
8. Conversation with Layne Carlin, Seattle Office of the E.P.A.
9. Egorov, O.; Ruzicka, J. *Analyst* **1995**, 120, 1959-62.
10. Luo, Y.; Al-Othman, R.; Ruzicka, J.; Christian, G. D. Analyst 1996, 121, 601-606
11. Saito, M.; Hibi, K.; Ishii, D.; Takeuchi, T. in *Introduction to Microscale High-Performance Liquid Chromatography*, Ishii, D., ed. , VCH, 1988, Chapter 2.
12. Fuh, M. S.; Burgess, L. W. *Anal Chem.* **1987**, 59, 1780-1783.
13. Skogerboe, K. J.; Yeung, E. S. *Anal. Chem.* **1987**, 59, 1812-1815.
14. DeGrandpre, M. G.; Burgess, L. W. *Anal. Chem.* **1988**, 60, 2582-2586.
15. Buffet, C. E.; Morris, M. D. *Anal. Chem.* **1982**, 54, 1824-1825.
16. Fujiwara, K.; Fuwa, K. *Anal. Chem.* **1985**, 57, 1012-1016.
17. Renn, C. N.; Synovec, R. E. *Anal. Chem.* **1991**, 63, 568-574.
18. Bender, W. J. H.; Dessy, R. E.; Miller, M. S.; Claus, R. O. *Anal. Chem.* **1994**, 66, 963-967.

19. Yang, L.; Saavedra, S. *Anal. Chem.* **1995**, 67, 1307-1314.

20. Arthur, C. ; Pawliszyn, J. *Anal. Chem.* **1990**, 62, 2145-2148.

21. Buchholz, K. D.;Pawliszyn, J. *Anal. Chem.* **1994**, 66, 160-167.

22. Synovec, R. E.; Bruckner, C. A.; Burgess, L. W.; Foster, M. D. *SPIE Chemical, Biochemical and Environmental Sensors;* SPIE: Bellingham, WA., 1994; Vol. 2293, pp167-177.

23. Synovec, R. E.; Sulya, A. W.; Burgess, L. W.; Foster, M. D.; Bruckner, C. A. *Anal. Chem.* **1995**, 67,473-481.

24. Foster, M. D., Synovec, R. E. *Anal. Chem.* **1996**, 68, 1456-1463.

25. Giuliani, J. F.; Jarvis, N. L. *J. Chem. Phys.* **1985**, 82, 1021-1024.

26. Giuliani, J. F.; Jarvis, N. L. *Sensors and Actuators* **1984**, 6, 107-112.

27. Kawahara, F. K.; Fiutem, R. A.; Silvus, H. S.; Newman, F. M.; Frazar, J. H. *Anal. Chim. Acta* **1983**, 151, 315-327.

28. Klainer, S. M.; Thomas, J. R.; Dandge, D. K.; Frank, C. A.; Butler, M. S.; Arman, H.; Goswami, K. *SPIE Environmental Sensing and Combustion Diagnostics* **1991**, Vol. 1434, pp. 119-126.

29. Novotny, M. *Anal. Chem.* **1988**, 60, 500A-510A.

30. Giddings, J. C.; Chang, J. P.; Myers, M. N.; Davis, J. M.; Caldwell, K. D. *J. Chromatogr.*, **1983**, 255, 359-369.

31. Karger, B. L.; Snyder, L. R.; Eon, C. *J. Chromatogr.* **1976**, 125, 71-88.

32. Schoenmakers, P. J.; Billiet, H. A. H.; de Galan, L. *J. Chromatogr.* **1983**, 282, 107-121.

33. Hafkenschied, T. L.; Tomlinson, E. *J. Chromatogr.* **1983**, 264, 47-62.

34. Sun, Z. L.; Liu, M. C.; Hu, Z. D. *Chromatographia* **1994**, 38, 599-608.

35. Harris, F.W.; Seymour, R.B. *Structure-Solubility Relationships in Polymers* Academic Press, New York, New York, **1977.**

36. Golay, M. J. E. in *Gas Chromatography, 1958*; Desty, D. H. ed., Academic Press, New York, N.Y., **1958.**

37. Glajch, J. L.; Kirkland, J. J.; Snyder, L. R. *J. Chromatogr.* **1982**, 238, 269.

38. Fazio, S. D.; Tomellini, S. A.; Shih-Hsien, H.; Crowther, J. B.; Raglione, T. V.; Floyd, T. R.; Hartwick, R. A. *Anal. Chem.* **1985**, 57, 1559.

39. Grushka, E. in *Preparative-Scale Chromatography, Chromatogr. Sci. Series: Volume 46*, Marcel Dekker, 1989.

40. Karger, B. L.; Snyder, L. R.; Horvath, C. in *An Introduction to Separation Science*, Wiley-Interscience, New York, NY, 1973, Chapter 5.

41. Giddings, J. C. in *Unified Separation Science*, Wiley-Interscience, New York, NY, 1991, Chapters 10-12.

42. Vera-Avila, L. E.; Covarrubias, R. Intern. J. Environ. *Anal. Chem.*. **1994**, 56, 33-47.

43. Williams, R.; Meares, J.; Brooks, L.; Watts, R.; Lemieus, R. *Intern. J. Environ. Anal. Chem.* **1994**, 54, 299-314.

44. Motohashi, N; Meyer, R.; Molnar, J.; Parkanyi, C.; Fang, X. *J. Chromatogr.* **1995**, 710, 117-128.

45. Driss, M.R.; Hennion, M.-C.; Bouguerra, M. L. *J. Chromatogr.* **1993**, 639, 352-358.

46. Vreeken, R. J.; Van Dongen, W. D.; Ghijsen, R. T.; Brinkman, U. A. TH. *Intern. J. Environ. Anal. Chem.* **1994**, 54, 119-145.

47. Van De Merbel, N. C.; Lagerwerf, F. M.; Lingeman, H.; Brinkman, U. A. TH. *Intern. J. Environ. Anal. Chem.* **1994**, 54, 105-118.

48. Dietz, E. A.; Cortellucci, N. J.; Singley, K. F. *J. Liquid Chromatogr.* **1993**, 16(15), 3331-3347.

49. Melcher, R. G.; Bakke, D. W.; Hughes, G. H. *Anal. Chem.* **1992**, 64, 2258-2262.

50. Virkki, L.; Knuutinen, J.; Hyotylainen, J. *Intern. J. Environ. Anal. Chem.* **1994**, 56, 133-147.

51. Husain, S.; Narsimha, R.; Alvi, S. N.; Rao, R. N. *J. High Res. Chrom.* **1993**, 16, 381-383.

52. Lehotay, J.; Baloghova, M.; Hatrik, S. *J. Liquid Chromatogr.* **1993**, 16(5), 999-1006.

53. Fujita, I.; Nishiyama, K.; Nagano, K.; Nakayama, M.; Sugii, A. *Intern. J. Environ. Anal. Chem.* **1994**, 56, 57-62.

54. Yokoyama, Y.; Kondo, M.; Sato, H. *J Chromatogr.* **1993**, 643, 169-172.

55. Lawton, L. A.; Edwards, C.; Codd, G. A. *Analyst* **1994**, 119, 1525.

56. Fiehn, O.; Reemtsma, T.; Jekel, M. *Anal. Chimica Acta* **1994**, 295, 297-305.

57. Joseph, M.; Kagdiyal, V.; Tuli, D. K.; Rai, M. M.; Jain, S. K.; Srivastava, S. P.; Bhatnagar, A. K. *Chromatographia* **1993**, 35(3/4), 173-176.

58. Horvath, C.; Melander, W.; Molnar, I. *J. Chromatogr.* **1976**, 125, 129-156.

59. Moore, L. K.; Synovec, R. E. *Anal. Chem.* **1993**, 65, 2663-70.

60. Renn, C. N.; Synovec, R. E. *Anal. Chem.* **1991**, 63, 568-74.

61. Small, H.; Soderquist, M. E. Patent # 4,732,686 Weak Eluant Ion Chromatography March 22, 1988.

66. Horvath, C.; Haidacher, D. *Theoretical Advancement in Chromatography and Related Separation Techniques*; Dondi, F.; Guiochon, G. ed's., Kluwer Academic Publishers, Netherlands, 1992.

67. Jandera, P.; Kubat, J. *J. Chromatogr.* **1990**, 500, 281-99.

68. Hartwick, R. A.; Colwell, L. F., Jr. *J. High. Res. Chrom.* **1986**, 9, 304-5.

69. Kronberg, B; Silveston, R. *J. Phys. Chem.*. **1989**, 93, 6241-6.

70. Kronberg, B.; Silveston, R. *J. Chromatogr.* **1994**, 659, 43-56.

71. Giesche, H.; Unger, K. K.; Esser, U.; Eray, B.; Trudinger, U. *J. Chromatogr* . **1989**, 465, 39-57.

62. Lambert, W. J. *J. Chromatogr* . **1993**, 656, 469-84.

63. Khaledi, M. G.; Dorsey, J. G. *J. Chromatogr.* **1993**, 656, 485-99.

64. Kaliszan, R. *J. Chromatogr.* **1993**, 656, 417-436.

65. Hansch, C. H. *Sci. Tot. Environ.* **1991**, 109, 17-29.

Chapter 2

Initial Development of the Theory of Operation and Characterization of the Mode Filtered Light Detection Scheme

2.1 Introduction to Chapter 2

There is an ongoing interest in optical waveguide-based chemical analyzers for a variety of applications such as process analysis and environmental monitoring.[1-8] Many of these reports use the optical waveguide as an intrinsic sensor element. In this context, a significant effort has been directed toward developing cladding materials, generally polymeric, that result in enhanced selectivity for a chemical compound or class of compounds. With the aim of building upon the fundamentals of this previous work, this work explores the potential benefit of incorporating into fiber optic-based sensors, chemical separation principles that translate into readily measurable differences in response time profiles for chemical species of interest. In other words, the possibilities of incorporating chromatographic principles into a fiber optic chemical analyzer design are being examined.[9-15] As a consequence of this examination of optical sensor design, an improved method for measuring the mode-filtered light emanating from an optical fiber is developed. The term mode-filtered light refers to the observation that light initially propagating down an optical fiber, can be decoupled from that fiber by an increase in the cladding refractive index (RI) at the core/clad interface by a permeating analyte, thus changing the allowable propagating modes within the fiber. Traditionally, mode-filtered light is measured as the change in the transmitted beam intensity.[1-4] Guiliani and Jarvis launched light into a bare core fiber optic and detected the decrease in the transmitted light when alkanes were adsorbed to the core.[1,2] They described this sensing mechanism as total internal optical scattering and related the signal to the change in refractive index at the core/analyte interface. Earlier, Kawahara et al. incorporated an optical fiber with an octadecyltrichlorosilane

derivatized coating into a similar instrument to selectively measure aromatics and oil products dispersed in water.[3] More recently, a selective fiber optic-based sensor for hydrocarbons has been developed for environmental application.[4] In all of the above examples, the sensing mechanism operates by detecting changes in the transmitted light at the end of a fiber optic, labeled as I_T in Figure 2.1. An alternative approach is discussed here in which one measures the mode-filtered light emanating from a small area at a right angle to the fiber primary axis, labeled as ϕI_F, as shown in Figure 2.1. This new approach is analogous to the advantage in signal-to-noise ratio (S/N) one obtains in fluorescence detection relative to absorbance detection, that is, measuring essentially the same signal against a low background instead of a large background. One will gain even greater advantage with this new detection approach by inserting the fiber optic, with a cladding providing chemical selectivity, into a relatively narrow capillary tube as shown in Figure 2.2. This configuration will be referred to as an annular column and provides a very small diffusional distance, thus allowing various chemical species to exhibit chromatographic behavior while simultaneously being selectively monitored by the mode-filtered light detection mechanism. One of the results is a small volume RI-type detector with additional chemical selectivity over traditional RI detection that is analogous to, and yet complimentary to, absorbance detection.

A discussion of the chromatographic issues for the annular column sensor design is essential in understanding the principles by which this sensor is governed. It has been established that open-tubular capillary chromatographic columns perform considerably better than packed columns, when compared objectively by the impedance function.[10] Unfortunately, the open-tubular capillary column has resulted in many difficulties in implementation for separation as well as detection, due to the severe volume constraints on the various instrumental components such as the pump, injector and detector. The annular column, as illustrated in Figure 2.2, is based upon the idea that open-tubular chromatographic performance can be achieved without the

Figure 2.1 Different approaches to measure mode-filtered light from a fiber optic with core RI n_1, clad RI n_2, and air RI n_0. At launch angle θ_0, I_0 is distributed between mode-filtered light I_F, and the transmitted light distribution I_T (centered at θ_T). The annular column sensor measures a fraction of the mode-filtered light ϕI_F, in a small area, as θ_2 is modulated near the critical angle by the partitioning analyte species.

I_F

ϕI_F

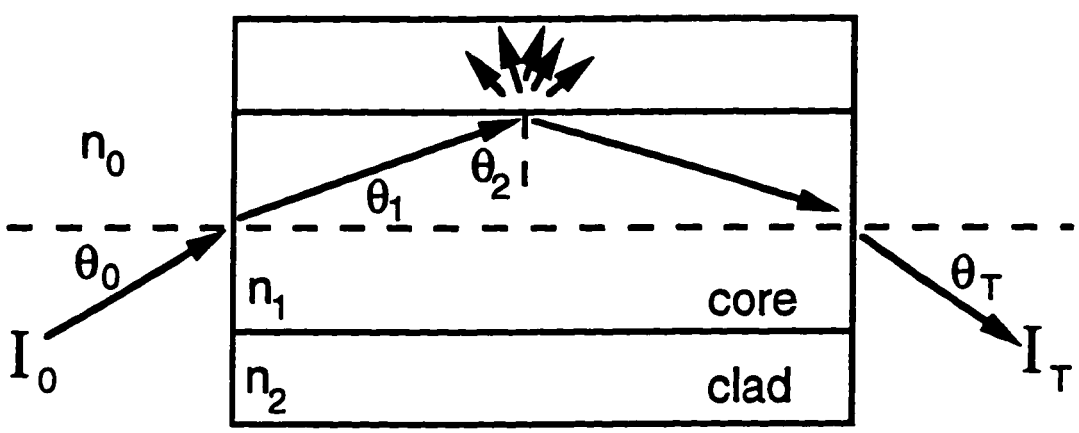

Figure 2.2 Design of the annular column sensor, where a fiber optic is inserted into a capillary tube (generally a fused silica capillary). The inside radius of the capillary is labeled as r_2, and the outside radius of the fiber optic core is labeled as r_1, while d_c is the cladding thickness.

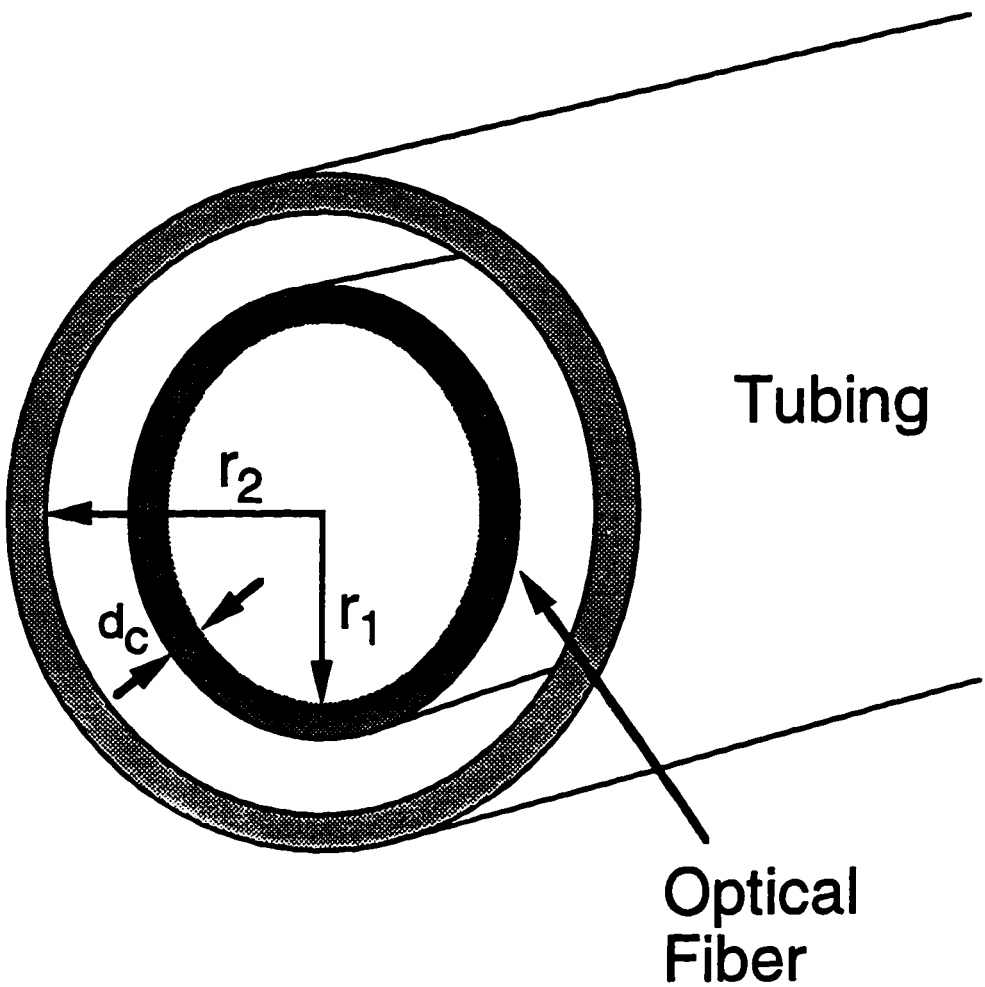
Tubing
r_2
r_1
d_c
Optical
Fiber

severe volume and maintenance constraints associated with either conventional scale packed columns or standard open-tubular capillary design. The annular column dimensions of interest are the fiber optic cladding thickness d_c, the difference r_2-r_1 between the fiber optic radius r_1 and the capillary inside radius r_2, and the volume per unit length. In practice the fiber ranges from being centered in the capillary to being against the capillary wall. Thus, the channel dimension will be a distribution ranging from zero to $2(r_2-r_1)$. One can imagine that r_2-r_1 and d_c can both be kept small, in the range of a few microns, thus maintaining good chromatographic separation efficiency, while the volume per unit length can simultaneously be large compared to the standard open tubular capillary column with an inside diameter on the order of the dimension r_2-r_1. The idea of achieving capillary performance in a larger volume per length device was first described by Giddings and co-workers, who investigated the concept of open-tubular chromatography in a narrow rectangular channel.[11] The annular column provides another advantage over other open-tubular designs with regard to on-column detection. The fiber optic cladding functions as the chromatographic stationary phase, and as such, retained analytes are readily sensed by a variety of fiber optic-based spectroscopic detection principles.[1-8]

This chapter describes the theory of detecting the mode-filtered light from an optical fiber in the annular column sensor design. The dependence of the signal upon the launch angle of the light, the injected analyte concentration, the distribution coefficient of the analyte between the mobile phase and the polymeric cladding, and the RI of the analyte is demonstrated. The practical application of the annular column mode-filtered light analyzer to low pressure, low resolution liquid chromatography (LC) is also demonstrated. Finally, the annular column is shown to function admirably as a robust, on-line solid phase extraction device, that also is a "smart" sampling system by providing a continuous detection readout of the sampling process. This on-line solid phase extraction and sampling application will build on previous work in the area of off-line solid phase extraction and sampling for GC using polymer coated fiber optics.[16-17]

2.2 General Theory for the Mode Filtered Light Detection Mechanism

To understand the basic operating principles, it is necessary to derive an expression that relates the detected analyte signal relative to background conditions as a function of the fiber optic properties, the beam intensity profile in the fiber optic, and the analyte properties such as RI, concentration, and analyte distribution coefficient, K_d, between the fiber cladding and mobile phase solvent. Illustration of the various optical quantities is presented in Figure 2.1. The intensity profile of light traveling within a fiber, also called the sum of the modes of propagation, can be investigated by observing the angular distribution of light at the exit plane of that fiber. Thus the transmitted beam intensity profile I_T was measured as a function of θ_T, which is equivalent to the launch angle reference frame, θ_0, for the purpose of illustrating the theory of the detector function. For an off-axis launching angle of 0.19 radians in Figure 2.1, which was just inside the specified numerical aperture of 0.22 for the fiber, the light intensity I_T observed at the end of the fiber is shown in Figure 2.3 (A) as a function of θ_2, in order to simplify the theoretical description. For a small θ_0 and θ_1, θ_2 is mapped from the transmitted beam reference frame θ_T by

$$\theta_2 = \pi/2 - (n_0/n_1)\,\theta_T \qquad (1)$$

where n_0 and n_1 are the RI of air and the fiber core, respectively. Thus, Figure 2.3 (A) should accurately describe the light distribution in the fiber, at the exit plane. Furthermore, as an acceptable approximation, I_T represents the intensity profile within the fiber optic at any position near the end of its length, and has been readily defined as a function of θ_2.

Consider when one directly observes the light that is mode-filtered along the fiber, defined as I_F in Figure 2.1, by placing a detector at a right angle to the fiber length axis. The detected intensity will essentially be proportional to the sum of the

Figure 2.3(A) Angular distribution of the transmitted light, I_T, just beyond the exit plane of a fiber optic, obtained at an off-axis launch angle of 0.19 radians. Each data point resulted from the transmitted intensity at a given angular position of a pin-hole aperture, mounted on a translational stage, with a spatial resolution of about 10 milliradians. I_T is plotted as a function of θ_2 as defined in Figure 2.1 and eq 1, thus the mode transmitted parallel to the fiber length axis is at θ_2 equal to 1.57 radians. The background (baseline) mode-filtered light signal is represented qualitatively as the shaded area ($\Delta\theta_C = 0$ radians, at $\theta_2 = \theta_C$), while an increase in the cladding RI (analyte) resulting in $\Delta\theta_C = 0.02$ radians (at $\theta_2 = \theta_{C,A}$) is represented as the additional cross-hatched area. **2.3(B)** Net analyte signal $S(\Delta\theta_C)$ as defined in eqs 2 and 3 over an analytically useful range of $\Delta\theta_2$. The baseline signal and analyte signal represented in Figure 2.3(A) are both labeled.

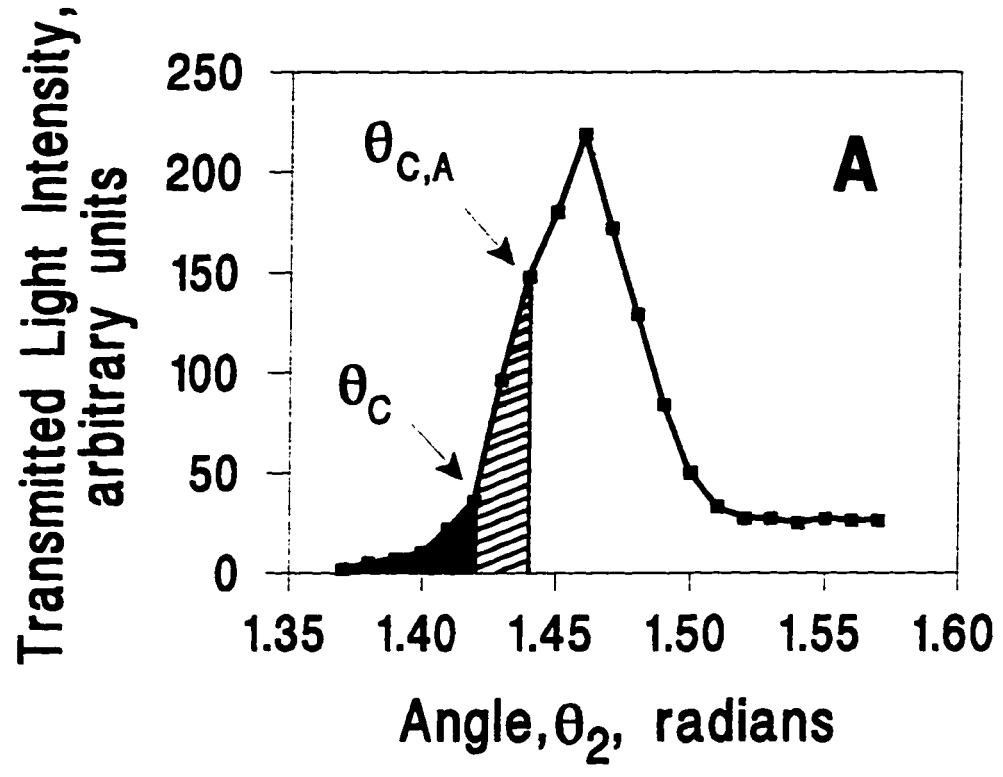
Transmitted Light Intensity, arbitrary units
250
200
150
100
50
0
$\theta_{C,A}$
θ_C
A
1.35
1.40
1.45
1.50
1.55
1.60
Angle, θ_2, radians

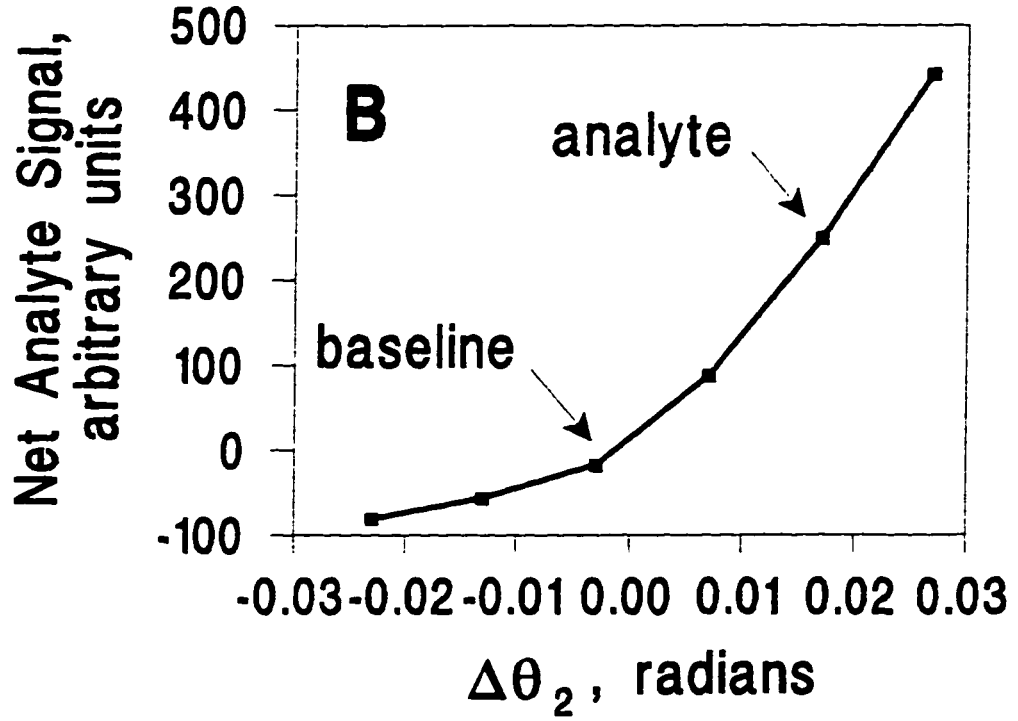
Net Analyte Signal, arbitrary units
500
400
300
200
100
0
-100
B
analyte
baseline
-0.03
-0.02
-0.01
0.00
0.01
0.02
0.03
$\Delta\theta_2$, radians

mode-filtered rays in the local environment of the detector, that occur when θ_2 is less than the critical angle θ_C for the fiber. One can measure a fraction of I_F, labeled as ϕI_F, which initially is the background signal intensity. This signal ($S(\theta_C)$) will be governed by the available light profile, which is proportional to I_T, and by the requirement that θ_2 be smaller than θ_C to achieve mode-filtering. For illustrative purposes, this background signal intensity is shown by the shaded region in Figure 2.3 (A) as the integral of $I_T(\theta_2)$ from 1.35 radians, where I_T goes to zero, to 1.42 radians, the critical angle for this particular fiber. Since the detector collects a portion of the mode-filtered light, the background intensity is actually only a constant fraction of this integrated signal. In order to detect a significant fraction of the mode-filtered light, the cladding must appreciably scatter it. Indeed, this was experimentally observed. Analyte partitioning will change the bulk RI of the cladding n_2, which in turn will alter θ_C. The result will be a change in mode-filtered light intensity, shown for a 0.02 radian increase in θ_C in Figure 2.3 (A) as an additional cross-hatched area under the I_T curve. This signal corresponds to the analyte plus background signal, and is defined as $S(\theta_{C,A})$. A shift in the integrated area to the left occurs if n_2 decreases, while a shift to the right occurs if n_2 increases. The change in observed intensity as a result of a change in θ_C can be represented as $\Delta\theta_C$, with the resultant net analyte signal, $S(\Delta\theta_C)$. The net analyte signal is given by

$$S(\Delta\theta_C) = S(\theta_{C,A}) - S(\theta_C) \tag{2}$$

with

$$\Delta\theta_C = \theta_{C,A} - \theta_C \tag{3}$$

where $\theta_{C,A}$ is the critical angle with the analyte contribution to n_2. The data in Figure 2.3(A) were applied to derive $S(\Delta\theta_C)$ as a function of $\Delta\theta_C$, with the result shown in Figure 2.3(B) for a limited range of $\Delta\theta_C$ which is considered to be relevant to most analytical measurements. Since most analytical measurements are made near $\Delta\theta_C$ equal

to zero (background conditions), one can anticipate from Figure 2.3(B) that the analyte signal will change in proportion to $\Delta\theta_C$, with a slight non-linearity.

The distinction between our method of directly detecting changes in I_F, and the conventional method of measuring changes in I_T, as illustrated in Figure 2.1, will now be made. The net analyte signal $S(\Delta\theta_C)$, is essentially the same for both methods, but the backgrounds are substantially different, as can be determined from inspection of Figure 2.3(A). The conventional method has a background approximated by the entire area under the curve, which is about 10 to 100 times larger than the background in our direct mode-filtered light measurement. Assuming the measurements are not shot noise limited, the signal-to-noise ratio (S/N) should simply be about 10 to 100 times better for our method. Even though in practice one would measure only a fraction of the direct mode-filtered light, ϕI_F, corresponding to a small volume in the annular column, the net analyte signal and background will be decreased by the same fraction, and again, if not shot noise limited, the same S/N advantage exists.[15]

We will now derive an expression for $\Delta\theta_C$ in terms of the analyte modifying the cladding refractive index by a solid phase extraction process. Subsequently, the derived expression will be experimentally examined. The critical angle θ_C, defined at θ_2, is well known and is given by

$$\cos\theta_C = NA / n_1 \tag{4}$$

as shown in Figure 2.1, where the numerical aperture NA, is given by

$$NA = (n_1^2 - n_2^2)^{1/2} = n_0 \sin\theta_{0,C} \tag{5}$$

where n_2 is the cladding RI, and $\theta_{0,C}$ the so called maximum allowed launching angle prior to any perturbation due to an analyte species. That is to say, θ_2 goes to θ_C, as θ_0 approaches $\theta_{0,C}$ in Figure 2.1.

We wish to calculate $\theta_{C,A}$ where $\theta_{C,A}$ is near θ_C for small changes in n_2. Using the identity $\cos\theta_C = \sin(\pi/2 - \theta_C)$, and since θ_C is near $\pi/2$, then the approximation

$$\cos\theta_C = \sin(\pi/2 - \theta_C) = \pi/2 - \theta_C \tag{6}$$

will be valid. For baseline conditions, the background signal $S(\theta_C)$ will be defined by

$$\theta_C = \pi / 2 - (n_1^2 - n_2^2)^{1/2} / n_1 \quad (7)$$

In the presence of a partitioning analyte, the RI of the cladding will become $n_2 + \Delta n$, where Δn is the RI change, approximately given by

$$\Delta n = C_{v,c}(n - n_2) \quad (8)$$

where $C_{v,c}$ is the analyte volume fraction in the cladding, and n is the analyte RI. The angle $\theta_{C,A}$ defining the analyte plus background signal is given by

$$\theta_{C,A} = \pi / 2 - (n_1^2 - (n_2 + \Delta n)^2)^{1/2} / n_1 \quad (9)$$

The analytical signal is based on $\Delta\theta_C$, and by substituting eqs 7 and 9 into eq 3 and simplifying,

$$\Delta\theta_C = NA / n_1 \left[1 - \left(1 - (2 n_2 \Delta n + \Delta n^2) / NA^2\right)^{1/2}\right] \quad (10)$$

Since relatively small Δn are to be measured, eq 10 can be approximated by a Taylor's series expansion, $(1+x)^a \approx 1 + ax$ for small x. The result is

$$\Delta\theta_C = NA / 2n_1\left((2n_2\Delta n + \Delta n^2) / NA^2\right) \quad (11)$$

Since $\Delta n \ll 2n_2$, eq 11 can be further simplified, and using eq 8,

$$\Delta\theta_C = n_2 / n_1 \left(C_{v,c} (n - n_2) / NA \right) \quad (12)$$

For a Δn increase of 0.0022 in the cladding of a 0.22 NA glass core fiber, a $\Delta\theta_C$ of 0.01 radians is calculated by eq 10, while the result from eq 12 is about 3% below the eq 10 result, thus the approximation is reasonable. Note that the angle change $\Delta\theta_C$ in eq 12 depends upon the analyte concentration in the cladding. Generally, partitioning processes are defined in terms of molar concentrations (or mole fractions). The distribution constant, K_d, for this partition process is

$$K_d = C_{v,c} / C_{v,m} \quad (13)$$

where $C_{v,m}$ is the volume fraction of the analyte in the mobile solvent phase at the point of detection. Note that eq 13 is equivalent to the ratio of the respective molar

concentrations. Equation 13 suggests that the detected concentration, $C_{v,c}$ can be selectively improved (amplified) relative to $C_{v,m}$ by proper selection of the cladding, thus providing a large K_d. One can further note that from eq 13,

$$C_{v,c} = (V_m/V_c)k'C_{v,m} \tag{14}$$

where k' is the analyte capacity factor as defined by chromatographic retention time, with V_c and V_m being the phase volumes of the cladding and mobile solvent phases, respectively. The inference that K_d is indeed a constant (eq 13) requires analyte equilibration between V_c and V_m, and is observed experimentally from the capacity factor, and from careful examination of the signal profile as a function of time, at various flow rates.

Combining eqs 12-14, one obtains an operative expression for $\Delta\theta_C$,

$$\Delta\theta_C = n_2 / n_1 ((n - n_2) / NA)) (V_m/V_c) k' C_{v,m} \tag{15}$$

which predicts the angle change from the original condition, θ_C, due to a partitioning analyte. In as much as Figure 2.3(B) is sufficiently linear for a small range of $\Delta\theta_C$, then

$$S(\Delta\theta_C) = \alpha\Delta\theta_C \tag{16}$$

where α is a proportionality constant. Evaluation and subsequent prediction capability of eqs 15 and 16 will follow.

2.3 Experimental Set-up for Chapter 2

A cross-sectional view of an annular column is shown in Figure 2.2, which is incorporated into an analyzer as shown in Figure 2.4, as described below. A typical annular column was made by sliding each end of a section of capillary tubing into a one inch length of PEEK tubing (Alltech Associates, Deerfield IL) fit with a PEEK nut and ferrule. One end was then inserted into an 0.5 μL injection valve (Rheodyne 7520, Cotati, CA), unless noted otherwise in the text, and the other end into a tee connector (Alltech Associates, Deerfield IL). For most experiments described in Chapter 2, a

Figure 2.4 Schematic of the annular column chemical analyzer: HeNe - laser; θ_0 - launch angle defined in Figure 2.1 (A); PMT - photomultiplier tube; Annular Column (illustrated in Figure 2.2); Pump - mobile phase introduction.

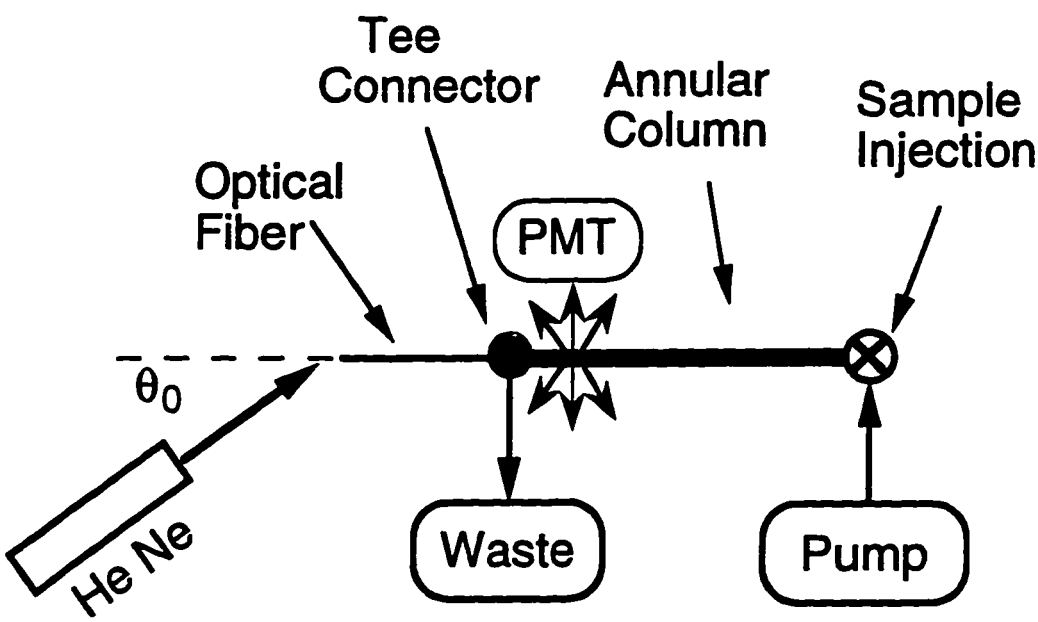
Tee
Connector
Annular
Column
Sample
Injection
Optical
Fiber
PMT
θ_0
He Ne
Waste
Pump

jacketless, polymer clad fiber optic (Fiberguide Industries, Anhydroguide, Stirling, NJ) was then slid through the tee connector into the capillary until it butted up against the injection valve, then it was moved back out about 3 mm. To reduce friction and subsequent damage to the polymer cladding of the fiber, the capillary tube was first filled with methanol for the insertion process. A seal was made between the exposed end of the fiber and the tee connector with an additional one inch length of PEEK tubing fit with a nut and ferrule. The outside diameter for the glass core fiber with a 15 μm thick polysiloxane cladding was 230 μm. Although the chemical composition of the cladding is proprietary, it is known that it is a polysiloxane with properties of a non-polar chromatographic stationary phase. The capillary tubing surrounding the fiber optic had an inner diameter of 300 μm, leaving an average 35 μm gap between the inner wall of the capillary and the fiber cladding to serve as a flow channel for the mobile phase and analytes.

For the experiments in which both the mode-filtered light and the transmitted light were measured as a function of the light launch angle the following conditions were used. The setup for these experiments were the same as described above except that a second tee was used at the end of the fluorinated silicone clad fiber (Fiberguide Industries, Anhydroguide, Stirling, NJ) adjacent to the injection valve so that the fiber could be run through the tee leaving both ends of the fiber exposed and thus allowing the transmitted light to be collected with a photodiode. In this case the injector was then also connected to this additional tee with a short piece of 0.005" ID PEEK tubing.

For all experiments, the exposed end of the optical fiber was cleaved to obtain a flat end, and fit into a fiber chuck (Newport, 460 XYZ, Fountain Valley, CA). This allowed the end of the fiber to be aligned with the 5 mW HeNe laser light source (Uniphase 105-1, Manteca CA) operating with continuous wave output at 632.8 nm, thus defining the launch angle. A positioning stage (Newport, 460 XYZ, Fountain Valley, CA) allowed alignment of the fiber and chuck such that the angle between the fiber optic and the laser, θ_0, was readily selected with 0.19 radians used for much of the liquid phase work. The mode-filtered light signal could be detected at any point along

the annular column by simply moving the detector along the length of the annular column between the injector and tee. The detector was a photomultiplier tube (PMT) (Hamamatsu, 1P28, Bridgewater NJ) fit with a black delrin box built to align the annular column with the PMT. A hole drilled through the delrin box parallel to the face of the PMT maintained the distance between the annular column and the face of the PMT housing at 1.25 cm. This box prevented stray light from entering the PMT and allowed light from a small region of the annular column to be sampled through a 3.2 mm diameter aperture. A power supply (Thorn EMI Gencom, 3000R, Fairfield, NJ) operating the PMT at 700 V typically produced a background photocurrent of 580 nA. It was determined that under these conditions the source of the limiting noise was due to intensity fluctuation of the laser.

In experiments in which the annular column was used as a simultaneous column and detector, various binary methanol and water mobile phases, were delivered with a microbore pump (either ISCO, μLC-500 Lincoln NE, or Beckman, 114M, Berkeley CA). Photocurrents from the PMT were converted to voltages with a picoammeter (Keithley, 485, Cleveland OH). The output from the picoammeter was connected either to a chart recorder or a personal computer equipped with an analog to digital converter (IBM, DACA, Boca Raton FL). Chromatograms that were collected on the computer were baseline corrected, boxcar averaged and smoothed with a 10 point algorithm. All software for data collection and processing was written in house. Commercially obtained reagent grade chemicals were used without purification.

2.4 Results and Discussion

2.4.1 Signal as a Function of Launch Angle

When evaluating the mode-filtered light detector, the parameters that effect the sensitivity must be investigated. Since the mode filtered light detector is to be used as chemical sensor, we are interested in how the sensitivity of the mode filtered light

detector is dependent upon the properties of the chemical to be sensed, i.e., the analyte. We are also interested in parameters which dictate the signal-to-noise ratio achievable for a given amount of chemical sensitivity. For example, the angle at which light is launched into the fiber optic is an important parameter and should be optimized to provide the best signal-to-noise ratio.

Figure 2.5 shows how the transmitted light, I_T, and mode-filtered light, I_F, vary with the angle of incidence. Actually, ϕI_F is shown, rather than I_F. Each data point on the x-axis represents a different launch angle condition with a beam spread of about 5 degrees. As one would expect, the intensity of the transmitted light decreases as the incident angle is increased. The intensity of the mode-filtered light is fairly constant, and very small, for launch angles between 0 and 27 degrees (0.47 radians), where 27 degrees corresponds to the launch angle resulting in the critical angle condition at the core/clad interface. The mode-filtered light background in this region can be ascribed to the scattering of mode stable light from the core of the fiber. As the incident launch angle is increased in the region near and beyond the critical angle condition, the intensity of mode-filtered light increases sharply, reaching a maximum near 27 degrees. Beyond the launch angle resulting in the critical angle condition, stable modes of propagation exist as skew modes which account for the transmitted light at angles beyond the critical angle condition. The mode-filtered light produces a positive, but decreasingly small signal beyond the critical angle condition as the skew modes are filtered out. The third feature in Figure 2.5, labeled as ΔI_F, is the change in the amount of mode-filtered light due to an analyte partitioning into the cladding which we refer to as the net analyte signal. The net analyte signal was obtained by injecting a small volume of analyte, in this case chlorobenzene, into the liquid phase annular column analyzer, and monitoring the intensity of mode-filtered light. The net analyte signal was

Figure 2.5 Data illustrating how the relative intensities of transmitted light, I_T, the intensity of the mode-filtered light, I_F, and the intensity of the mode-filtered light net analyte signal (chlorobenzene), ΔI_F, varies with launch angle. Magnitude of the transmitted intensity has been reduced in order to compare with the direct mode-filtered light intensities.

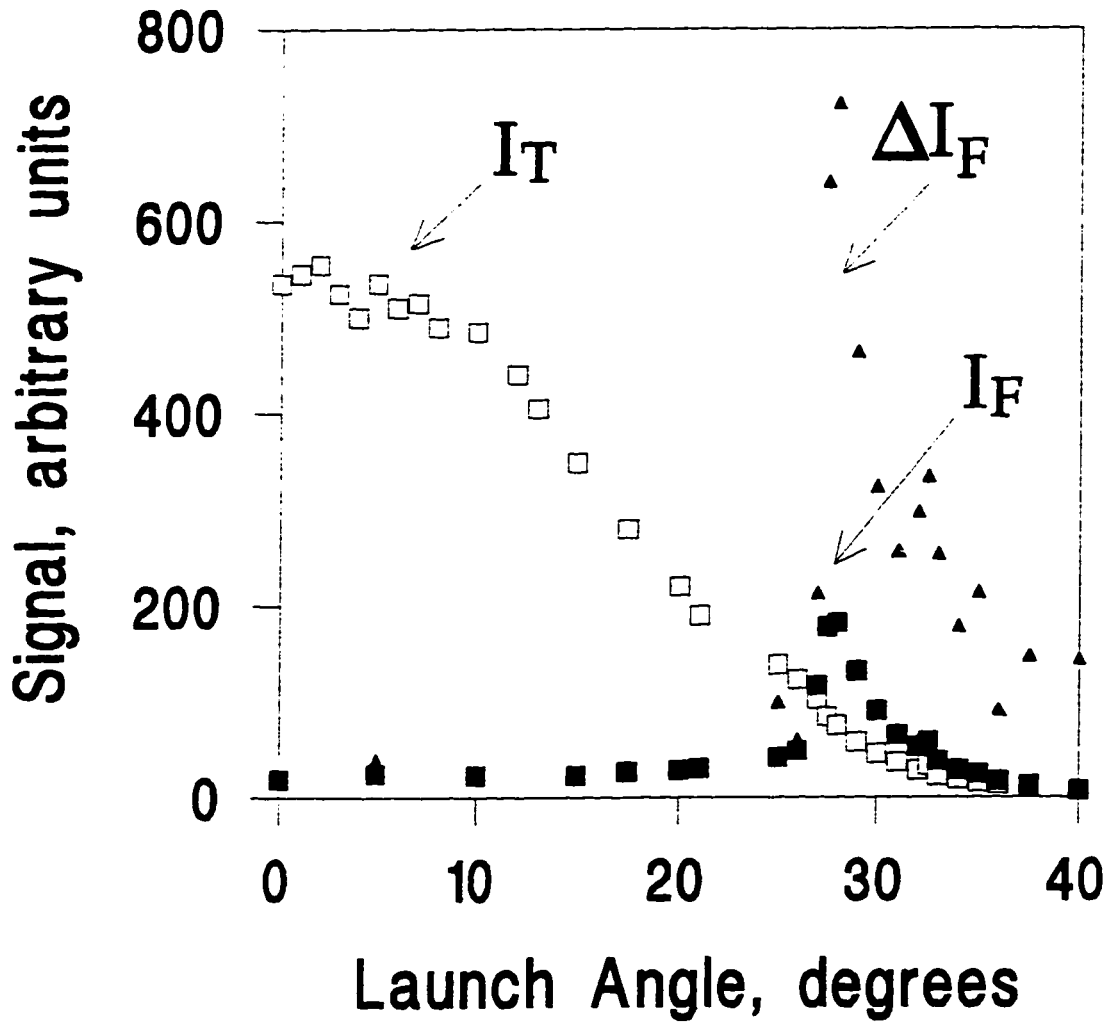
800
600
400
200
0
Signal, arbitrary units
I_T
ΔI_F
I_F
0
10
20
30
40
Launch Angle, degrees

taken as the maximum signal due to the partitioning analyte minus the background signal without the analyte. Note that the net analyte signal is much larger than the background signal which allows the measurement of the net analyte signal to be made with less noise than would be expected from the traditional, transmission method. Figure 2.6(A) shows the S/N ratio measured for the same chlorobenzene data. The S/N ratio was found to increase linearly beyond the critical angle condition. As described in the theory section, the signal due to mode-filtered light is created by a change in the critical angle by the partitioning analyte. The ratio of ΔI_F to I_T, which is plotted in Figure 2.6(B), will provide some insight into the launch angle condition required to observe a sensitive mode-filtered light signal. This ratio effectively normalizes the analyte signal data with respect to the diminishing available light level as a function of increasing launch angle. As one can see in Figure 2.6(B), the true sensitivity for the mode-filtered light measurement is nearly a step change from about zero sensitivity to a considerable level of sensitivity at the launch angle due to the resulting critical angle condition.

2.4.2 Signal as a Function of Injected Analyte Concentration

The signal, according to eq 15, is expected to depend upon the injected concentration, the refractive index of the analyte and the degree that the analyte partitions into the cladding. These dependencies were examined to substantiate our understanding of the detection mechanism.

It is necessary to determine if the detector responds linearly to concentration. Using the analyzer described in Figure 2.4, the signal relative to the baseline was measured for injections of samples with increasing concentration of toluene in the mobile phase. A representative signal for a toluene sample is shown in Figure 2.7 (A). A nearly linear relationship between the injected concentration and the signal (peak height relative to baseline) was observed for toluene samples as shown in Figure 2.7(B). The slight non-linearity may be attributed to the non-linearity of the mode-

Figure 2.6(A) Signal to noise as a function of launch angle for the mode-filtered light analyzer, resulting from the same data set as in Figure 2.5. The signal was defined as the peak height produced by a 0.2 μL injection of chlorobenzene into an 80:20 methanol/water mobile phase flowing at 3 μL/min, while the noise was defined as the RMS noise of the baseline measured with the flow of mobile phase but in the absence of analyte. **2.6(B)** True sensitivity of the mode-filtered light measurement as a function of launch angle, calculated as the ratio of $\phi\Delta I_F$ to I_T. Notice that the sensitivity appears as a step change near the launch angle corresponding to the critical angle matching condition.

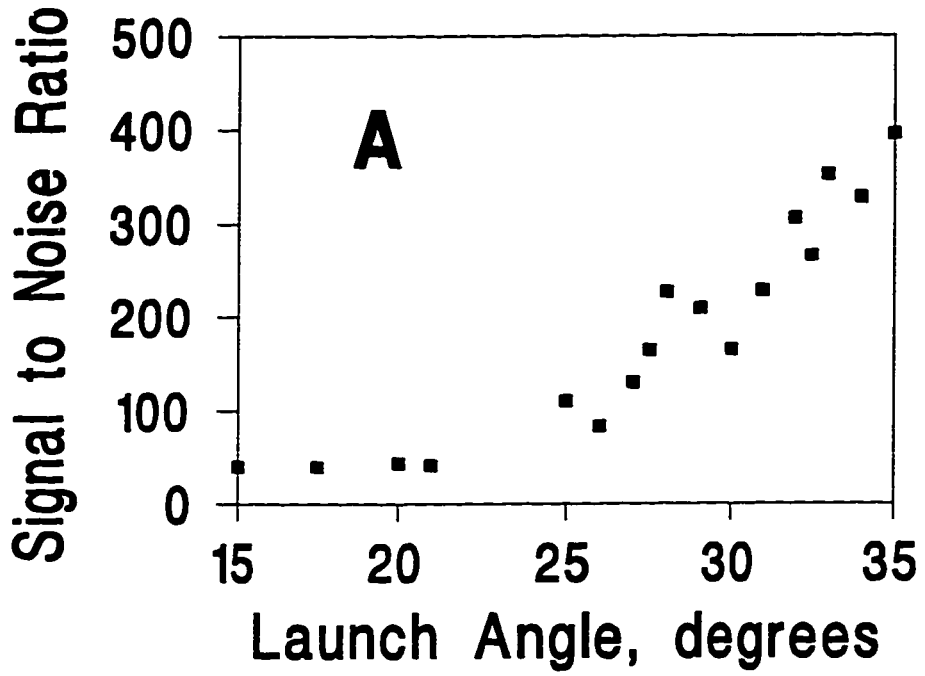
Signal to Noise Ratio
500
400
300
200
100
0
A
15
20
25
30
35
Launch Angle, degrees

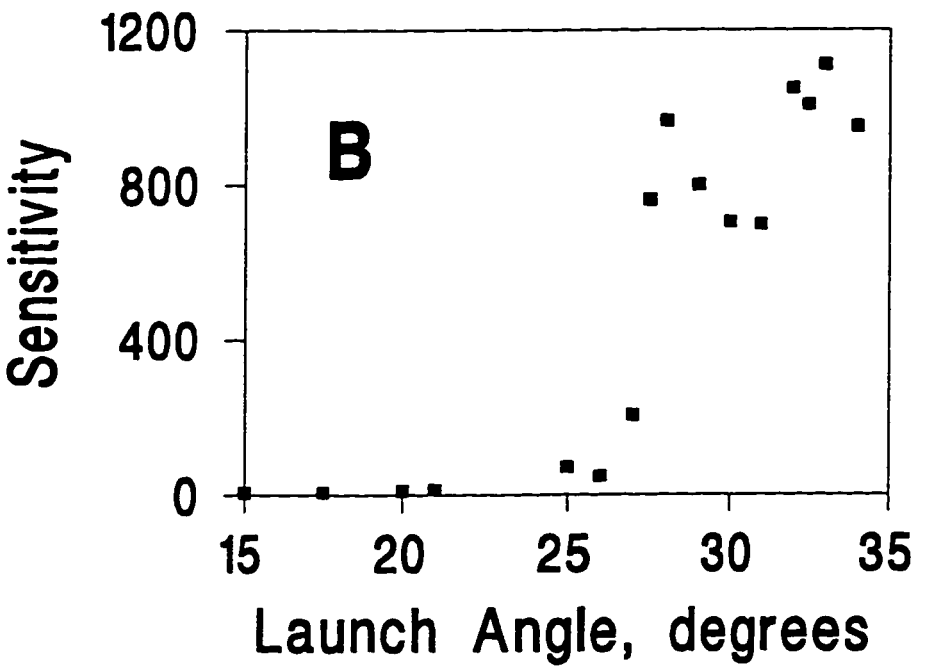
Sensitivity
1200
800
400
0
B
15
20
25
30
35
Launch Angle, degrees

Figure 2.7(A) Mode-filtered light signal for a 25 μL sample of 0.4 % (by volume) toluene in 70 % methanol to 30 % water (by volume) mobile phase, at 20 μL/min. Precision for 3 trials was 2.5 % relative standard deviation in peak height. **2.7(B)** Calibration curve for toluene obtained under these conditions.

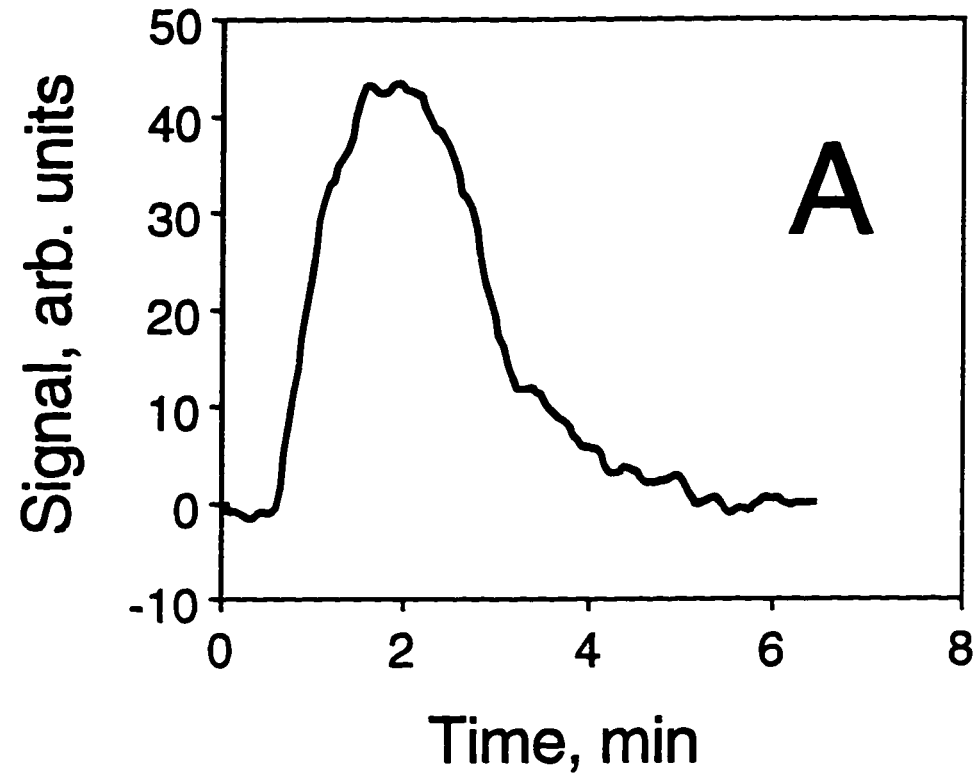
Signal, arb. units
50
40
30
20
10
0
-10
0
2
4
6
8
Time, min
A

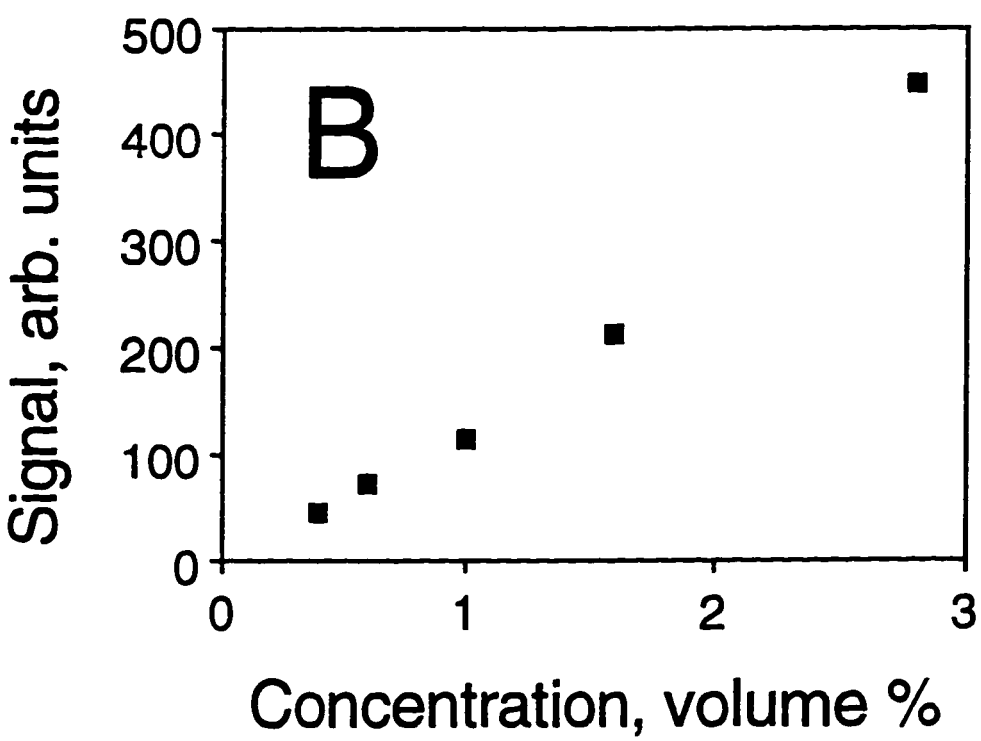
Signal, arb. units
500
400
300
200
100
0
0
1
2
3
Concentration, volume %
B

filtered light signal as a function of $\Delta\theta_2$, as shown in Figure 2.3(B). The near linear response in Figure 2.7(B) suggests that the signals can be corrected for concentration changes in order to determine the dependencies on analyte RI and the distribution coefficient. The linear dependence is more evident at low concentration, near the detection limit. Thus, to a good approximation, the signal $S(\Delta\theta_C)$ in eq 16 is linear with $\Delta\theta_C$ defined in eq 15.

2.4.3 Signal as a Function of Mobile Phase Composition

By increasing the fraction of water in the mobile phase, one might expect the analytes to partition more into the cladding, thus increasing the detection sensitivity. Equations 13-16 predict the signal dependence on the distribution coefficient. It was necessary to test eq 15 by measuring the change in sensitivity with changing distribution coefficient. Sensitivity is defined as the ratio of $S(\Delta\theta_C)$ to $C_{v,m}$, as defined in eqs 15 and 16. The K_d, and thus the sensitivity, for an analyte can be changed by changing the mobile phase composition. It is well known that for an analyte partitioning between a relatively non-polar stationary phase, and binary mobile phase of methanol and water, at a fixed phase volume ratio V_m/V_c as defined in eq 14, that

$$\log K_d = mW + b \quad \alpha \quad \log(\text{Sensitivity}) \tag{17}$$

where W is the % water by volume in the mobile phase, with m dependent upon the relative polarities of the two phases and the analyte. The sensitivities of a few representative analytes were measured at different % water compositions, W, with sensitivity in arbitrary units. Note that the RI differences of the analytes will be incorporated into the b-term in eq 17, which does not affect the slope information we seek. Figure 2.8 shows that log(Sensitivity) increases linearly with W as described by eq 17. Conditions applied to obtain the data shown in Figure 2.8 included a large injection volume, to eliminate hydrodynamic dilution effects that may be capacity factor

Figure 2.8 Log(Sensitivity) as a function of % water in methanol (by volume), as defined in eq 17, for three analytes measured with a 200 μL injection loop to ensure the analyte had equilibrated between the cladding stationary phase and the mobile phase solvent: Bb - butylbenzene; Tol - toluene; Bp - butyrophenone. Note that all of these analytes have roughly the same RI, so the differences in sensitivity are attributable to the differences in partitioning into the cladding.

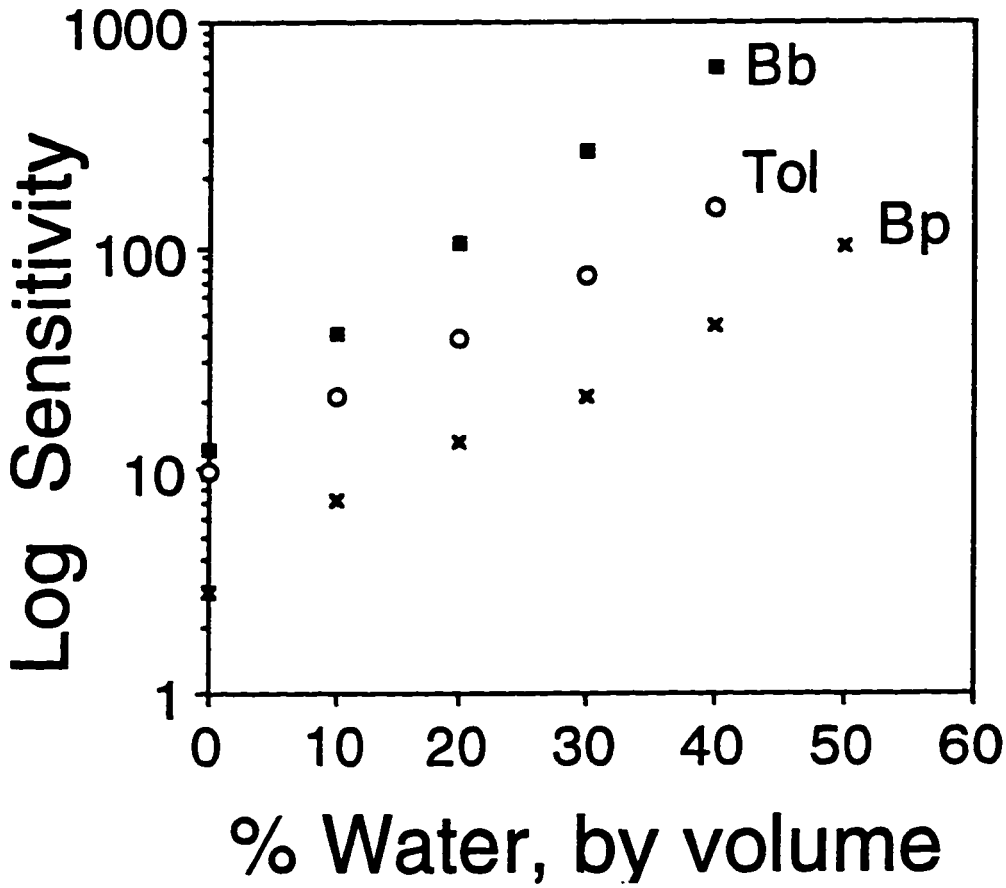
1000
100
10
1
Log Sensitivity
Bb
Tol
Bp
0
10
20
30
40
50
60
% Water, by volume

dependent, and low sample concentration to allow the linear approximation between signal and concentration as observed in Figure 2.7(B). Thus, in all injections the concentration in the mobile phase at the detector is the same as the injected concentration. Upon consideration of the linearity of Figure 2.8 and eqs 15-17, it may be inferred that the sensitivity depends linearly with the distribution coefficient, and the capacity factor as well.

Figure 2.8 also indicates that the detector is more sensitive to non-polar analytes. Butylbenzene is substantially more sensitive than butyrophenone, since butylbenzene structurally differs from butyrophenone by the absence of a polar carbonyl group. This suggests the present form of the mode-filtered light detector may be useful to selectively detect non-polar analytes in the presence of polar species. The limit of detection (LOD) is reasonable for many applications, as well. From Figure 2.7(A), a LOD of 200 parts-per-million (ppm) was obtained for toluene. Based upon the data in Figure 2.8 for butylbenzene and toluene, a LOD of about 20 ppm is achieved for butylbenzene at 60 % methanol to 40 % water, by volume. The detector may find application as a selective detector following microbore LC.

2.4.4 Signal as a Function of Analyte Refractive Index

Next, it was interesting to test eq 15 with respect to the dependence of the signal on the refractive index of the analyte. For this study the annular column was used as a chromatographic device by injecting the sample directly on the column and measuring the retention time, chromatographic dilution, and signal height. The analyte sensitivity was corrected for changes in capacity factor, as well as for the different concentration at the detector in the mobile phase, $C_{v,m}$. The corrected sensitivity is obtained from combining eqs 15, and 16,

$$S(\Delta\theta_C)/k'C_{v,m} = m'(n - n_2) \qquad (18)$$

where m' is the slope of the data set. The data presented were obtained in the following manner. Analytes with different RI were injected at concentrations necessary to produce signals of nearly the same magnitude, to ensure the linear approximation as in Figures 2.3(B) and 2.7(B). The analytes were injected directly into the detector and allowed to migrate along 5 cm of the annular column before being detected. Figure 2.9 shows the chromatographic signal of three representative analytes, octane, trichloroethlyene, and cyclohexane, that were determined in this fashion. This allowed measurement of a retention time on the annular column, based upon the time corresponding the center of mass of the detected peak. From the measured retention times, the capacity factor of the analytes were calculated. Figure 2.10 shows that there is a near linear relationship between analyte RI, n, and the corrected sensitivity defined in eq 18. It was assumed that the RI at 633 nm is essentially the same as the RI at the sodium-D line, which were used in Figure 2.10. Based upon the results in Figure 2.10, it is likely that the primary RI change in the fiber is due to the presence of the partitioned analyte in the fiber cladding, and that swelling of the cladding does not contribute significantly to the observed signal. Octane was the most strongly retained of all the analytes tested as indicated by the large capacity factor of 27. A small, negative signal for octane was observed, since the octane RI was slightly below the cladding RI and due to the high relative retention, resulting in a wide peak. Although it is likely that the octane was partitioned into the cladding enough to cause swelling, the adjusted sensitivity of the octane signal fits on the line in Figure 2.10 and suggests a secondary signal mechanism due to swelling of the cladding is insignificant.

The RI of the analyte where the corrected sensitivity is zero, as defined by eq 18 and shown in Figure 2.10, is 1.40. The intercept corresponds with the RI of the cladding. This experimentally obtained cladding RI is consistent with a reduced cladding RI due to methanol partitioning that increases the effective fiber NA. There must be a difference between the analyte RI and the cladding RI in order to see a signal. This provides an additional selectivity advantage which is separate from the

Figure 2.9 Transient signal of the annular column with mode-filtered light detection, for the analyzer shown in Figure 2.4 with a 0.5 mL sample volume for three analytes of varying RI and k', with the baselines offset for clarity: O - octane (1 % concentration by volume at peak max); T - trichloroethlyene (2 %); C - cyclohexane (0.7 %). Note that the back pressure is essentially zero for these measurements, in 20 % water to 80 % methanol by volume at 4 μL/min.

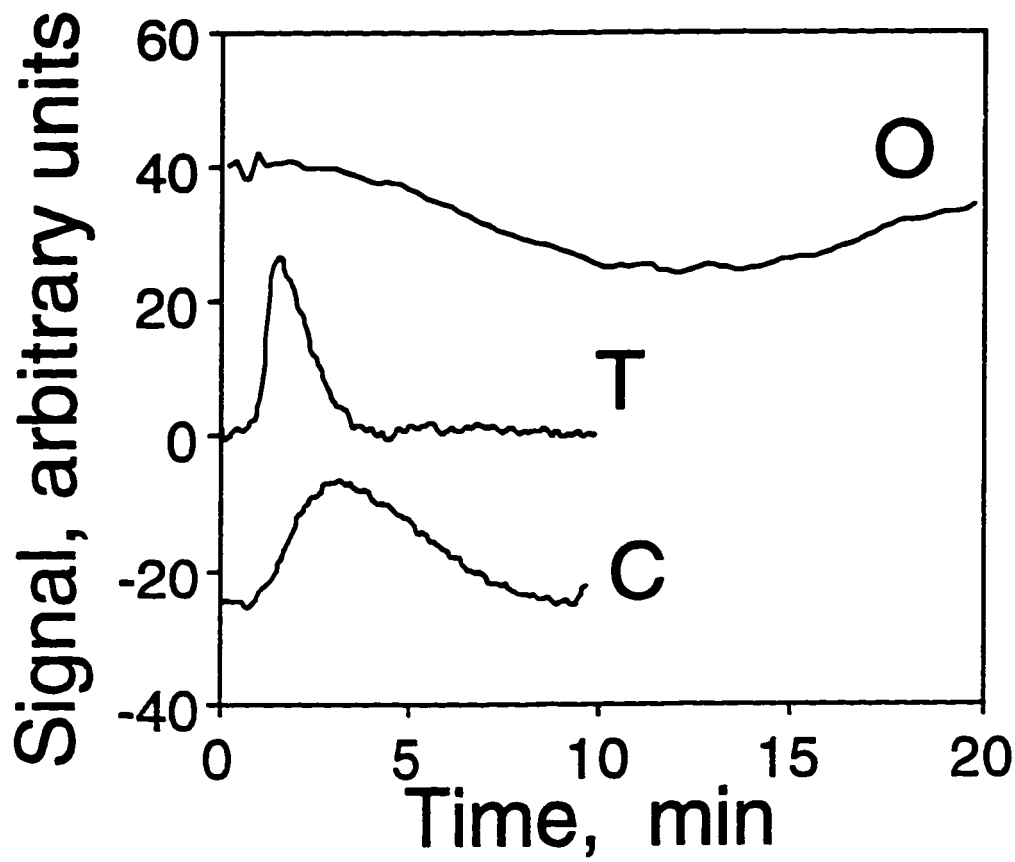
Signal, arbitrary units
60
40
20
0
-20
-40
0
5
10
15
20
Time, min
O
T
C

Figure 2.10(A, top) Capacity factor, k', as a function of analyte RI, determined from experimental data as shown in Figure 2.7(A): a, pentane; b, heptane; c, octane; d, cyclohexane; e, trichloroethylene; f, butybenzene. **(B, middle)** Sensitivity, as a function of analyte RI, for analytes and data in (A). **(C, bottom)** Normalized sensitivity, as defined in eq 18, as a function of analyte RI, for analytes and data in (A) and (B). The relative standard deviation in normalized sensitivity is typically 6%.

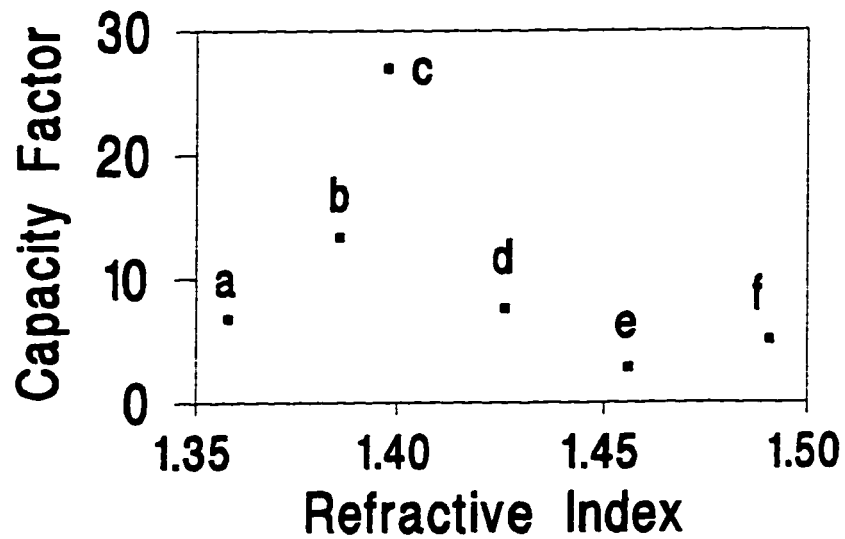
Capacity Factor
30
20
10
0
a
b
c
d
e
f
1.35
1.40
1.45
1.50
Refractive Index

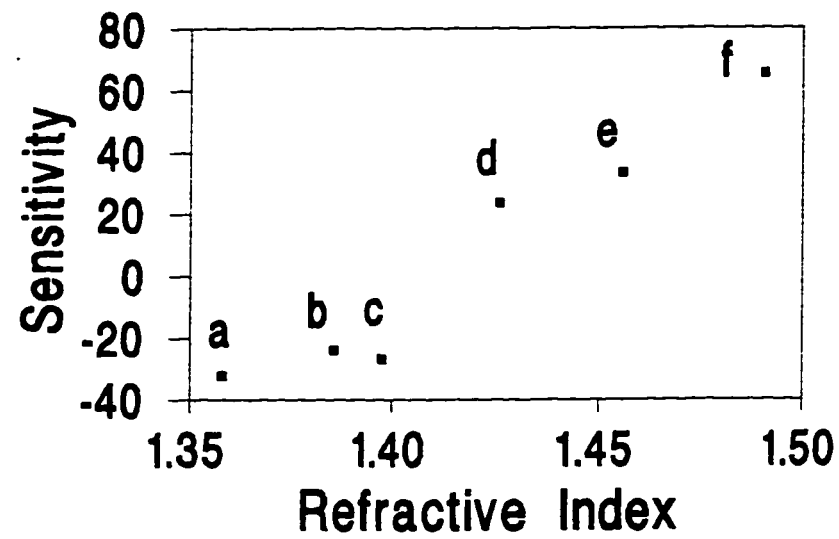
Sensitivity
80
60
40
20
0
-20
-40
a
b
c
d
e
f
1.35
1.40
1.45
1.50
Refractive Index

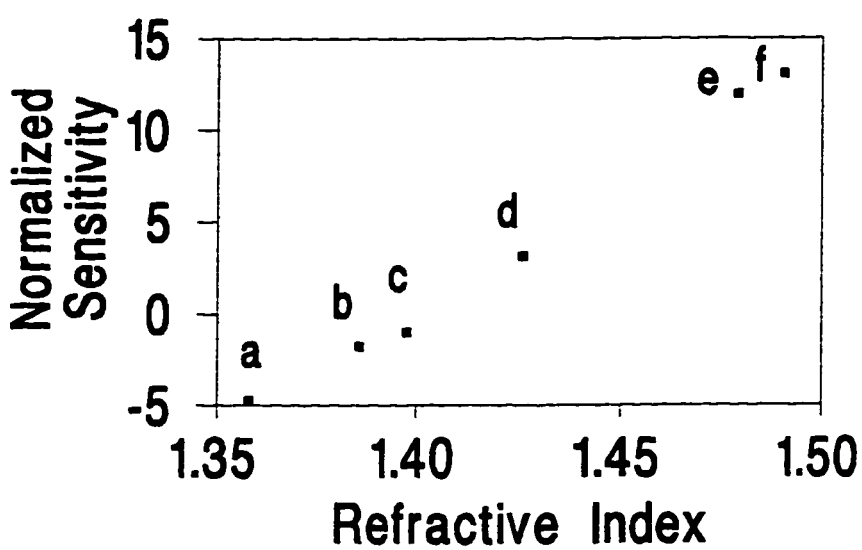
Normalized Sensitivity
15
10
5
0
-5
a
b
c
d
e
f
1.35
1.40
1.45
1.50
Refractive Index

selectivity achieved by differences in the distribution coefficient. Analytes with RI's equal to the cladding RI are not detected. This allows the creation of a detection scheme in which certain species are selectively tuned out by carefully selecting the cladding RI to match the RI of the interfering species.

2.4.5 On-line Preconcentration and Analysis of Trace Organics in Water

While the thickness of the stationary phase (cladding thickness of 12-15 μm range) limits the chromatographic efficiency of the annular column, the large capacity and stationary to mobile phase ratio of a relatively thick stationary phase would be desirable for an application in which the annular column were used essentially as a solid phase extraction device. There has been widespread interest in developing novel methods for sample preparation, i.e., the steps required to prepare a raw sample for analysis.[16-17] Sample preparation may be necessary to remove particulates, to separate the analyte from other components of the raw sample matrix, to preconcentrate the analyte or for a number of other reasons. The most common approach to sample preparation where the raw sample is a liquid is to find a solid adsorbent for which the analyte has a very large affinity and then allow the liquid sample sufficient contact with the solid adsorbent such that the analyte is quantitatively transferred to it. A well known example of this type of sample preparation is the use of solid phase extraction cartridges for the analysis of trace organics in water, for example. Recently, the utility of optical fibers for off-line solid phase extraction of organics from water for analysis by gas chromatography was reported.[16,17] While these methods[16,17] provide useful analytical results, they do still require that an analyst perform these steps which can be expensive and quite time consuming. We believe the annular column is well suited for continuous use as an on-line sample preparation device for process analysis or environmental compliance monitoring. Because the flow path is straight, the annular column should have relatively less resistance to flow than a packed column and should therefore be less prone to clogging.[10] The annular column should also be less likely to

clog, in general, than an open tubular column since for columns of each type, with a given diffusional distance, the annular column will have a larger cross sectional area of mobile phase. An interesting feature of the annular column is that analyte detection is done on-column, and can in some cases be done at any point along the column. Detection is best performed at the end of the column as illustrated in Figure 2.4. If detection is performed somewhere before the end of the column, previously detected analytes will continue to partition into the cladding downstream from the detector thus attenuating the incident beam available at the detector. This effect can be quite small if the total RI change within the cladding is reasonably low. One can imagine monitoring the accumulation of analytes on the annular column in real time and controlling the sampling process. In a sense, the annular column could be used as a smart sampling device which could detect when an appropriate amount of analyte had been accumulated, elute these analytes, and select appropriate heart cuts to be sent to the primary analyzer. Preliminary work towards this end has been accomplished. Some fundamental characteristics of the column were investigated with a flow rate study. Linear flow velocities from below 1 to above 100 mm/sec were used and a plot of plate height versus linear flow velocity was found to be linear throughout that range (not shown for brevity). A plot of peak area (as signal height times width in volume) versus linear flow velocity was constant up to a linear flow velocity of approximately 20 mm/sec (9 μL/min) at which point the plot deviated sharply from this flat region and peak shapes acquired a skewed appearance. We interpreted the velocity of 20 mm/sec to be the maximum flow rate for this system to avoid analyte breakthrough. Breakthrough occurs when the analyte in a flowing stream does not have a sufficient resident time to diffuse through the mobile phase and partition into the stationary phase. Avoiding breakthrough is one requirement to obtaining quantitative extraction of the analyte from the mobile phase. Of course another requirement is that the analyte have a much higher affinity for the stationary phase than for the mobile phase. To test the ability of the annular column to preconcentrate and detect a test analyte, a saturated solution of methylene chloride in water was prepared. Figure 2.11 shows the results

Figure 2.11. Transient signal for methylene chloride samples under various sample volume and concentration conditions, illustrating the preconcentration and "smart" sampling capability of the annular column detector design. The mobile phase is 20 % water to 80 % methanol by volume at 2 μL/min.

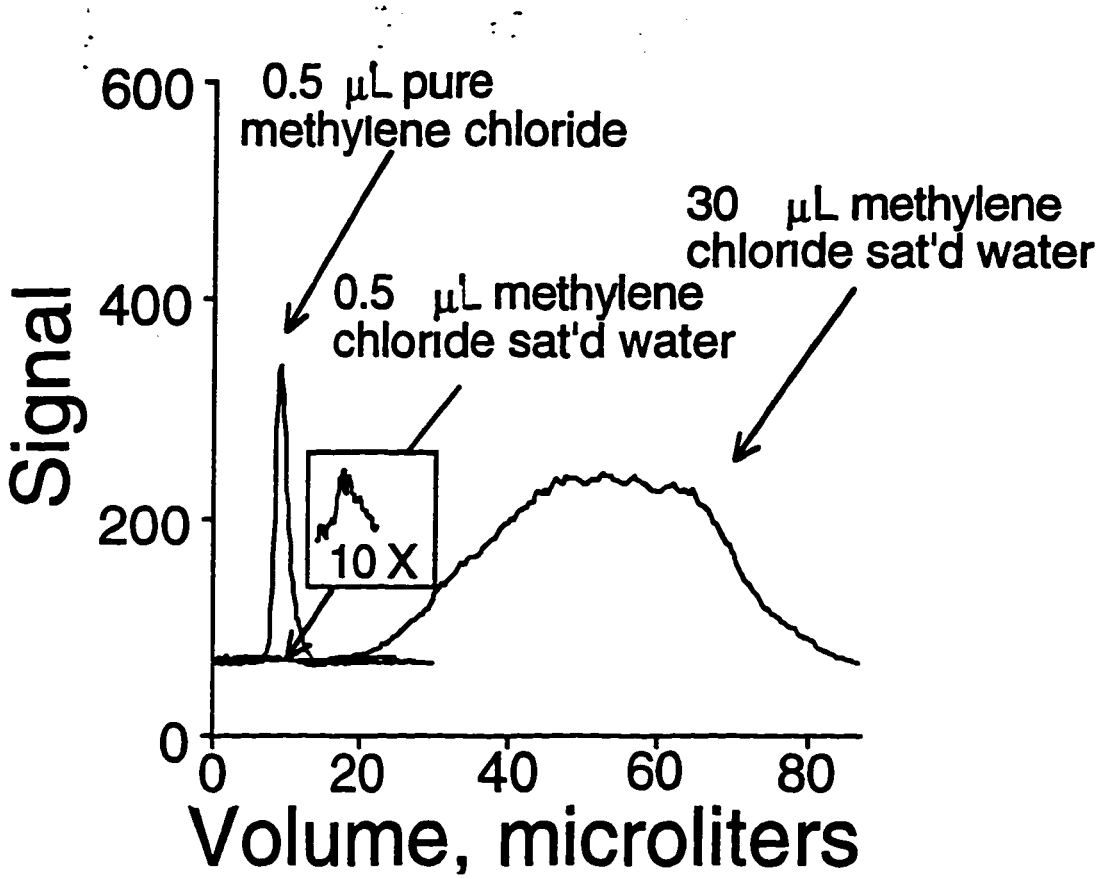
600
400
200
0
Signal
0.5 µL pure
methylene chloride
30 µL methylene
chloride sat'd water
0.5 µL methylene
chloride sat'd water
10 X
0
20
40
60
80
Volume, microliters

obtained for injection of 0.5 μL of pure methylene chloride, 30 μL of methylene chloride saturated water, and 0.5 μL of methylene chloride saturated water into an 80:20 methanol/water mobile phase. The solubility of methylene chloride in water is about 2 % at a temperature of 25 ^{0}C. One might first note that the much larger signal obtained from the 30 μL plug of methylene chloride saturated water as compared to the 0.5 μL plug of methylene chloride saturated water indicating that a considerable preconcentration of methylene chloride in the stationary phase was achieved. One can also note that the signal from the 30 μL plug of methylene chloride saturated water does not begin until well after the signals for the smaller injection sizes. The time lag for the larger plug is reasonable since the effective mobile phase for the larger sample is the sample itself which is a much weaker mobile phase than methanol/water. Consequently, as the sample passes through the column, it partitions into the cladding and continues to preconcentrate until the stronger mobile phase at the tail of the 30 μL plug begins to elute the sample.

2.5 Conclusions

Several improvements and applications for liquid phase analyses are envisioned. Thinner claddings will improve chromatographic performance, allowing the annular column to be used as a gas or liquid sensor that provides temporal information. Reducing cladding thickness while keeping the other annular column dimensions constant reduces the phase volume ratio. Thus, thinner claddings will allow one to operate at conditions resulting in a high distribution constant while keeping the capacity factor favorably low. The result will be substantially improved detection limits. One can predict detection limits improving by a factor of 100 by using a 1 μm clad instead of a 10 μm clad, so sub-ppm detection limits should be achieved in the future. If an analyte is in the presence of a large interferent that has a different RI than the analyte, the cladding RI can be matched to that of the interferent

so that the analyte will be selectively detected. Alternately, a short section of the annular column can be used as a detector only, in conjunction with microbore LC.

2.6 Notes to Chapter 2

1. Giuliani, J. F.; Jarvis, N. L. *J. Chem. Phys.* **1985**, 82, 1021-1024.
2. Giuliani, J. F.; Jarvis, N. L. *Sensors and Actuators* **1984**, 6, 107-112.
3. Kawahara, F. K.; Fiutem, R. A.; Silvus, H. S.; Newman, F. M.; Frazar, J. H. *Anal. Chim. Acta* **1983**, 151, 315-327.
4. Klainer, S. M.; Thomas, J. R.; Dandge, D. K.; Frank, C. A.; Butler, M. S.; Arman, H.; Goswami, K. *SPIE Environmental Sensing and Combustion Diagnostics* **1991**, Vol. 1434, pp. 119-126.
5. Marcus, M. A.; Hartog, A. H.; Purdum, C. F.; Leach, A. P. *SPIE Chemical, Biochemical, and Environmental Sensors* **1989**, Vol. 1172, pp. 194-201.
6. Carey, W. P.; DeGrandpre, M. D.; Jorgenson, B. J. *Anal. Chem.* **1989**, 61, 1674-1678.
7. DeGrandpre, M. D.; Burgess, L. W. *Anal. Chem.* **1988**, 60, 2582-2586.
8. DeGrandpre, M. D.; Burgess, L. W.; White P. L.; Goldman, D. S. *Anal. Chem.* **1990**, 62, 2012-2017.
9. Xi, X.; Yeung, E. S. *Anal. Chem.* **1990**, 62, 1580-1585.
10. *Chromatogr.*, **1983**, 255, 359-369.
12. Moore, L. K.; Synovec, R. E. *Anal. Chem.* **1993**, 65, 2663-2670.
13. Renn, C. N.; Synovec, R. E. *Anal. Chem.* **1991**, 63, 568-574.
14. Murugaiah, V.; Synovec, R. E. *Anal. Chem.* **1992**, 64, 2130-2137.
15. Synovec, R. E.; Bruckner, C. A.; Burgess, L. W.; Foster, M. D. *SPIE Chemical, Biochemical and Environmental Sensors;* SPIE: Bellingham, WA., 1994; Vol. 2293, pp167-177.
16. Arthur, C. ; Pawliszyn, J. *Anal Chem.* **1990**, 62, 2145-2148.
17. Buchholz, K. D.; Pawliszyn, J. *Anal. Chem.* **1994**, 66, 160-167.

Chapter 3

Development of the Annular Column Chemical Analyzer for Sensing of Trace Organics in Flowing Aqueous Streams

3.1 Introduction to Chapter 3

Fiber optics have provided a tremendous source of innovation and improvement in the field of analytical chemistry. Most often, fiber optics are extrinsic detection elements of common spectroscopic detection schemes where the fiber optic is used as a path to provide the spectroscopic information to the detector.[1-6] Fiber optic chemical sensors (FOCS) have also been developed. FOCS provide chemical information based on a number of different mechanisms for analyte interaction with the light source along the fiber optic pathway. A review of FOCS was recently reported in 1992.[7] One common way to use optical fibers as intrinsic sensors is to make a Michelson interferometer from an optical fiber so the change of optical path length in the optical fiber can be correlated to the resulting change in fringe pattern of the interfering light.[8] Evanescent field measurements with FOCS is also an effective way to utilize fiber optics as intrinsic sensors. Evanescent field measurements can be used for quantitation of a wide variety of analytes, as for example, dissolved chlorine.[9] Evanescent field measurements can even be used as a tool for studying interfaces using evanescent wave induced fluorescence.[10] Additionally, sensing based on surface plasmon resonance which can provide very sensitive refractive index responses.[11] Indicator chemistry in thin Sol-Gel coated fiber optic has also been used as a novel method of probing the evanescent field.[12] In recent reports,[13,14] fiber optics with polymer claddings were used for the purpose of solid phase microextraction of organics from aqueous solutions with direct injection into a GC, although the optical properties of the fiber optic were not exploited.

In Chapter 2 we discussed an intrinsic fiber optic chemical sensor that provides selective detection based upon an affinity for the polymeric coating of the fiber optic.

The detection mechanism is called mode filtered light detection (MFLD) and has been described in detail and theoretically developed and tested, regarding the refractive index (RI) and partitioning mechanisms both in Chapter 2 and in previous publications.[15,16] The sensor incorporates a bare glass core section of fiber optic which is coated with a polymeric film which has a refractive index lower than the glass core, allowing for propagation of light in the fiber. By inserting this fiber optic with an appropriate coating into a section of capillary tubing which is just larger than the outside diameter of the fiber optic, an annular column sensor is produced as illustrated in Figure 2.2 of Chapter 2. The annular gap allows a mobile phase to be introduced. The polymeric coating of the fiber optic can then serve as the cladding for the fiber optic as well as a chromatographic stationary phase for separation of species in the mobile phase. The term mode-filtered light refers to the observation that light initially propagating down an optical fiber, can be decoupled from that fiber by an increase in the cladding RI at the core/clad interface by a permeating analyte, thus changing the allowable propagating modes within the fiber resulting in a continuous and nearly linear increase in mode filtered light with increasing clad RI. Traditionally, mode-filtered light is measured as the change in the transmitted beam intensity.[17-20] The MFLD approach measures the mode-filtered light emanating from a small area at a right angle to the fiber primary axis[15,16] as described in Chapter 2. This new approach is analogous to the advantage in signal-to-noise ratio (S/N) one obtains in fluorescence detection relative to absorbance detection, that is, measuring essentially the same signal against a low background instead of a large background. Additionally, an annular column should perform favorably in terms of the chromatographic impedance function while easing constraints on the pump and sample injector. [21,22]

Chapter 3 is devoted to introducing an improved annular column chemical sensor which could be used with a pure water mobile phase and with much better detectability than prior efforts. The result of Chapter 2 showed a linear increase in sensitivity with distribution constant which resulted in a exponential increase in sensitivity for a given analyte as the percentage of water in the mostly methanol mobile phase was increased.

However, increasing the water content also caused broadening of peaks so that the detectability in terms of the injected concentration, for a typical analyte such as toluene, did not improve with increasing water content beyond about 30 percent water in methanol. The results demonstrated in Chapter 3 will show that the detectability for this sensor is improved by decreasing the cladding thickness and thereby decreasing the phase volume ratio, i.e., the ratio of the volume of stationary phase to mobile phase. Peak broadening is proportional to the capacity factor, which is the product of the distribution constant and the phase volume ratio, so that a decrease in the phase volume ratio allows a proportional increase in distribution constant while keeping the capacity factor, and peak broadening, constant. Thus, detectability of an analyte, for a given stationary phase, can be increased by reducing the phase volume ratio by using a thinner cladding and increasing the distribution constant by using a weaker mobile phase while maintaining the same capacity factor and peak broadening. The data in Chapter 2 were obtained with a commercially available, 15 μm thick poly[oxy(dimethylsilylene)] (PDMS) clad fiber optic which produced a phase volume ratio of 0.35 in the annular column. Here, is reported work with about a custom made 0.1 micron cladding on a bare glass core fiber, which should be about the thinnest layer that can guide a 633 nm He/Ne light source without a large increase in the background signal due to scattered light. The PDMS stationary phase was not used since extrapolations from previous results indicated that capacity factors and peak broadening would be larger than desired for target analytes such as toluene in a pure water mobile phase. The PDMS would have likely produced better detection limits in pure water, but at the cost of wider peaks and longer analysis times. By consideration of solubility parameter theory,[23-26] which relates capacity factor to phase volume ratio and the polarity of the stationary phase, mobile phase and analyte, a poly[oxy[methyl(3,3,3 trifluoropropyl)silylene]] (TFPS) cladding which is more commonly called trifluoropropyl polysiloxane should be a more appropriate choice. This particular material was chosen because it had a higher polarity as indicated by a solubility parameter value of 9.0 as compared to the PDMS value of 7.4.[27] The higher

solubility parameter for TFPS should lead to slightly lower retention for the most hydrophobic analytes. Thus, the TFPS has good qualities for the development of a liquid chromatographic sensor for the analysis of trace organics in pure water, which should eliminate the generation of hazardous waste.

In Chapter 3, a case will be made that decreasing the phase volume ratio allows the use of weaker solvents and a consequent increase in the distribution coefficient, thus resulting in improved detectability for the annular column sensor. Additionally, it will be shown that a decreased phase volume ratio coupled with a moderate polarity stationary phase allows reasonable capacity factors for hydrophobic analytes in a pure water mobile phase. A theory is developed which estimates the expected signal from the MFLD which takes into account the hydrodynamic dilution of an analyte band as it travels down the annular column, in terms of the capacity factor of the analyte and the linear flow velocity of the mobile phase. To model the broadening of the analyte zone, the expected behavior of the annular column is approximated as the behavior expected with flow through parallel open plates.[28] While this is an approximation, the experimental results are in fair agreement. The hydrodynamic aspects of the annular column sensor will be characterized in terms of the sensor response throughout a wide range of flow rates in order to establish applicability with reasonably short analysis times. The utility of the annular column chemical sensor is demonstrated by showing chromatographic sensing of aromatic and chlorinated hydrocarbons on the annular column, using water as the mobile phase, with excellent sensitivity and good chemical selectivity by MFLD. Additionally, distribution coefficients, as derived from the analyte signal after eliminating the RI dependence, correlated well to octanol/water partition coefficients for a wide range of analyte species. Analyte sensitivity can be predicted by this correlation. The dynamic range of the MFLD is evaluated over a wide range of mobile phase composition.

3.2 Theory

The theoretical mechanism of operation for MFLD has been discussed in detail in Chapter 2. In summary, with MFLD, the analyte signal is measured by a photodetector which detects light emerging perpendicular to the primary axis of the fiber. There is always some background signal due to scattered light from the fiber optic, but the net analyte signal is the change in the amount of light coupled out of the fiber and reaching the photodetector due to an analyte partitioning into the cladding and changing the refractive index of the cladding thus producing a localized change in the numerical aperture of the fiber. The expression derived which related the detected analyte signal relative to background condition as a function of the fiber optic properties, the beam intensity profile in the fiber optic, and the analyte properties such as refractive index (RI), concentration and analyte distribution coefficient (K_D) between the fiber cladding and the mobile phase solvent was shown to obey

$$\text{signal} = \frac{\alpha\, n_2 (n - n_2) K_D C_{v,m}}{n_1\, NA} \qquad (1)$$

where α is a proportionality constant relating the change in the critical angle of the fiber due to the partitioning analyte to the flux of light reaching the PMT, n_2 is the refractive index of the cladding, n_1 is the refractive index of the fiber core, n is the refractive index of the analyte, NA is the numerical aperture of the fiber optic in the absence of analyte, and $C_{v,m}$ is the volume fraction of the analyte in the mobile phase at the detector. Inspection of this equation reveals that detector sensitivity for a given configuration is primarily determined by two terms. The $(n-n_2)$ term predicts increasing sensitivity with increasing difference between RI of the analyte and cladding. This term is similar to the term which describes analyte selectivity for standard RI detectors except that the RI difference is relative to the stationary phase in MFLD, rather than the mobile phase as with standard RI detection. The K_D term is significant for chemical analysis because this predicts increased analyte sensitivity with increased affinity for the polymeric cladding. This term is interesting because it suggests that the MFLD method

is governed both by chemical selectivity and RI sensitivity. It is obvious that increased analyte affinity for the stationary phase will increase K_D and analyte sensitivity by MFLD. The distribution constant can be made quite large for hydrophobic analytes by increasing the water content of the mobile phase since the distribution coefficient increases exponentially with increasing water content of the mobile phase for hydrophobic analytes. However, an increase of the distribution coefficient also causes an increase in the capacity factor and increased retention which results in increased analysis times and consequent broadening and dilution of the analyte zone in the mobile phase. The capacity factor, k', is a common chromatographic term which serves as a measure of retention and is defined for a particular component as

$$k' = \frac{V_R - V_M}{V_M} \qquad (2)$$

where V_R is the retention volume of the component and V_M is the total volume of mobile phase in the annular column between injection and detection. The capacity factor is related to the distribution constant as

$$k' = \left(\frac{V_S}{V_M}\right) K_D \qquad (3)$$

where V_S/V_M is the ratio of the volume of stationary phase to mobile phase and k' is the capacity factor. Equation 1 predicts the signal for an analyte based upon the concentration of the analyte in the mobile phase at the detector, but does not account for dilution of the analyte zone due to band broadening prior to the detection volume. Using a Gaussian distribution as a reasonable model for the analyte zone, then the maximum concentration of the analyte zone in the mobile phase at the area of detection will be inversely proportional to the volume standard deviation of the of the analyte zone, σ_V

$$C_{V,m} = \frac{C_{inj} V_{inj}}{\sigma_V \sqrt{2\pi}} \qquad (4)$$

where C_{inj} is the injected concentration as a volume fraction and V_{inj} is the volume of sample injected. The dispersion of the analyte zone can be related to the chromatographic efficiency of the annular column sensor, H, which is given by

$$H = \frac{L\sigma_V^2}{V_M^2(1+k')^2} \qquad (5)$$

where L is the length of the annular column. Thus if H is known or can be predicted, it can be used to relate σ_V to k'. Since the annular gap formed between the fiber and the capillary is very small compared to the overall radius of the annular ring, the characteristics of flow through the annular column ought to be very similar to flow through two parallel plates. Golay derived an equation predicting H for flow between two parallel plates[28] which approximates the band broadening dependence for the annular column for the conditions used as

$$H = \frac{4UR^2(1+9k'+25.5k'^2)}{105D_m(1+k')^2} \qquad (6)$$

where U is the linear flow velocity, D_m is the analyte diffusional coefficient in the mobile phase and R is one half of the distance across the annular gap. Equation 1 can be manipulated with respect to eqs 2 through 6 to predict the signal as a function of the capacity factor of the analyte, refractive index of the analyte, injected volume and concentration of analyte and the mobile phase linear flow velocity

$$\text{Signal} = \frac{\alpha' (n-n_2) C_{inj} V_{inj} k'}{\sqrt{U(1+9k'+25.5k'^2)}} \qquad (7)$$

where the constant, α', includes a number of terms which remain constant for a given sensor configuration and analyte,

$$\alpha' = \frac{\alpha n_2 \sqrt{105 L D_m}}{n_1 NA V_S R\sqrt{8\pi}} \qquad (8)$$

Equation 7 predicts a signal which is proportional to the injected volume and concentration of analyte and inversely proportional to the square root of the linear flow velocity of the mobile phase. The signal dependence on capacity factor can be seen by

plotting the expected signal, normalized to a value of 1 for infinite capacity factor, versus capacity factor while keeping the other terms of eq 7 constant. This plot is shown in Figure 3.1. Note that there is a rapid increase in signal while k' is less than one and little increase beyond that point. The shape of the function of Figure 3.1 is due to two factors which are related to capacity factor. The signal increases linearly with capacity factor but the peak concentration decreases at the detector with increasing capacity factor due to increased hydrodynamic dilution. With all parameters other than capacity factor held constant, the relative signal as defined in eq 7 should be equal to the capacity factor divided by the peak width, W, of the analyte band at the detector

$$\text{signal} = \beta(k' / W) \qquad (9)$$

where β is a constant for a given analyte, and W is equal to four times σ_V. Also note that eq 1 predicts a linear increase in signal with distribution constant. What is desired for optimum performance is a device with a large distribution constant for the analyte but also a capacity factor near one. To achieve this goal one need only consider the relationship between the capacity factor and the distribution coefficient as indicated in eq 3. It follows that a decrease in stationary phase thickness results in a lower phase volume ratio so that the distribution constant, for hydrophobic analytes, can be increased by increasing the polarity of the mobile phase while maintaining a reasonable capacity factor.

3.3 Experimental

The thin clad fiber was prepared in the following manner. A short length of the cladding, as supplied by the manufacturer, was removed and replaced with TFPS. The original cladding was removed from the fiber (FT200URT, 3M, Westhaven CT) by burning it off with a flame leaving a 200 micron diameter glass core. The exposed glass core was then rinsed successively with methanol, acetone and water. The exposed glass surface was then soaked in 1 normal sodium hydroxide overnight to roughen the surface and promote adhesion by the stationary phase. A 10% solution of the TFPS (OV 215, Supelco, Bellefonte PA) in ethyl acetate was then placed into a glass tube of sufficient length and diameter to hold the length of fiber to be coated. Coating of the

Figure 3.1 The predicted relative peak signal for an analyte on the annular column chemical sensor as a function of the capacity factor of the analyte. The plot illustrates that signal increases with capacity factor, but that there is a concomitant increase in peak dilution due to band broadening which leads to less real gain in detectability above a capacity factor of about two, as predicted by equation 7.

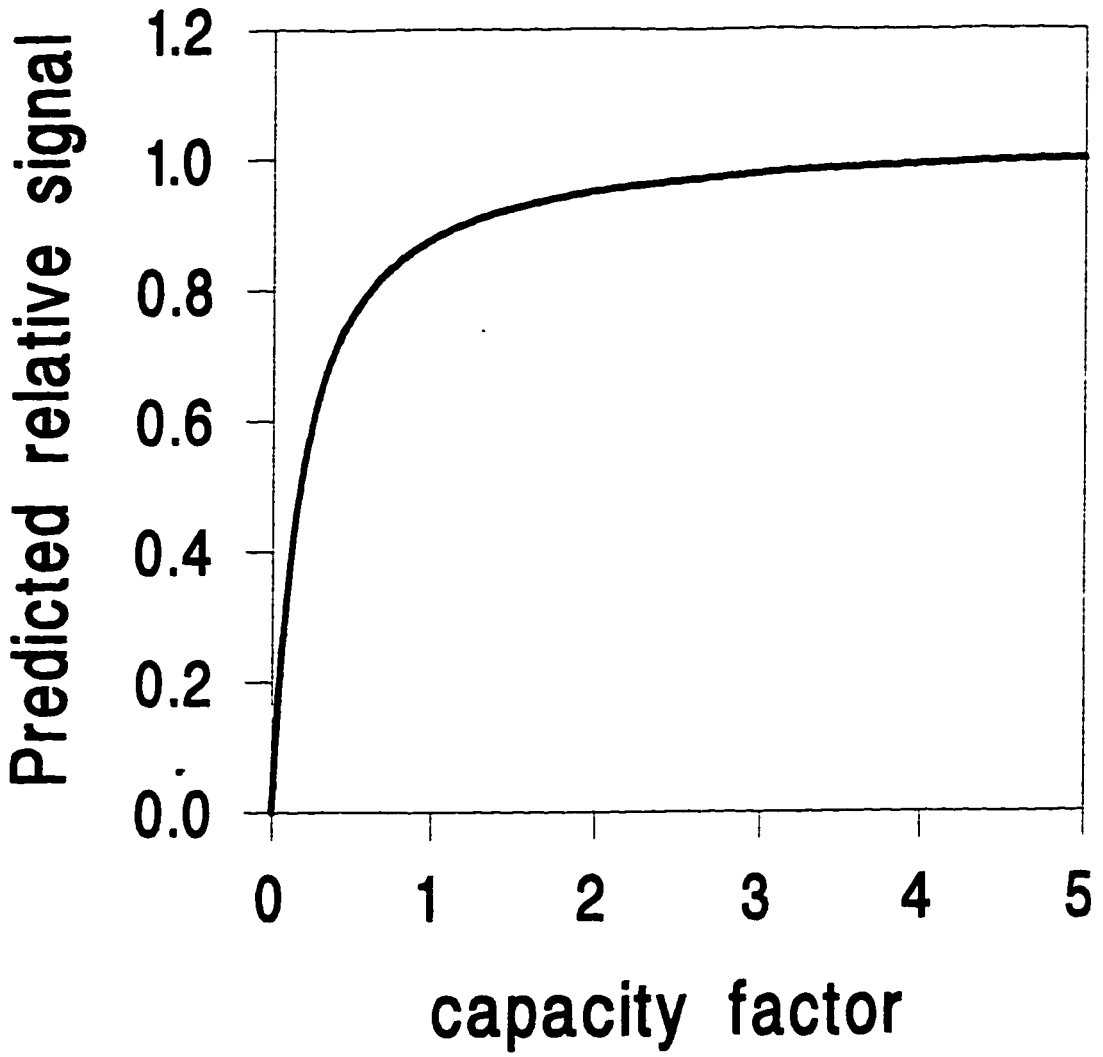
Predicted relative signal
1.2
1.0
0.8
0.6
0.4
0.2
0.0
0
1
2
3
4
5
capacity factor

fiber was accomplished by immersing the fiber into the solution and then withdrawing the fiber at a rate of 1.6 cm/sec which has been found to leave a film of approximately 0.1 μm in thickness.[29] This thickness resulted in a phase volume ratio of 3.6×10^{-3} after inserting the thin clad fiber as described below.

A cross-sectional view of the annular column is incorporated into a sensor, as shown in Figures 2.2 and 2.4 of Chapter 2, and as described below. The annular column was made by sliding each end of a 17 cm length of 250 micron ID fused silica capillary tubing (J&W Scientific, Folsom CA) into a one inch length of PEEK tubing (Alltech Associates, Deerfield IL) fit with a PEEK nut and ferrule. One end was then inserted into an 0.2 μL injection valve (Rheodyne 7520, Cotati, CA) and the other end into a tee connector (Alltech Associates, Deerfield IL). The thin clad optical fiber was then slid through the tee connector into the capillary until it butted up against the injection valve, then it was moved back out about 3 mm. To reduce friction and subsequent damage to the polymer cladding of the fiber, the capillary tube was first filled with methanol for the insertion process. A seal was made between the exposed end of the fiber and the tee connector with an additional one inch length of PEEK tubing fit with a nut and ferrule.

The exposed end of the optical fiber was cleaved to obtain a flat end, and fit into a fiber chuck (Newport, 460 XYZ, Fountain Valley, CA). This allowed the end of the fiber to be aligned with the He/Ne laser light source (Uniphase 105-1, Manteca CA) operating with continuous wave output at 632.8 nm. A positioning stage (Newport, 460 XYZ, Fountain Valley, CA) allowed alignment of the fiber and chuck such that the angle between the fiber optic and the laser was readily selected, with 0.19 radians used for most of the work. A photomultiplier tube (PMT) (Hamamatsu, 1P28, Bridgewater NJ) was fit with a black delrin box built to align the annular column with the PMT was used for detection of light from the annular column. A hole drilled through the delrin box parallel to the face of the PMT maintained the distance between the annular column and the face of the PMT housing at 1.25 cm. This box prevented stray light from entering the PMT and allowed light from a small region of the annular column to be sampled through a 3.2 mm diameter aperture. The effective detection volume was taken to be the mobile

phase contained within that 3.2 mm section of column which was calculated to be 17 nL. The mode-filtered light signal could be detected at any point along the annular column by simply moving the PMT along the length of the annular column between the injector and tee. For the work described here the detector was positioned 11 cm away from the injection valve so that the total mobile phase volume between injection and detection was approximately two microliters. A power supply (Thorn EMI Gencom, 3000R, Fairfield, NJ) operating the PMT at 700 V typically produced a background photocurrent of 580 nA. The background photocurrent and analyte sensitivity remained essentially constant from day to day suggesting that the fiber maintained a constant distance from the capillary wall, although, not necessarily centered. It was determined that under these conditions the limiting source of the noise was intensity fluctuations of the laser as observed by a PMT perpendicular to the main fiber axis.

Various binary methanol and water mobile phases, were delivered with a syringe pump (ISCO, μLC-500 Lincoln NE). Photocurrents from the PMT were converted to voltages with a picoammeter (Keithley, 485, Cleveland OH). The output from the picoammeter was connected to a personal computer equipped with an analog to digital converter (IBM, DACA, Boca Raton FL). Collected datapoints were baseline corrected, boxcar averaged and smoothed with a 10 point algorithm, except data used for calculation of detection limits which was not smoothed. All software for data collection and processing was written in house. Commercially obtained reagent grade chemicals were used without purification.

3.4 Results and Discussion

3.4.1 Analyte Capacity Factor and the MFLD Signal

Figure 3.2 shows a typical response produced by the annular column sensor after injection of a 200 nL sample plug containing 2 μg of toluene into a flowing, pure water mobile phase. Slight tailing was observed as a function of linear flow velocity, as will be

described in more detail later along with Figures 3.5, 3.6, and 3.7 and as described in the theory section. To illustrate the dependence of analyte sensitivity on mobile phase composition, data as shown in Figure 3.2 were collected for both toluene and cumene in mobile phases which were composed of varying percentages of methanol and water by volume. Figure 3.3 shows a plot of the logarithm of the analyte sensitivity versus percent water in the mobile phase for the analytes toluene and cumene, where sensitivity is taken to be the peak maximum signal-to-noise ratio, divided by the concentration of the analyte at the detector for the transient signal produced in the annular column chemical sensor. Figure 3.3 demonstrates an exponential increase in signal-to-noise as the capacity factor rises exponentially with increasing percentage of water in the mobile phase. Note that, in Figure 3.3, dilution of the analyte does not effect the sensitivity because the sensitivity is calculated from the concentration at the detector. Figure 3.4 shows the signal-to-noise divided by the injected concentration (net sensitivity) for cumene as a normalized least squares fit to the signal predicted by eq 7 and illustrated in Figure 3.1. Though an approximation was made in developing eq 7, the net sensitivity data shows qualitative agreement with the signal predicted by eq 7 by showing a linear increase in the relative signal with increasing capacity factor for small capacity factors with a leveling off at capacity factors greater than one. Also, the normalized least squares fit of the measured capacity factor divided by the measured peak width for cumene at the detector as a function of the capacity factor is shown. As predicted by eq 9, the capacity factor divided by peak width should be proportional to the predicted relative signal, and after normalization, the two are in excellent agreement as seen in Figure 3.4. The toluene data shown in Figure 3.3 is not included in Figure 3.4 because the capacity factor for most of the toluene data were too small to be accurately measured. One should also note that the detector monitored approximately 3.2 mm of the annular column after elution across 110 mm of annular column. MFLD could be adapted to provide small volume detection with very little peak dilution by simply using a much shorter length of annular column. We have shown that decreasing the stationary phase thickness provides a decreased phase volume ratio and consequent

Figure 3.2 Annular column sensor response to a small sample volume of toluene in water. Conditions: Mobile phase is pure water. Flow rate is 1.0 μL/min. A 200 nL sample containing 2 μg of toluene was injected.

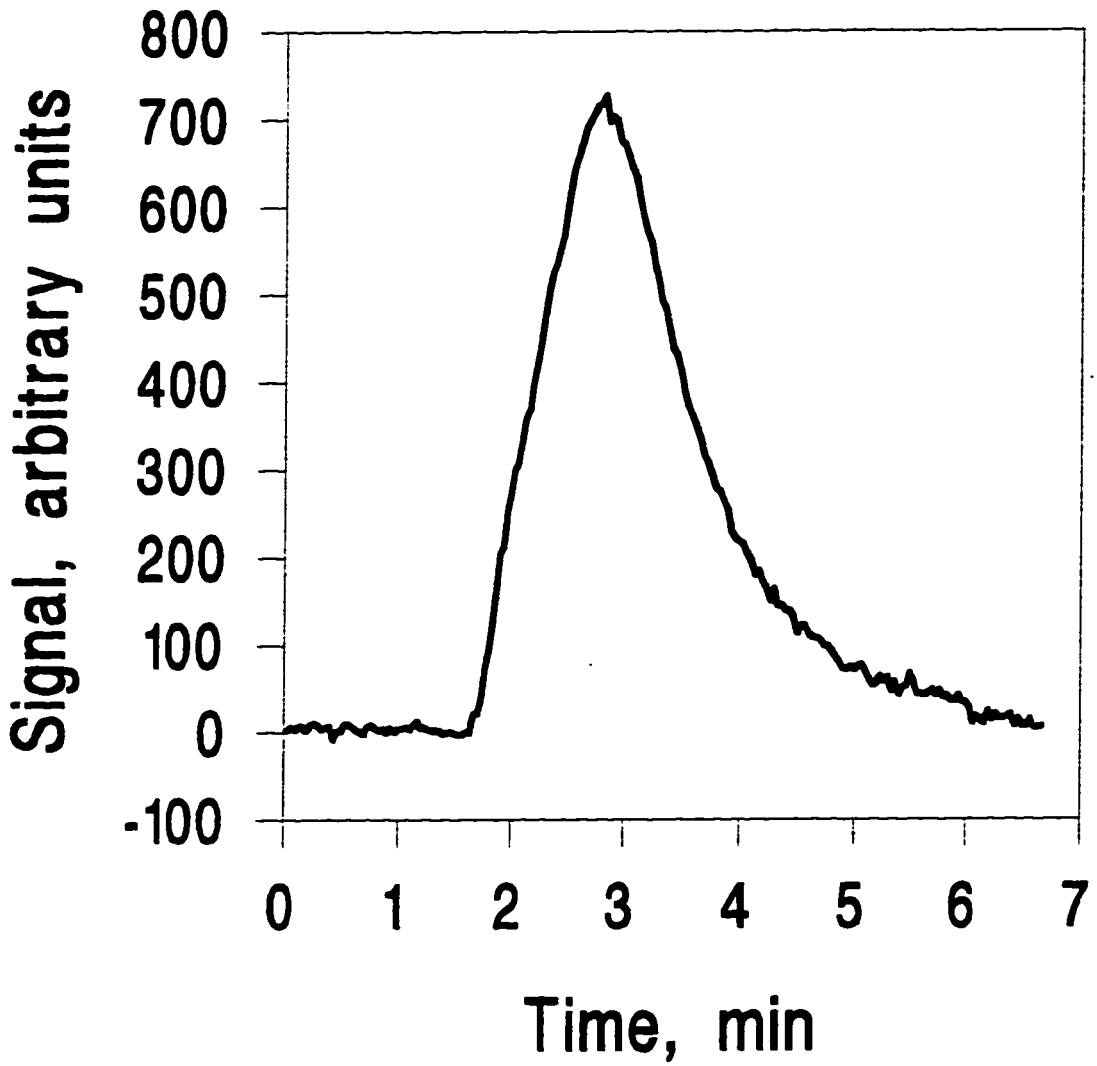
Signal, arbitrary units
800
700
600
500
400
300
200
100
0
-100
0
1
2
3
4
5
6
7
Time, min

Figure 3.3 Sensitivity vs. % water in the mobile phase obtained for: C=cumene and T=toluene where sensitivity is taken as the peak height divided by the concentration at the detector. The signals were obtained by injection of 200 nL of standards containing individual analytes, into a mobile phase of various compositions of methanol/water at a flow rate of 1 μL per minute.

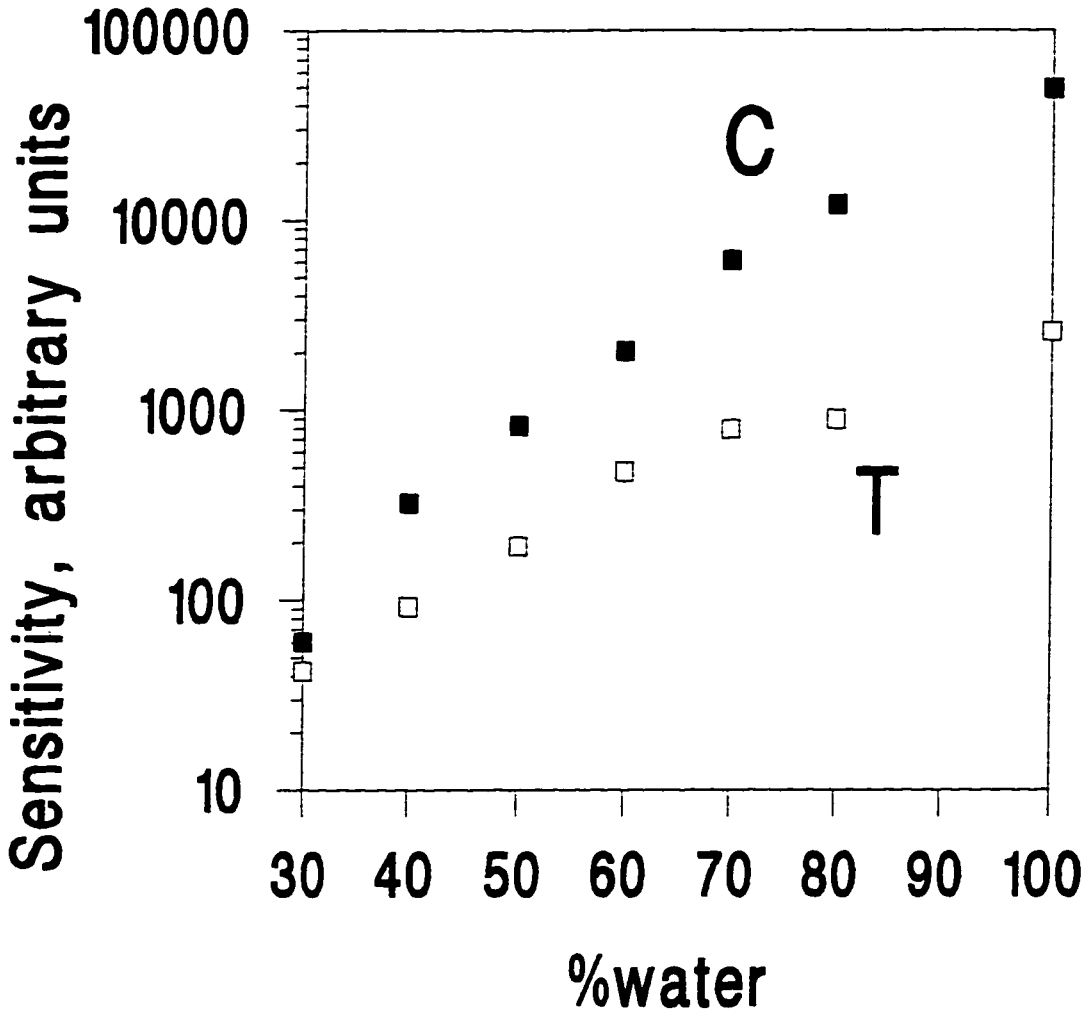
100000
10000
1000
100
10
Sensitivity, arbitrary units
C
T
30
40
50
60
70
80
90
100
%water

Figure 3.4 The solid line is the same function plotted in Figure 1 showing the predicted signal for the annular column sensor as a function of capacity factor of the analyte. The larger, open squares show a least squares fit of the capacity factor divided by peak width following eq 9 obtained for cumene in various percentages of methanol/water versus the measured capacity factor and normalized fit to the solid line. The closed squares show the least squares fit of the actual signal fit to the predicted signal as a function of capacity factor, thus testing eq 7.

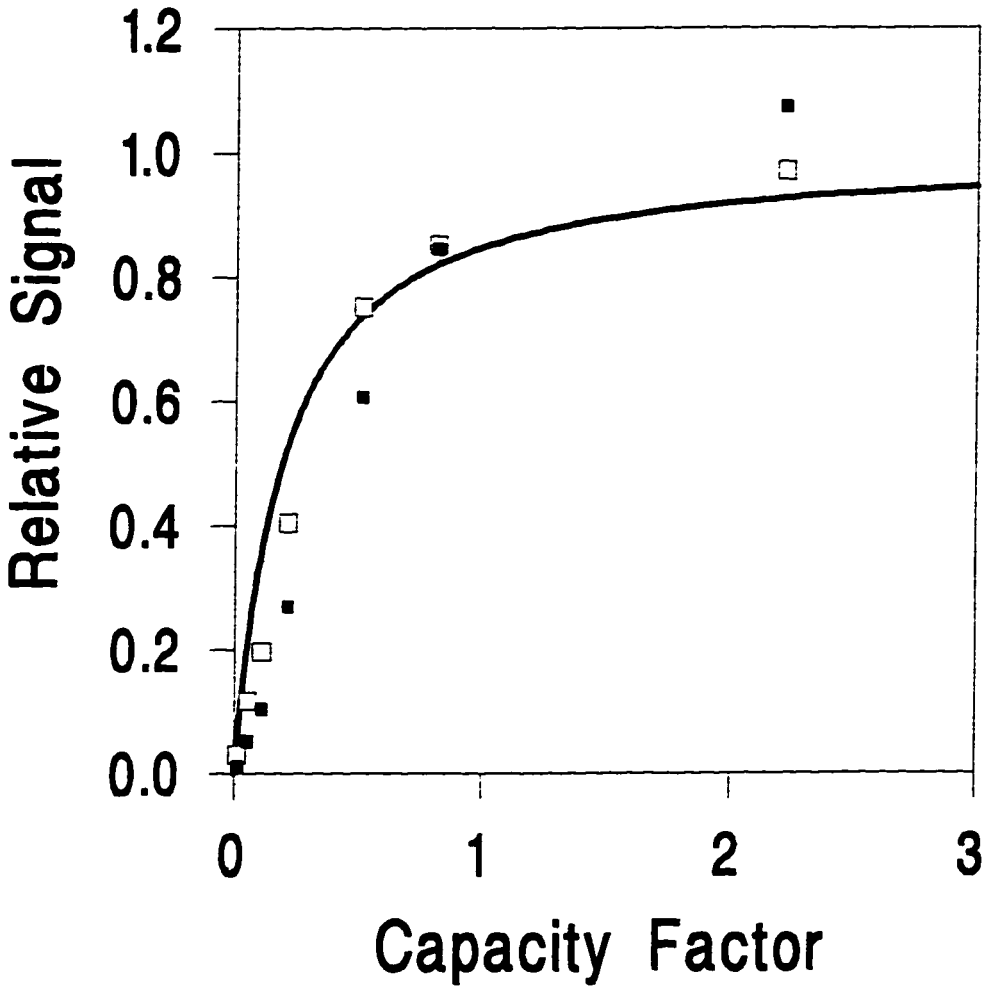
Relative Signal
1.2
1.0
0.8
0.6
0.4
0.2
0.0
0
1
2
3
Capacity Factor

decreased capacity factors, while maintaining a large distribution coefficient which improves analyte detectability. At the same capacity factor, the limit of detection (LOD) for toluene for the present work on the 0.1 μm thick cladding can be compared to the previous work on the 15 μm thick cladding. Previously an LOD of 3 parts-per-thousand was obtained in pure methanol at a capacity factor of about 1 for toluene using the 15 μm thick cladding[16], while the present work produced an LOD of 7 ppm for toluene in a pure water mobile phase with a capacity factor of much less than one. Thus, the LOD for toluene is about 400 times better, due primarily to the thinner clad allowing a higher distribution constant, while keeping k' essentially constant. To achieve a more useful capacity factor for toluene, a thicker TFPS cladding than we used would be required.

3.4.2 Flow Rate and the MFLD Signal

Rather than decrease the cladding thickness, the phase volume ratio could also be reduced by increasing the mobile phase diffusional distance, which is given as the distance from the O.D. of the fiber optic to the I.D. of the capillary, but this approach will necessitate a slower analysis since the time required to diffuse across this channel is proportional to the square of the distance across. Thus, there are two important effects to consider with regard to increasing the linear flow velocity for a particular mobile phase diffusional distance which are, decreased detectability due to increased peak width as predicted by eq 7, and also, breakthrough, which occurs when analyte traveling in flow streamlines away from the stationary phase does not have time to diffuse through the mobile phase to the stationary phase. The effect of increased linear flow velocity was examined by the following analysis. Since the annular column sensor had a small phase volume ratio and since rapid analysis was desired, peak broadening was dominated by slow diffusion in the mobile phase so that the signal should be inversely proportional to the square root of the linear flow velocity as predicted by eq 7. The signal at the peak due to injection of a dilute benzene solution was measured at

a number of different flow rates to test the effect of increasing flow rate on the peak signal maximum for the diluted concentration profile. Figure 3.5 shows the annular column sensor response to 200 nL injections of a 0.5 % benzene solution into a 30:70 methanol/water mobile phase at a variety of flow rates, offset for clarity. The peak maximum signal was expected to be inversely proportional to the square root of the linear flow velocity as predicted by eq 7 so that a plot of peak signal maximum versus the reciprocal of the square root of the linear flow velocity ought to be linear. This was observed as illustrated by the plot shown in Figure 3.6. Breakthrough occurred when the linear flow velocity was increased to the point that analyte present in flow stream lines away from the stationary phase was swept through without ever partitioning into the stationary phase. The flow velocity at which breakthrough began to have an observable effect was identified by examination of the running total integration of the peak area with increasing flow rate.[30] Peak width increased with flow rate as illustrated in Figures 3.5 and 3.6, but the peak area should remain constant until the onset of breakthrough. The onset of breakthrough was not observed in Figure 3.6 because the signal height measurement dependence on flow rate was dominated by normal band broadening as described by eq 6, and not breakthrough. The integration of the signals shown in Figure 3.5 versus eluted volume is shown in Figure 3.7. Note that the integration reached a constant volume for flow velocities of 0.1 mm/sec to 3.3 mm/sec but occupied a larger volume with increasing flow velocity. These flow velocities are produced by volumetric flow rates of 0.1 μL/min and 3.3 μL/min, respectively. At flow velocities above 3.3 mm/sec the signal integration in Figure 3.7 decreased with increasing flow rate as expected with the onset of breakthrough. This is in agreement with the calculation of the onset of breakthrough by the following analysis. Since the observed flow region of the annular column monitors a 3.2 mm section of the column, a flow velocity of 3.33 mm/sec allows approximately a 1 second residence time in the detection volume to diffuse through the mobile phase to the stationary phase. For the diffusional coefficient of benzene in water, a 1 second residence time should allow approximately 95% of analyte molecules within 25 microns of the stationary phase a

Figure 3.5 Annular column sensor response to injection of a small sample volume of benzene in water with a pure water mobile phase at several different flow rates. A 200 nL sample containing 1.0 μg of benzene was injected. The transient signals obtained were offset for clarity and were obtained at flow rates of (from top to bottom) 0.1 μL/min, 1 μL/min, 3.33 μL/min, 10 μL/min, 33.3 μL/min, 100 μL/min.

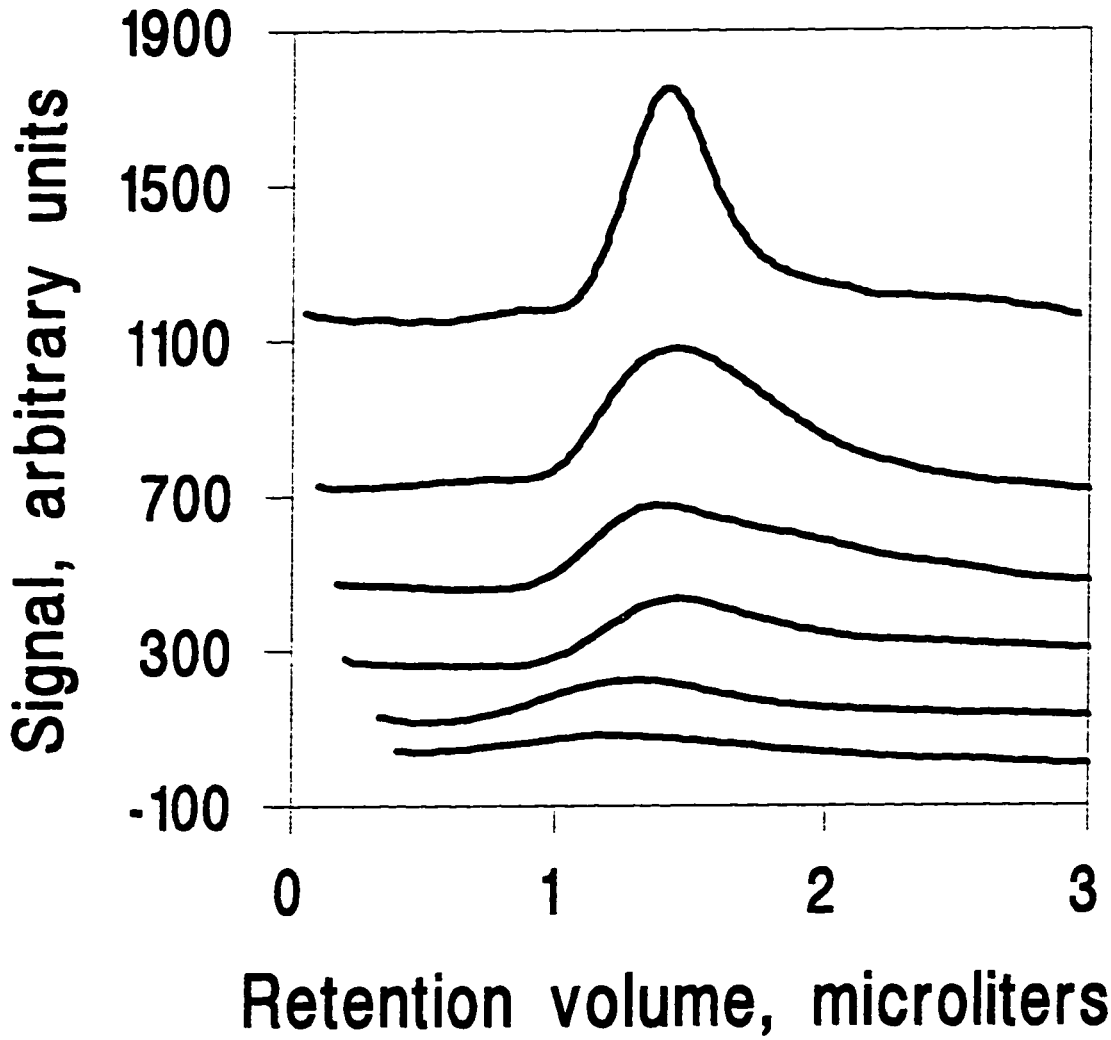
1900
1500
1100
700
300
-100
Signal, arbitrary units
0
1
2
3
Retention volume, microliters

Figure 3.6 The logarithm of the peak signal maxima from the sensor responses shown in Figure 3.5 were plotted against the reciprocal of the square root of the corresponding linear flow velocity (mm/sec).

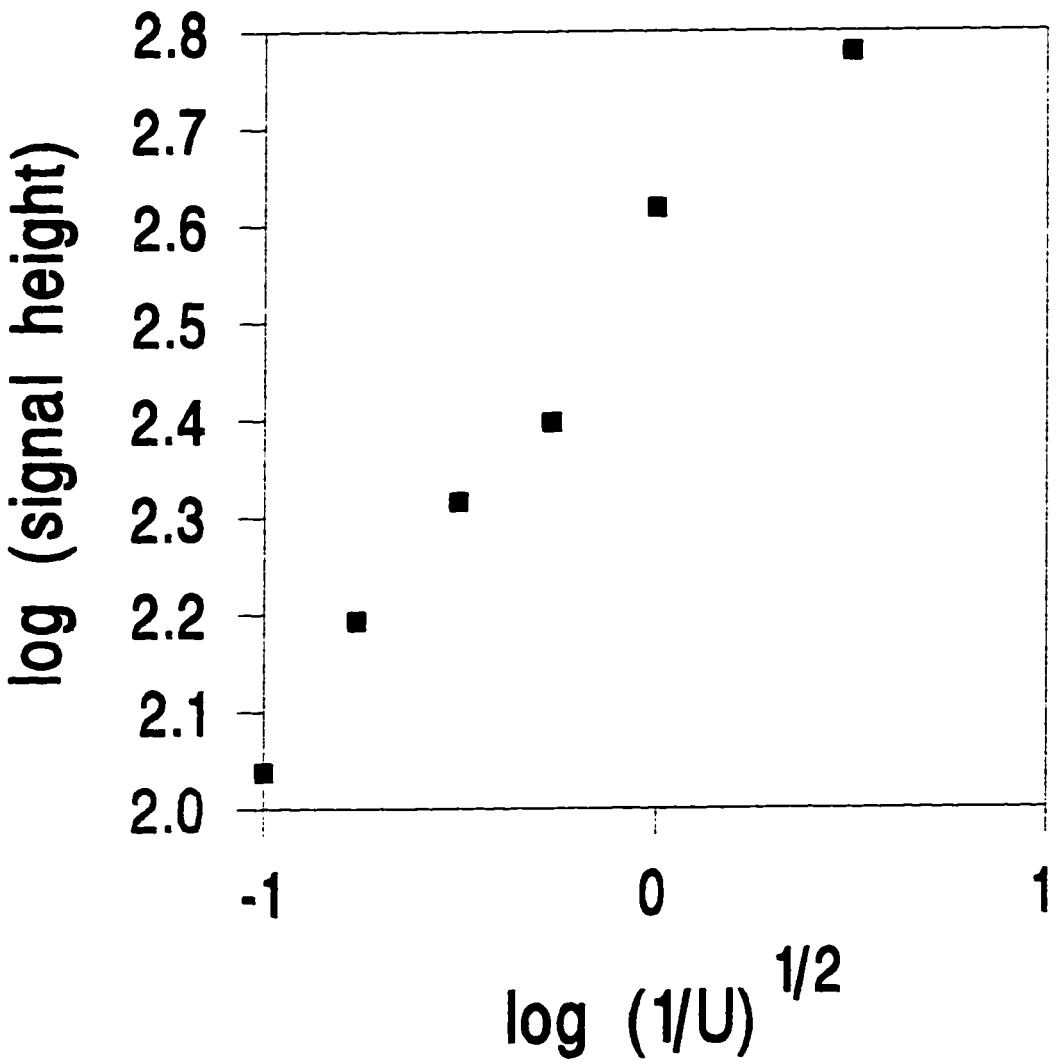
2.8
2.7
2.6
2.5
2.4
2.3
2.2
2.1
2.0
log (signal height)
-1
0
1
log (1/U) 1/2

Figure 3.7 The sigmoidal curves were obtained by integrating the sensor responses shown in Figure 3.5 and plotting the running total integration versus the total volume of mobile phase passed through the annular column.

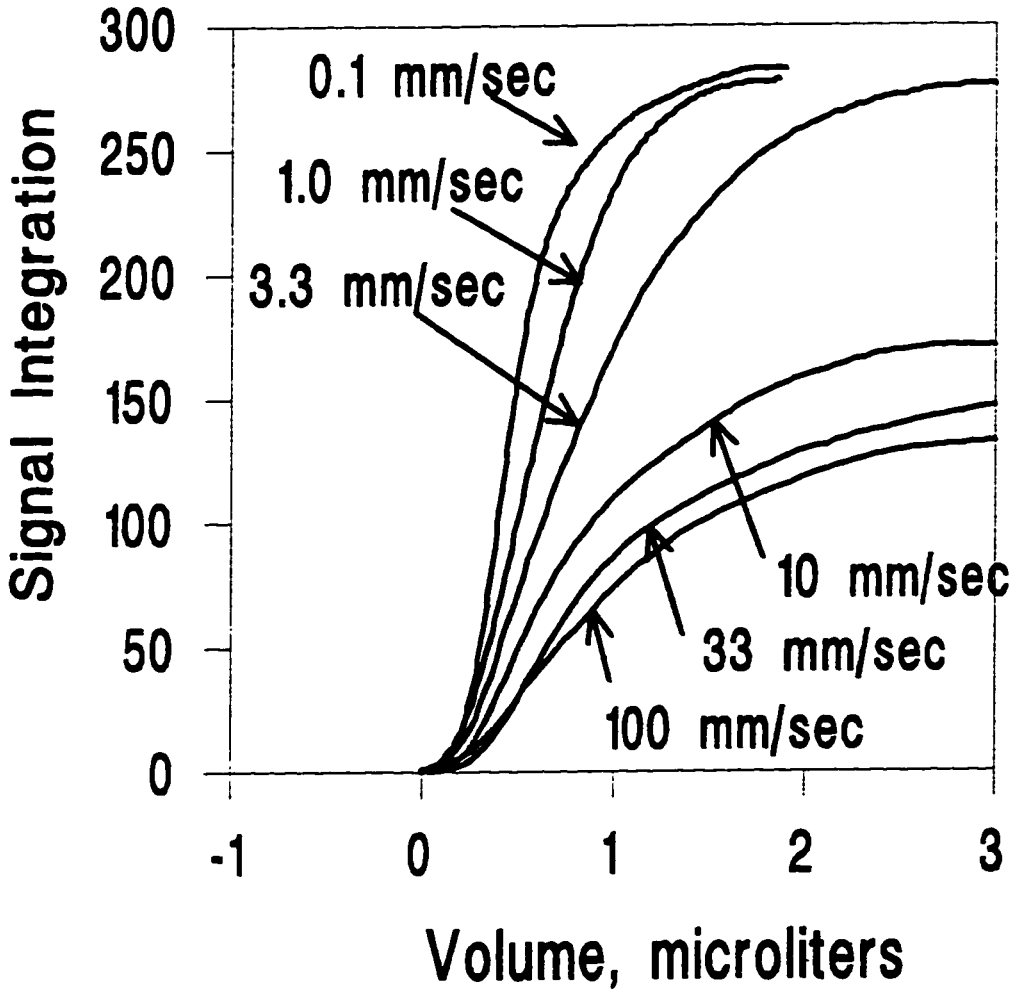
300
250
200
150
100
50
0
Signal Integration
0.1 mm/sec
1.0 mm/sec
3.3 mm/sec
10 mm/sec
33 mm/sec
100 mm/sec
-1
0
1
2
3
Volume, microliters

chance to reach the stationary phase. This is in agreement of the best case diffusional distance of 25 microns for the mobile phase with the fiber centered in the capillary tubing, or off-centered as well. The equilibration time for the analyte, benzene, in the 0.1 μm thick TFPS stationary phase is negligible at less than a millisecond with a diffusional coefficient of 1 x 10^{-6} cm^2/sec. Thus, slow mass transfer in the mobile phase dominates the signal broadening.

3.4.3 Examples of Sensing of Trace Organics in Water

The annular column sensor provides excellent detectability for a small volume RI based sensor but also offers additional selectivity advantages. The sensitivity for a given analyte is due to a combination of refractive index difference between analyte and cladding and distribution coefficient for the analyte between the stationary phase and the mobile phase. Additional discrimination is offered by means of temporal displacement due to the chromatographic retention mechanism. The annular column sensor worked well for the detection of chlorinated organics in water. Figure 3.8(A) shows the response of the annular column sensor to saturated solutions of chlorinated organics in water. An analysis time of five minutes is achieved, with a detection limit of 1 ppm for trichloroethylene with a pressure drop of less than 10 psi. The rapid analysis time and virtually zero pressure drop are very desirable characteristics of chemical sensors. The trade off is little resolution of components as seen by comparing the overlaid trace of chlorinated organics. Good quantitative results can still be obtained for very low resolution separations by using chemometric techniques.[31-33] Figure 3.8(B) shows the sensor response to two aromatic hydrocarbons, toluene and cumene, in water. The peak concentrations for toluene and cumene are 900 ppm and 74 ppm respectively. From the data in Figure 3.8(B) the LOD's for toluene and cumene were calculated to be 7 ppm and 0.5 ppm, respectively. The RI values for cumene and toluene are very similar and the factor of 14 lower LOD for cumene demonstrates the selectivity which can be obtained for species which are very similar chemically.

Figure 3.8(A) Annular column response to 200 nL injections of saturated solutions of chlorinated hydrocarbons in water. TCE= trichloroethylene, TCA= Trichioroethane, Chlor= chloroform. The flow was pure water at 1 μL/min. **(B)** Annular column response to injections of T= toluene and C= cumene. The mobile phase was pure water and was operated at a flow rate of 1 μL/min. 200 nL samples were injected containing a total of 2 μg of toluene and 0.5 μg of cumene, and the peak concentrations are 900 ppm for toluene and 74 ppm for cumene.

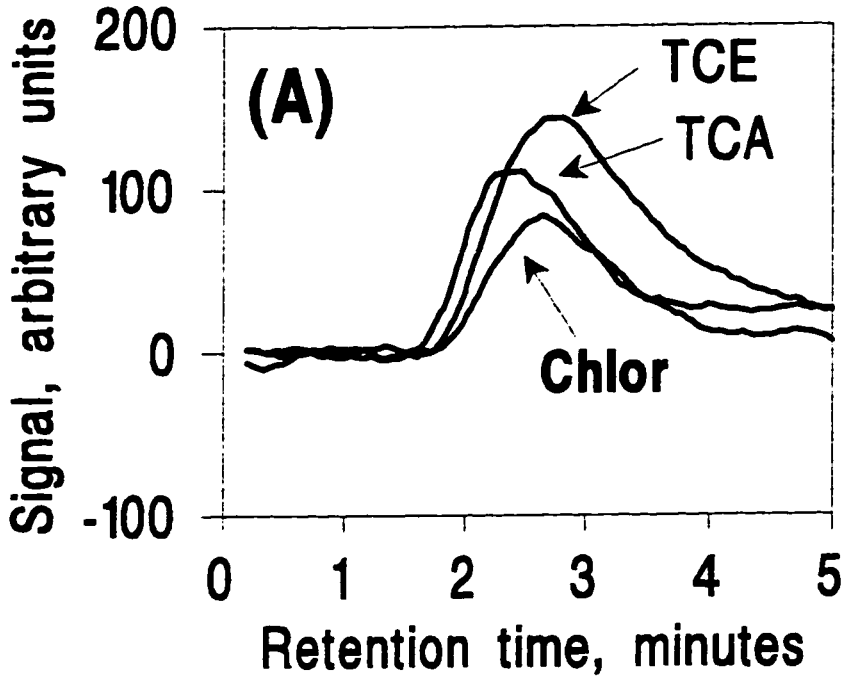
200
100
0
-100
Signal, arbitrary units
(A)
TCE
TCA
Chlor
0
1
2
3
4
5
Retention time, minutes

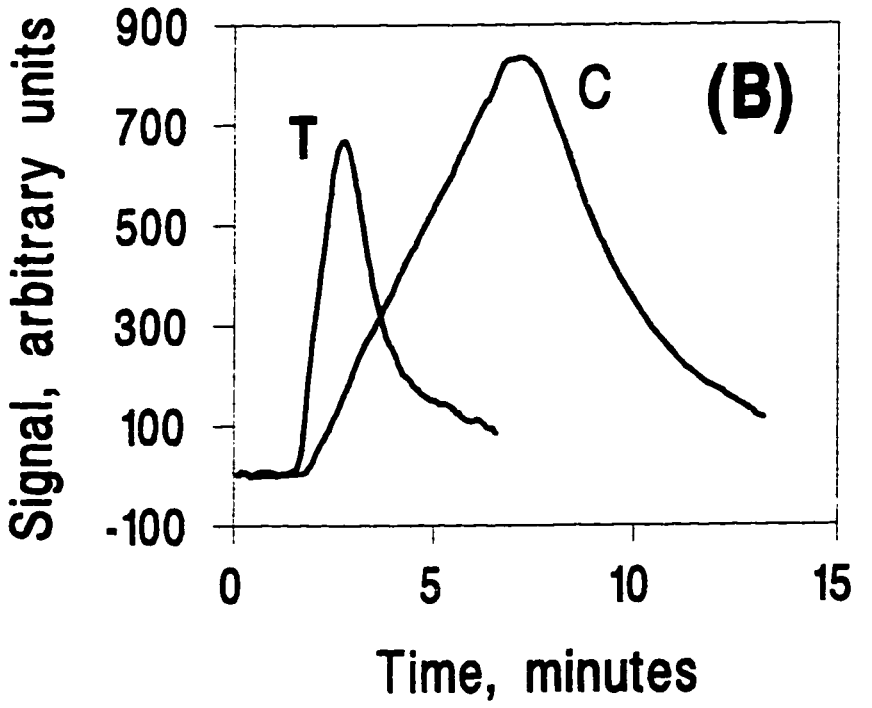
900
700
500
300
100
-100
Signal, arbitrary units
T
C
(B)
0
5
10
15
Time, minutes

Figures 3.8(A) and (B) demonstrate excellent sensitivity for the hydrophobic species tested but also demonstrate that reasonable capacity factors can be obtained for these types of compounds using pure water as the mobile phase. There is great potential for development of reversed phase liquid chromatography columns which provide reasonable capacity factors for very hydrophobic analytes in a pure water mobile phase and this subject will be addressed in future work.

3.4.4 Correlation of the MFLD Signal to the Octanol/Water Partition Coefficient

Numerous compounds were tested in an effort to fully characterize the selectivity of the TFPS phase by the MFLD scheme. Selectivity is gained in two ways. Sensitivity increases as the RI difference of the analyte and clad increase, and also as the affinity of the analyte for the cladding increases as described in eq 1. Overall selectivity for the MFLD scheme is seen as a product of both effects. Selectivity due to RI difference is easily understood and predicted knowing the cladding RI and analyte RI and need not be further examined. In order to examine the signal enhancement due to partitioning selectivity, the total signal was measured as the peak area for an injection of analyte as shown in Figure 3.2, and then divided by the RI difference between cladding and analyte. When the data that are obtained are divided by the concentration of each analyte that was injected, the relative analyte signal is obtained, which should be linearly dependent upon the distribution coefficient for the analyte between the cladding stationary phase and the mobile phase according to eq 1. Recall that in Figure 3.8(B) the LOD for cumene was approximately 14 times lower than for toluene due to a larger distribution coefficient for cumene between the mobile phase and the cladding stationary phase. The more hydrophobic cumene would be expected to have a larger affinity for the relatively nonpolar stationary phase in the mobile phase of water. There is a large body of data containing the distribution coefficient for organic molecules between octanol and water which is a measure of hydrophobicity[34] and should correlate well with the signal selectivity of the MFLD if partitioning into the TFPS is dominated by analyte

hydrophobicity under these solvent conditions. A plot of the relative analyte signal versus the octanol water partition coefficient (P_{ow}) for 11 compounds over a wide polarity range is shown in Figure 3.9. There is good correlation between the relative analyte signal and P_{ow} which provides an *a priori* method for predicting the performance of the MFLD for an analyte, provided the P_{ow} value for the analyte can be found.

3.4.5 Dynamic Range for MFLD

The dynamic range of the MFLD is a function of the RI difference of the analyte and cladding and also of the distribution coefficient of the analyte between the mobile phase and cladding. The low end of the dynamic range for a given analyte occur at the LOD and the high end is governed by a maximum concentration in the stationary phase, which is approximately 10% by volume. Both the LOD and maximum concentration of analyte in the stationary phase are dependent upon the distribution coefficient which increases exponentially with the water content of the mobile phase. From Figure 3.10, optimum dynamic range for a given analyte and concentration range can be tuned by selecting the proper mobile phase.

3.5 Conclusions

The annular column sensor has excellent promise as a stand alone sensor but also compares well to very small volume, refractive index based detectors that might be used for capillary chromatography or electrophoresis. The effective volume of our detection cell was 17 nL based on the 3.2 mm length of column which was seen by the PMT. It should also be noted that with a 5 mW He/Ne laser, we were not shot noise limited so the effective detection volume could be considerably reduced by reducing the length of column viewed by the PMT. The detection limit for cumene in water was 0.5 ppm as determined from the data presented in Figure 3.8(B), which corresponded to a true RI-LOD of 23 μRIU in the stationary phase, which is good for waveguide based

Figure 3.9 Plot of the relative analyte signal versus the octanol/water partition coefficient (ref. 34) for 11 different analytes. The relative analyte signal refers to the peak area of the analyte response, obtained as in Figure 2, divided by the injected concentration and the RI difference between analyte and cladding according to eq 1. Signals were obtained in duplicate in a 20:80 methanol/water flowing at 2 μL/min. 1=2-butanone; 2=tetrahydrofuran; 3=1-butanol; 4=dichloromethane; 5=trichloroethylene; 6=carbon tetrachloride; 7=toluene; 8=butyrophenone; 9=pentane; 10=cumene; 11=butylbenzene.

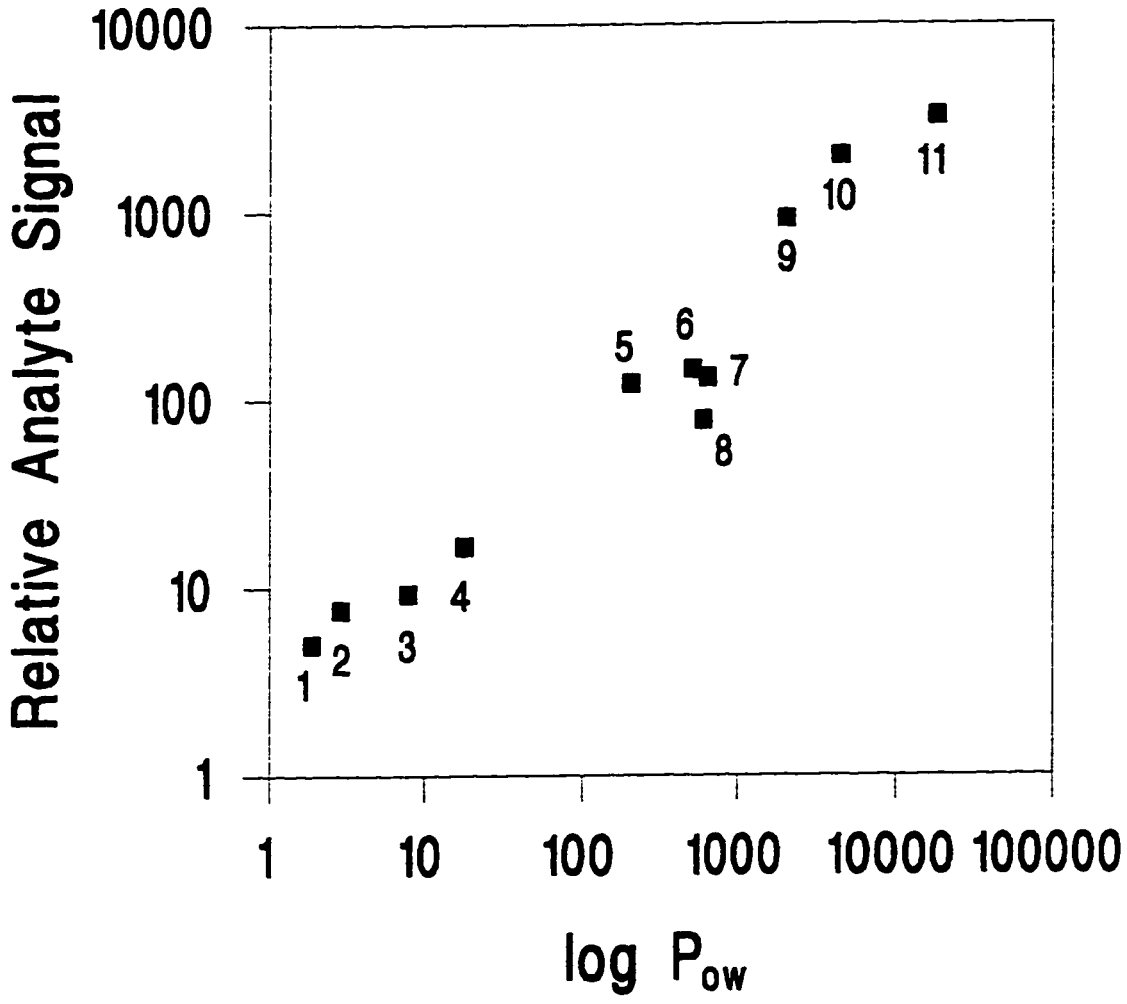
Relative Analyte Signal
10000
1000
100
10
1
1
10
100
1000
10000
100000
log P_{ow}
1
2
3
4
5
6
7
8
9
10
11

Figure 3.10 The dynamic range is shown as a function of methanol/water mobile phase for cumene as the area between the two set of data. The points making up the lower curve are the detection limits for cumene as determined in the various mobile phase compositions. The points making up the upper curve are the concentrations of cumene which would create a concentration of 10 % by volume in the stationary phase.

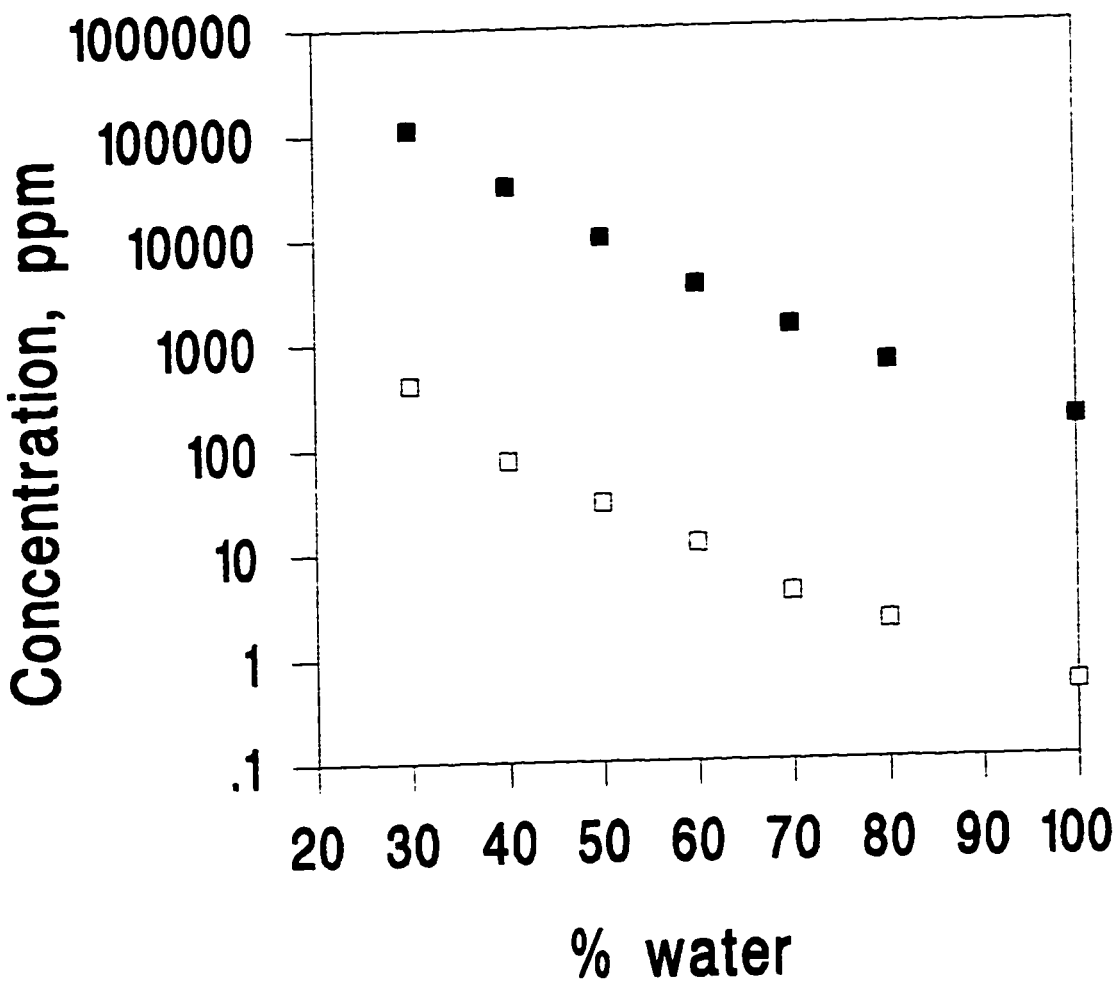
1000000
100000
10000
1000
100
10
1
.1
Concentration, ppm
20 30 40 50 60 70 80 90 100
% water

RI detection. One should note that a key advantage to detecting refractive index changes in the stationary phase rather than the mobile phase is increased detectability since the concentration of analyte in the stationary phase relative to the mobile phase is amplified by the distribution constant, thus improving the effective RI detection limit. The advantage can be illustrated by noting that the RI change in the mobile phase due to 500 ppb of cumene is only 0.08 μRIU while the RI change in the stationary phase is 23 uRIU because the distribution coefficient for cumene is 620 with the pure water mobile phase. The detectability is modified by changing the linear flow velocity and mobile phase, as discussed with Figures 3.5, 3.6, 3.7 and 3.10. A recent article[35] quoted refractive index LOD values ranging from 0.6 μRIU in a 500 μm capillary tube to 10 μRIU in a 5 μm capillary tube, by a number of different RI and thermooptical techniques, which would correspond to cumene concentration LOD's of 3.7 ppm and 62 ppm respectively. Based on the excellent detection limits and selectivity advantages, MFLD with a chromatographic sensor has excellent potential for application as a small volume detector for microbore and capillary liquid chromatography, and also capillary electrophoresis.

3.6 Notes to Chapter 3

1. Fuh, M. S.; Burgess, L. W. *Anal Chem.* **1987**, 59, 1780-1783.
2. Skogerboe, K. J.; Yeung, E. S. *Anal. Chem.* **1987**, 59, 1812-1815.
3. DeGrandpre, M. G.; Burgess, L. W. *Anal. Chem.* **1988**, 60, 2582-2586.
4. Buffet, C. E.; Morris, M. D. *Anal. Chem.* **1982**, 54, 1824-1825.
5. Fujiwara, K.; Fuwa, K. *Anal. Chem.* **1985**, 57, 1012-1016.
6. Renn, C. N.; Synovec, R. E. *Anal. Chem.* **1991**, 63, 568-574.
7. Arnold, M. A. *Anal. Chem.* **1992**, 64, 1015A-1025A.
8. Richmond, E. W.; Dessy, R. E. *Anal. Chem.* **1992**, 64, 1379-1382.
9. Piraud, C.; Mwarania, E.; Wylangowski, G.; Wilkinson, J.; O'Dwyer, K.; Schiffrin, D. J. *Anal. Chem.* **1992**, 64, 651-655.
10. Lundgren, J. S.; Bekos, E. J.; Wang, R.; Bright, F. V. *Anal. Chem.* **1994**, 66, 2433-2440.
11. Bender, W. J. H.; Dessy, R. E.; Miller, M. S.; Claus, R. O. *Anal. Chem.* **1994**, 66, 963-967.
12. Yang, L.; Saavedra, S. *Anal. Chem.* **1995**, 67, 1307-1314.
13. Arthur, C. ; Pawliszyn, J. *Anal. Chem.* **1990**, 62, 2145-2148.
14. Buchholz, K. D.;Pawliszyn, J. *Anal. Chem.* **1994**, 66, 160-167.
15. Synovec, R. E.; Bruckner, C. A.; Burgess, L. W.; Foster, M. D. *SPIE Chemical, Biochemical and Environmental Sensors;* SPIE: Bellingham, WA., 1994; Vol. 2293, pp167-177.
16. Synovec, R. E.; Sulya, A. W.; Burgess, L. W.; Foster, M. D.; Bruckner, C. A. *Anal. Chem.* **1995**, 67,473-481.
17. Giuliani, J. F.; Jarvis, N. L. *J. Chem. Phys.* **1985**, 82, 1021-1024.
18. Giuliani, J. F.; Jarvis, N. L. *Sensors and Actuators* **1984**, 6, 107-112.
19. Kawahara, F. K.; Fiutem, R. A.; Silvus, H. S.; Newman, F. M.; Frazar, J. H. *Anal. Chim. Acta* **1983**, 151, 315-327.

20. Klainer, S. M.; Thomas, J. R.; Dandge, D. K.; Frank, C. A.; Butler, M. S.; Arman, H.; Goswami, K. *SPIE Environmental Sensing and Combustion Diagnostics* **1991**, Vol. 1434, pp. 119-126.

21. Novotny, M. *Anal. Chem.* **1988**, 60, 500A-510A.

22. Giddings, J. C.; Chang, J. P.; Myers, M. N.; Davis, J. M.; Caldwell, K. D. *J. Chromatogr.*, **1983**, 255, 359-369.

23. Karger, B. L.; Snyder, L. R.; Eon, C. *J. Chromatogr.* **1976**, 125, 71-88.

24. Schoenmakers, P. J.; Billiet, H. A. H.; de Galan, L. *J. Chromatogr.* **1983**, 282, 107-121.

25. Hafkenschied, T. L.; Tomlinson, E. *J. Chromatogr.* **1983**, 264, 47-62.

26. Sun, Z. L.; Liu, M. C.; Hu, Z. D. *Chromatographia* **1994**, 38, 599-608.

27. Harris, F.W.; Seymour, R.B. *Structure-Solubility Relationships in Polymers* Academic Press, New York, New York, **1977.**

28. Golay, M. J. E. in *Gas Chromatography, 1958*; Desty, D. H. ed., Academic Press, New York, N.Y., **1958.**

29. Novotny, M.; Blomberg, L.; Bartle, K. D. *J. Chromatgr. Sci.* **1970**, 8(7), 390-393.

30. Synovec, R. E.; Yeung, E. S. *Anal. Chem.* **1985**, 57, 2162-2167.

31. Bahowick, T. B.; Synovec, R. E. *Anal. Chem.* **1995**, 67, 631-40.

32. Linn, Z.; Burgess, L. W.; *Anal. Chem.* **1994**, 66, 2544-51.

33. Linn, Z.; Booksh, K. S.; Burgess, L. W.; Kowalski, B. R.; *Anal. Chem.* **1994**, 66, 2552-60.

34. Leo, A.; Hansch, C *Subtsituent Constants for Correlation Analysis in Chemistry and Biology*, John Wiley & Sons, New York, N. Y., **1979**.

35. Bruno, A. E.; Bruin, G. J. M.; Krattiger, B. *Anal. Chem.* **1994**, 66, 1-8.

Chapter 4 Development of HPLC Columns for Water Only Reversed Phase Separation of Hydrophobic Species in Water

4.1 Introduction to Chapter 4

Reversed phase high performance liquid chromatography (RP-HPLC) of organic analytes with significant hydrophobicity is traditionally performed on stationary phases that require a large fraction of an organic solvent in the mobile phase, such as 70% to 80% methanol or acetonitrile in water.[1] The scope of RP-HPLC is large, and a broad range of chemical species can be separated for either preparative or chemical analysis goals. The stationary phase is generally octadecylsilane (ODS), i.e., C18 bonded to a highly porous silica-based material , resulting in a high surface area per gram of stationary phase.[2] The high surface area per gram of stationary phase leads to a relatively high phase volume ratio column (ratio of stationary phase volume to mobile phase volume), well-suited for the task of preparative chromatography.[3] Unfortunately, the price paid for using a column with a high phase volume ratio is the necessity for a large fraction of organic solvent in the mobile phase in order to achieve a good separation in a reasonable time.[4,5] The high organic solvent content in the mobile phase is now considered a significant source of chemical waste. For the application of RP-HPLC as a chemical analysis tool, in contrast to preparative chromatography, many samples require trace analysis and it is not necessary to use columns with a high phase volume ratio, because there is little worry that column overload will be approached. Thus, it should be possible to design stationary phases for RP-HPLC that function with a lower phase volume ratio, but with a polarity comparable to traditional C18, while providing reasonable capacity factors for analytes exhibiting hydrophobic interactions using only water as the mobile phase. Essentially, it is reasonable to anticipate that for any aqueous sample, as long as the analytes are soluble in the original sample matrix, then the RP-HPLC of the sample should be achievable in only water or the appropriate inorganic buffer (without organic solvent). Use of a water mobile phase will eliminate organic solvent use in many applications dealing with the direct analysis of aqueous systems. Gradients can still be applied

without organic solvents by using a thermal gradient[6,7] or by using a gradient of non-toxic surfactants or buffering compound such as those used for biological systems.

There are many compelling reasons to develop RP-HPLC that depends only upon water as the mobile phase. First, the cost of disposing of chromatographic waste will be minimized. For routine RP-HPLC analysis, a trend has been to use mini-bore (2.1 mm I.D.) and microbore (1 mm I.D.) columns rather than the more traditional 4.6 mm I.D. columns in order to save on solvent consumption while maintaining separation performance.[8] Use of water as the mobile phase in RP-HPLC will complement this trend toward narrow bore columns. Second, the water only mobile phase will be easier and less expensive to prepare than a mixed mobile phase. Third, the water mobile phase can be readily re-circulated and used over again by simply trapping any eluted analytes on a C18 column with a higher phase volume ratio. Fourth, reduced phase volume offers an inherent advantage of improved peak capacity as opposed to a higher phase volume column. Finally, water provides a low background for many detection methods, such as UV/Vis absorbance and conductivity, thus detection limits for many analytes will improve.[9]

Use of only water as the mobile phase is an underdeveloped concept. Most of the work has been directed toward ion exchange methodology[9] and hydrophobic interaction chromatography (HIC) for the separation of proteins.[10] Small discussed the merits of water-only ion exchange and developed a technique for the separation of inorganic ions using a weak ion-exchange column and water as the mobile phase.[9] The use of aqueous buffer gradients for the separation of proteins by HIC has been introduced out of the need to avoid protein denaturation that occurs with addition of organic modifier to the mobile phase.[10] Our work is complementary because we are focusing on the overall control of phase volume ratio and stationary phase polarity to achieve separations of organics in water with a reversed phase retention mechanism. To a limited extent Jandera and Kubat[11] demonstrated RP-HPLC with water as the mobile phase during a study of commercial C18 materials. Very short columns were packed to compensate for the huge capacity factors

observed due to the high phase volume ratio.[11] Several authors have explored the use of non-porous silica packing materials of low surface area with traditional bonded phases, e.g., C18 or similar materials for a number of special applications or purposes.[12-15] Work with non-porous silica based packing materials has demonstrated reduced requirements for organic modifiers, yet, the use of a water mobile phase to obtain reasonable retention times in RP-HPLC has not been developed and reported. As discussed in Chapter 3, work on reversed phase liquid chromatographic sensing, using a thin-clad fiber optic inserted down a capillary producing an annular column produced reasonable capacity factors, in the range of zero to three, for analytes such as toluene and cumene using only water as the mobile phase.[16] This result is a consequence of using a stationary phase which is of the correct polarity and phase volume ratio. The results demonstrated the potential for the development of water-only RP-HPLC.

An additional benefit of water only RP-HPLC will be improved correlation of analyte capacity factors to the octanol/water partition coefficient (P_0) and aqueous solubility values (X_0) of the analyte. These correlations are very useful in biological toxicity modeling and predictions. For instance, log P_0 and log X_0 values are often used for quantitative structure activity relationships (QSAR) for predicting the effects of nonspecific toxins in biological systems.[17-20] Capacity factor data for hydrophobic analytes obtained with mixed organic/aqueous mobile phases and RP-HPLC has long been used as a method for obtaining P_0 and X_0 and has been the topic of numerous publications.[19,20] Accurate prediction of P_0 and X_0 values by RP-HPLC provides savings in solvent and time, in comparison to solvent extraction techniques, but has met with limited success due to the difficulty of extrapolating results from a mixed organic/aqueous phase to a 100% water phase. Application of water-only RP-HPLC allows for very rapid and accurate predictions of P_0 and X_0 values from the determination of the capacity factor directly in water.

The development and evaluation of a new stationary phase packing material for water-only RP-HPLC is reported here. The same stationary phase (TFPS) as applied in the chromatographic sensor work of Chapter 3 was coated on non-porous spherical

silica (14 micron diameter, nominal), resulting in a phase volume ratio about two orders of magnitude less than traditional C18 columns, and consequently a significantly lower capacity factor at a given mobile phase composition. The TFPS stationary phase is also slightly more polar than C18, further reducing the capacity factor for a given analyte and mobile phase. The chromatographic performance achieved by using the new stationary phase material and methodology is similar to current practices using standard packing materials, but can operate with water only. Two columns for water-only reversed phase liquid chromatography (WRP-LC) were packed with the new stationary phase material, prepared to have a factor of two difference in phase volume ratio. The factor of two difference in phase volume ratio produced separations with a factor of two difference in capacity factor, for a given analyte. Thus, two different analyte polarity ranges could be analyzed while providing evidence that the polymeric stationary phase was quantitatively adsorbed to the surface of the silica packing material. Band broadening as a function of linear flow velocity was measured to evaluate chromatographic efficiency with the first generation WRP columns. The mass loading characteristics of the new packing materials has been investigated and the results presented, in order to demonstrate that the new columns provide a useful mass dynamic range for most applications. A broad range of neutral, hydrophobic organics, along with ionic compounds containing a hydrophobic group (surfactants) were studied, to demonstrate general applicability. The separation of four aromatic hydrocarbons is shown with water as the mobile phase in about ten minutes. The capacity factor data in water for a broad range of compounds was used for log P_0 and -log X_0 correlations to demonstrate that accurate predictions of these important parameters can be obtained without the need to extrapolate from capacity factor measurements in several aqueous/organic mobile phase compositions. Detection was performed with UV/Vis absorbance in most cases and evidence of the improved detection limits for a water mobile phase is demonstrated.

4.2 Theory

One of the main goals of the work demonstrated in this dissertation was to develop a column for reversed phase high performance liquid chromatography (RP-HPLC) for hydrophobic analytes such as aromatic hydrocarbons using only water as the mobile phase. Based upon the earlier result on the annular column chemical sensor, it seemed likely that it should be possible achieve reasonable capacity factors for these types of compounds without the need for toxic and costly organic modifiers in the mobile phase by. Review of chromatographic theory suggest that WRP columns could be made by substantially decreasing the phase volume ratio of stationary phase relative to the mobile phase volume, and also by increasing the polarity of the stationary phase relative to stationary phase materials commonly used for RP-HPLC.

In RP-HPLC, a reasonable retention time is achieved by generating the proper polarity differences between the analyte and the stationary phase, and between the analyte and the mobile phase. The polarity differences will determine the distribution coefficient, K_d, for the analyte, which is the concentration of analyte in the stationary phase relative to the concentration in the mobile phase. Retention is most often described by the capacity factor, k', which is related the distribution coefficient by

$$k' = K_d \varphi \qquad (1)$$

where φ is the phase volume ratio, i.e., the ratio of stationary phase volume to mobile phase volume. To a certain extent, retention times can be calculated from thermodynamic quantities which are related to the polarities of the analyte, stationary phase and mobile phase. The solubility parameter model originally developed by Scratchard, Hildebrand and Scott[21] to describe the thermodynamics of mixing of regular solutions has been applied by many authors to estimate capacity factors in RP-HPLC.[21-27] While the solubility parameter model is problematic with aqueous systems, it is instructive to apply the model to obtain a qualitative understanding. The solubility parameter (polarity), δ, for the analyte, stationary phase, initial mobile phase, and water

are referred to as, δ_i, δ_s, δ_m, and δ_w respectively. The capacity factor can be related to solubility parameter data as

$$\log k' = \log k_o' + \frac{2V_i}{2.3\,RT}(\delta_m - \delta_i)(\delta_w - \delta_m)(\%\text{water}) + \frac{V_i}{2.3\,RT}(\delta_w - \delta_m)^2(\%\text{water})^2 \quad (2)$$

where:
$$\log k_o' = \frac{V_i}{2.3RT}\left[(\delta_m - \delta_i)^2 - (\delta_s - \delta_i)^2\right] + \log\varphi \quad (3)$$

and V_i is the molar volume of the analyte, R is the gas constant, T is the absolute temperature and log k_o' represents the capacity factor which would be obtained in pure solvent, i.e., with zero percent water. With conventional stationary phase materials used for RP-HPLC (typically C18), the values for δ_s and δ_i are very similar for most hydrocarbon analytes so the term, $(\delta_s - \delta_i)$, is nearly zero and a reasonable retention time is achieved by decreasing the magnitude of the $(\delta_m - \delta_i)$ term, i.e., by using an initial solvent with a lower δ_m, and by keeping the % water low as well. In Figure 4.1(A) is illustrated the typical log(k') plot as a function of % water in methanol for a typical hydrophobic analyte on a traditional C18 column.

The basic principles in the development of a WRP stationary phase is as follows. First, the effect of increasing the stationary phase polarity a few solubility parameter units is shown in line (B) of Figure 4.1. By increasing the polarity of the stationary phase, the $(\delta_s - \delta_i)$ term can become significant and will begin to diminish the effect of the $(\delta_m - \delta_i)$ term thus resulting in a lower capacity factor for a given analyte, mobile phase and phase volume ratio.[28,29] Note that a similar reduction in k' can be achieved by reducing δ_s from the initial equality with δ_i as has been reported.[30,31] Second, the effect of decreasing the phase volume ratio by a factor of 32, in concert with the increased polarity stationary phase is shown in plot (C). A lower phase volume ratio can be achieved by a combination of reducing the stationary phase thickness, and by reducing the surface area to volume ratio for the stationary phase substrate material,

Figure 4.1 Illustration of the concepts involved in reducing the amount of organic modifier required in the mobile phase for RP-HPLC according to eq 2. **(A)** Log k' (capacity factor) versus % water in mobile phase for a hydrophobic analyte on a common C18 porous silica packed column. A capacity factor of one is achieved with 80% organic solvent such as methanol. **(B)** By increasing the polarity of the stationary phase, i.e., δ_s of equation 3, the magnitude of eq 3 is reduced and a lower y-intercept is obtained for eq 2, so that a capacity factor of one can be obtained with only 50% organic solvent in the mobile phase. **(C)** The amount of organic solvent required to get a capacity factor of one is further reduced by reducing the phase volume ratio, φ , in addition to increasing the polarity of the stationary phase. The line in **(C)** is for the same polarity stationary phase as in **(B)** added to the effect of arbitrarily reducing φ by a factor of 32.

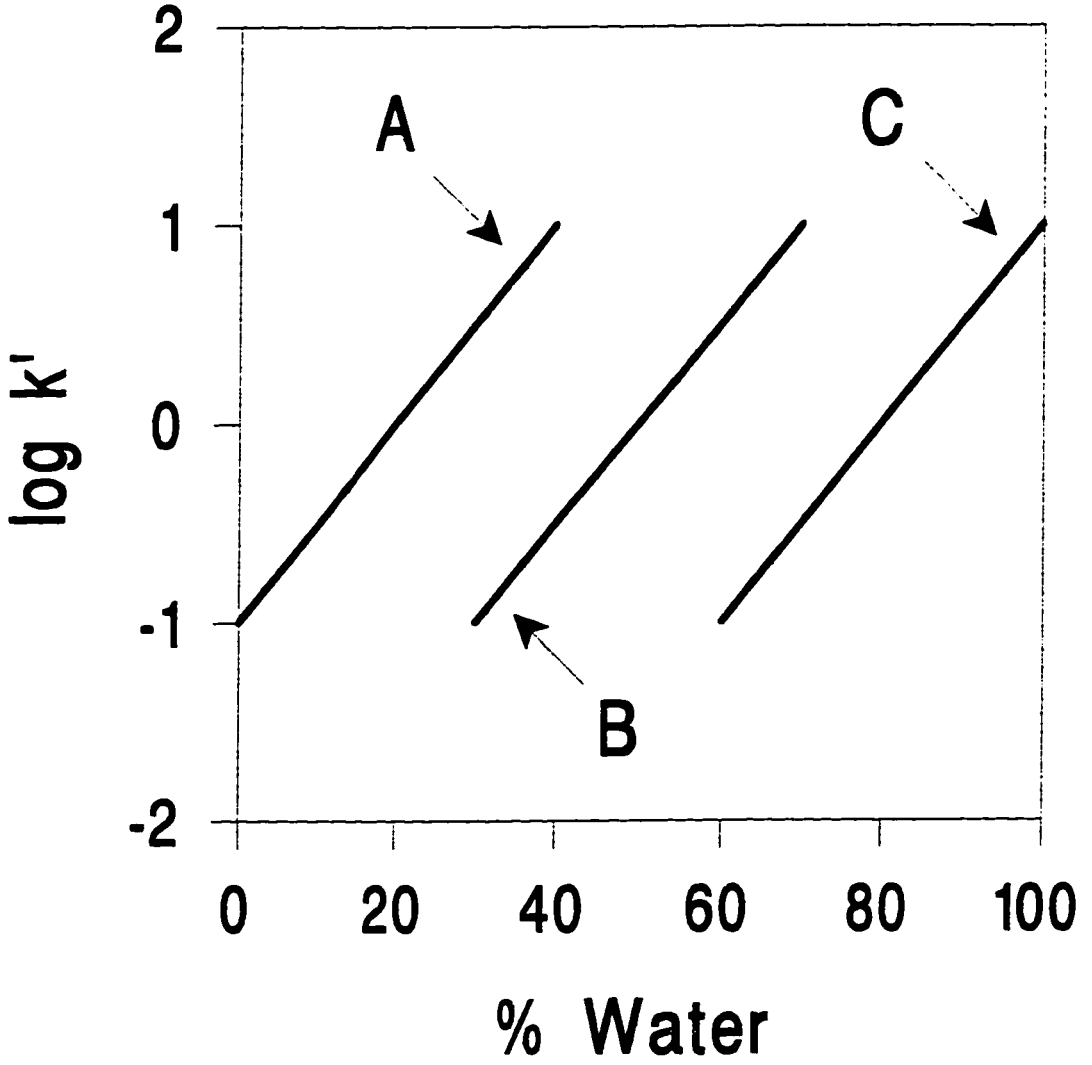
2
1
0
-1
-2
log k'
A
B
C
0
20
40
60
80
100
% Water

i.e., by using non-porous spherical silica instead of the highly porous silica traditionally used in commercially available packing materials. The immediate outcome is that for this typical analyte, which required about 20% water in 80% methanol for a reasonable k' on the traditional column, a reasonable k' can be achieved in 100% water by the combined effect of increasing the polarity of the stationary phase and reducing the phase volume ratio as illustrated in Figure 4.1.

Applying a stationary phase of trifluoropropyl siloxane (TFPS), which is a common gas chromatographic stationary phase material, to non-porous glass microspheres yields a stationary phase with a phase volume ratio reduced by about two orders of magnitude as compared to common liquid chromatographic packing materials. Additionally, the TFPS has a solubility parameter of 11, indicating that it is considerably more polar than traditional C18 stationary phases. As a result of these two factors, the columns obtained were able to perform separations of hydrophobic organic analytes such as benzene, toluene, ethylbenzene and isopropyl benzene using a water mobile phase at ambient temperature.

4.3 Experimental

Two different WRP columns were made by adsorbing a polymer onto the surface of non-porous glass spheres. Non-porous glass spheres were from obtained from Potters Industries (Spheriglass 4000E, Potters Industries, Valley Forge, PA) and had a rather large size distribution with 90% of the material by mass smaller than 36 μm, 50% smaller than 12 μm and 10% smaller than 4 μm. The average size by mass is 14 μm. Analysis by BET nitrogen indicated a specific surface area for this material of 0.40 m^2/g. The polymer coated on these glass spheres was a high molecular weight gum of trifluoropropylsiloxane (TFPS) which is a common gas chromatographic stationary phase material (OV 215, Supelco, Bellefonte, PA).

Coating of the packing material for column #1 was achieved by dissolving 0.1010 g of the stationary phase polymer in 25 mL of reagent grade ethyl acetate (J.T. Baker,

Phillipsburg, MA) in a 100 mL round bottom flask and adding 20.20 g of the glass spheres. The mixture was stirred on a rotovap and the solvent then evaporated off to leave the polymer adsorbed to the surface of the glass spheres. The coated beads were then placed under a high vacuum until all trace of solvent was gone. The surface area of the round bottom flask was less than 0.1 % of the surface area of the glass spheres so a quantitative transfer of stationary phase to packing material was assumed. At a density of 1.3 g/cm^3, the total volume of stationary phase was 0.078 cm^3 resulting in a calculated stationary phase thickness of 98 Angstroms. The mobile phase volume of column #1 was determined to be 0.75 mL by using sodium nitrate as a dead volume marker. The total volume of glass spheres in column #1 is 1.75 mL based on the calculated empty column volume of 2.5 mL. Since the density of the sphere material is 2.4 g/mL there was a total of 16 μL of polymer in column #1 which results in a phase volume ratio of 0.02. Column #2 was prepared in the same way as column #1 except that half as much polymer was used per gram of packing material resulting in a packing material with a stationary phase thickness of 49 Angstroms and a phase volume ratio of 0.01.

For column packing, the coated beads were made into a slurry by adding a small amount of 10:90 methanol/water and stirring until a paste-like consistency was achieved. The columns were successively filled with this slurry and compacted at a constant flow of 1.8 mL/min with a water mobile phase until no void volume remained at the top of the column. The final operating pressure of column #1 once fully packed was 1000 psi at 0.5 mL/min using a water mobile phase. The dimensions of column #1 were 4.6 mm I.D. by 150 mm long and the dimensions of column #2 were 4.6 x 100 mm. Separations on a traditional C18 column were achieved with a 150 x 3.2 mm Hyperprep column (Keystone Scientific, Bellefonte, PA) with a particle size of 12 μm and a specific surface area of 200 m^2/g.

A third WRP column was made by chemically bonding chloro dimethyl cyanopropyl silane to monodisperse glass beads. Two grams of monodisperse glass beads (Duke Scientific, Palo Alto, CA) with a mean diameter of 8 microns and an

approximately gaussian distribution of beads resulting in 67% of the particles in the range of 7 to 9 microns were boiled in concentrated nitric acid for 24 hours to assure complete hydroxylation of the glass surface and also to remove any metal impurities which might be present. The beads were then washed with deionized water and dried at 200 C overnight. The dried beads were then placed into a 50 mL round bottomed flask containing 20 mL of toluene which was freshly distilled from sodium/potassium alloy. Next, twenty microliters of dimethyl, chloro cyanopropy siloxane (Geleste, Tullytown, PA) and 1 mL of pyridine were added and a reflux condenser fit with a drierite filled drying tube was set in place. The pyridine had been dried by placing it over sodium hydroxide pellets overnight. The mixture was refluxed for 48 hours. After the initial reflux period, the beads were endcapped by adding 10 microliters of hexamethyldisilazane (Geleste, Tullytown, PA) and refluxing for an additional 24 hours. The reaction mixture was then filtered to remove the solvent and then washed with 40 mL portions of solvent in the following order: toluene, tetrahydrofuran, methanol, 50:50 methanol/water, water, 50/50 methanol/water, tetrahydrofuran and toluene. The chemically bonded beads were then passed through a 25 micron stainless steel mesh to remove any fibers or particulates. The stationary phase was packed into a 2.1 x 250 mm stainless steel column (Alltech Associates, Deerfield, IL) by a slurry packing technique as described below. The chemically bonded beads were added to 10 mL of a 70:30 mixture of methanol/water which was saturated with sodium dodecyl sulfate and sodium chloride. This slurry was then transferred to a 10 x 250 mm stainless steel column which served as the slurry reservoir. The outlet from the packing pump was then immediately connected to the slurry reservoir and a constant flow of 20 mL/min was applied with an 8700 psi upper pressure maximum. The outlet from the slurry reservoir was fitted directly to the 2.1 x 250 mm column to be packed via a swagelock fitting. The solvent supplied by the pump was pure methanol and pumping was applied for 30 minutes although the column appeared to have been packed in about one minute. The slurry reservoir and column to be packed were immersed in an

ultrasonic bath for the first ten minutes of the packing to help stimulate migration of material to the highest density of packing.

The mobile phase for most experiments was water obtained from a millipore nanopure water system. Methanol, when used, was HPLC grade from Burdick and Jackson. Mobile phase delivery was accomplished with a syringe pump (ISCO 2600, Lincoln, NE). Two different injection valves were used, one (Rheodyne 7125, Cotati, CA) for 20 μL injection volumes and one (Rheodyne 7520) for 1.0 μL injections. Detection of eluting components was done with either a UV/Vis absorbance detector (Dionex VDM-2, Sunnyvale, CA) at 260 nm in a flow cell volume of 8 μL or a conductivity detector (Milton Roy ConductoMonitor III, Riviera Beach, FL). The analog detector signal was sent to a digital acquisition board connected to a 486 PC at a sampling rate of 10,000 data points per second. Datapoints were reduced on-the-fly by a running boxcar average.

Most of the analytes studied were of reagent grade or better and obtained from either J.T. Baker or from Aldrich (Aldrich Chemical Co., Milwaukee, WI). The chlorobenzene purity was 98+ % and was obtained from Alfa (Ward Hill, MA). The sodium dodecylsulfate was 98 % pure and the sodium octyl sulfate was 95% pure and both were obtained from Aldrich.

4.4 Results and Discussion

4.4.1 Comparison of Separations on WRP Columns and Traditional C18 Columns

The benefits of a RP-HPLC column which works with a water mobile phase have been thoroughly discussed so a demonstration of the feasibility is in order. The first question which might be asked is whether or not a separation of very hydrophobic compounds in a pure water mobile phase is possible. Figure 4.2(A) shows a three minute separation of a mixture of four hydrophobic components using a water mobile phase at a flow rate of 1.6 mL/min on WRP column #1 which had a phase volume ratio

Figure 4.2(A) RP-HPLC separation of four hydrophobic analytes with a water mobile phase at a flow rate of 1.6 mL/min on a 4.6 mm x 150 mm water based reversed phase (WRP) column #1 with UV/Vis absorbance detection at 260 nm. Identity and injected concentration of analytes are: 0.75 ppm sodium benzoate [SB], 0.05 ppm benzaldehyde [BA], 20 ppm benzene [B] and 1 ppm butyrophenone [BP]. **4.2(B)** Separation of the same mixture as in (A) but the column is a standard C18 column on traditional porous silica and requires 70% methanol in the mobile phase to achieve capacity factors similar to the separation shown in (A).

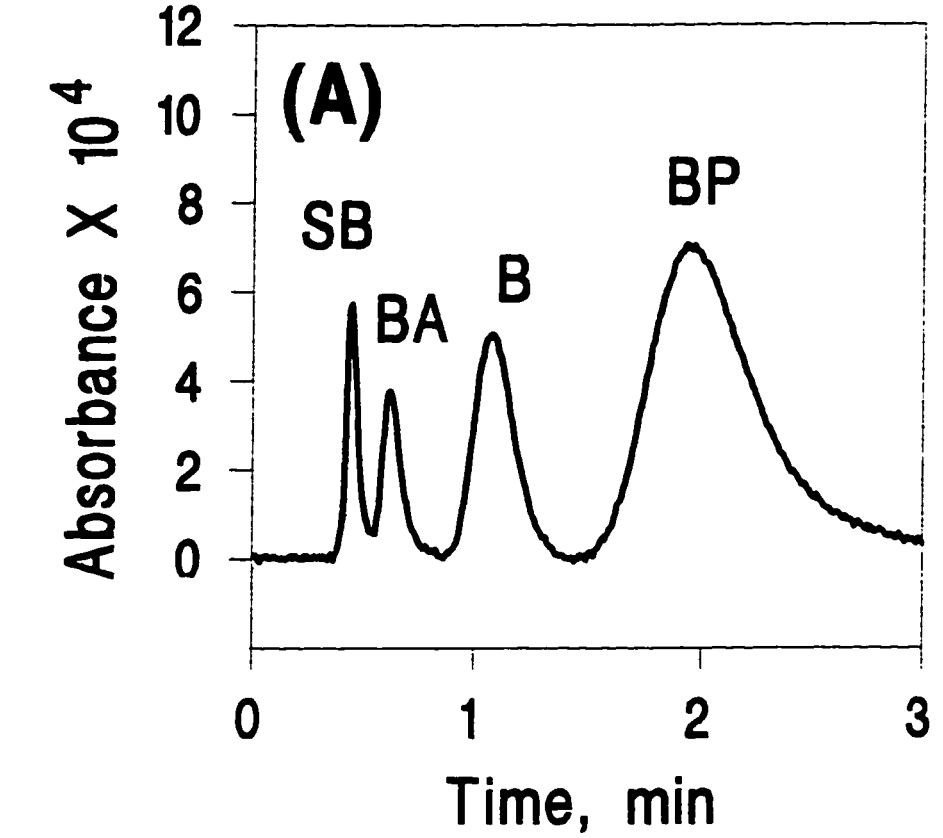
(A)
SB
BA
B
BP
Absorbance X 10^4
12
10
8
6
4
2
0
0
1
2
3
Time, min

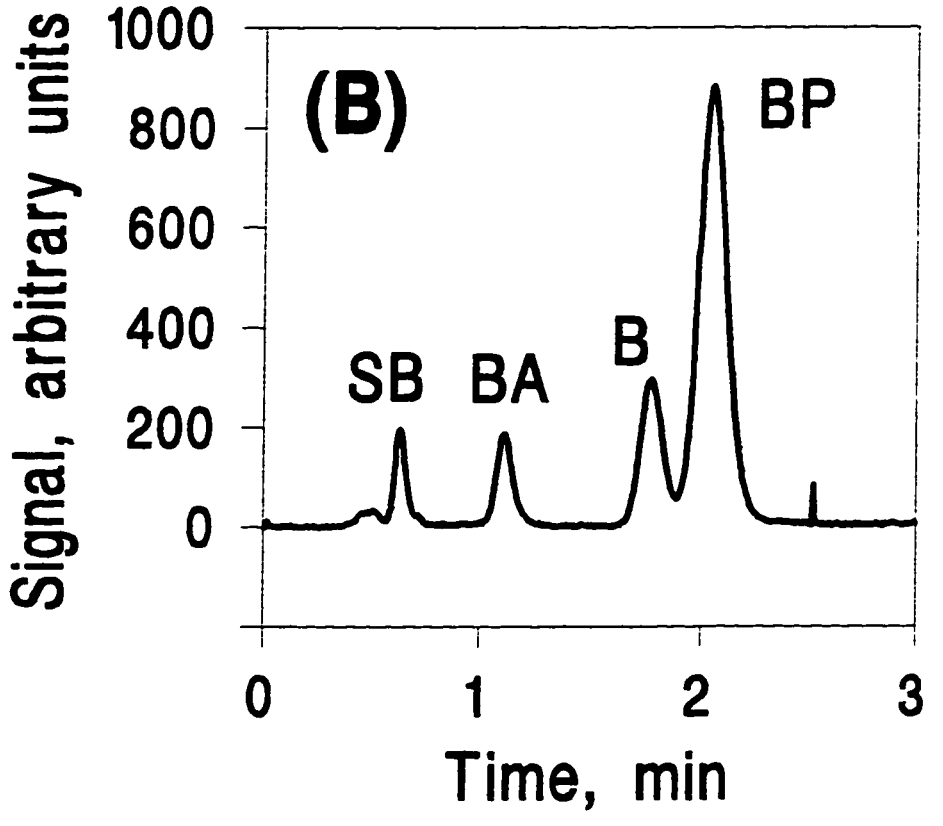
(B)
SB
BA
B
BP
Signal, arbitrary units
1000
800
600
400
200
0
0
1
2
3
Time, min

of 0.02. The next question which should be asked is how does this compare to traditional C18 chromatographic columns. Figure 4.2(B) shows the separation obtained on a standard C18 column requiring a mobile phase containing 70 % methanol to achieve a capacity factors similar to the same components as Figure 4.2(A). A separation of aromatic hydrocarbons was also achieved on WRP column #1 as shown in Figure 4.3(A). The corresponding separation on a traditional C18 column is shown in Figure 4.3(B) with a mobile phase requiring 60 % acetonitrile.

One interesting fact about the WRP column is that the mobile phase volume of the column was found to be 0.5 mL out of a total column volume of 2.5 mL, indicating that the mobile phase took up only 20% of the total volume of the column. A column packed with perfect spheres to the maximum density would have a mobile phase volume which made up 33% of the total column volume. The higher packing density for the WRP column must be due to the ability for the smaller spheres to occupy the interstitial volume of the network of larger spheres.

4.4.2 Demonstration and Explanation of Enhanced Separative Ability of Reduced Phase Volume Columns

Another interesting feature of the WRP column separation is the much larger difference in capacity factor observed as compared to the C18 separation. The WRP column separation of aromatic hydrocarbons shown in Figure 4.3(B) covers a capacity factor range of 1.53 for benzene to 17.6 for isopropyl benzene with water as the mobile phase while the C18 column separation of Figure 4.3(A) covered a capacity factor range of 2.36 to 7.02 respectively with 60% acetonitrile in water as the mobile phase. Note that the mobile phase strength for the C18 separation was designed to achieve similar capacity factors for the second component which was equal to 4.5 for both columns. The mobile phase for the C18 separation could have been made of appropriate elution strength to obtain an equal capacity factors for any one of the components of the mixture separated on the WRP column, but the range of capacity factors for the WRP column would still have been much larger. The increased range of

Figure 4.3(A) RP-HPLC separation of four aromatic hydrocarbons with a water mobile phase at a flow rate of 1.0 mL/min on a 4.6 mm x 150 mm water based reversed phase (WRP) column #1 with UV/Vis absorbance detection at 260 nm. Sample was twenty microliters of water containing an impurity in the isopropyl benzene [I] , 10 ppm benzene [B], 14 ppm toluene [T], 48 ppm ethyl benzene [E], 120 ppm isopropyl benzene (or Cumene) [C]. **4.3(B)** RP-HPLC separation of four aromatic hydrocarbons with traditional porous C18 column (Keystone, 2.1 x 74 mm) with a mobile phase of 65% acetonitrile in water at a flow rate of 0.20 mL/min with UV/Vis absorbance detection at 260 nm. Sample was one microliter of acetonitrile containing several impurities [I] , 30 ppm benzene [B], 50 ppm toluene [T], 80 ppm ethyl benzene [E], 115 ppm isopropyl benzene [C].

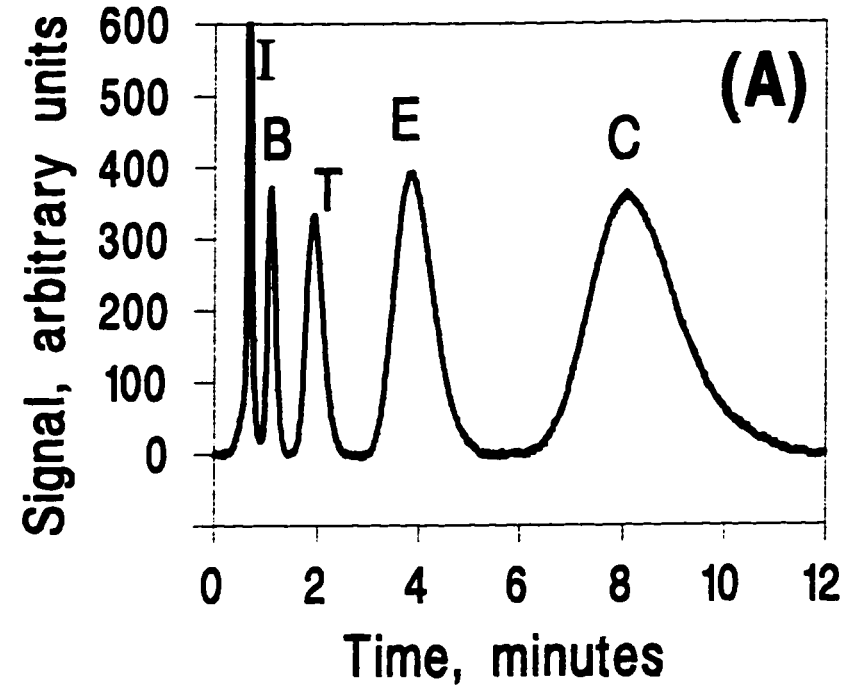
Signal, arbitrary units
600
500
400
300
200
100
0
I
B
T
E
C
(A)
0
2
4
6
8
10
12
Time, minutes

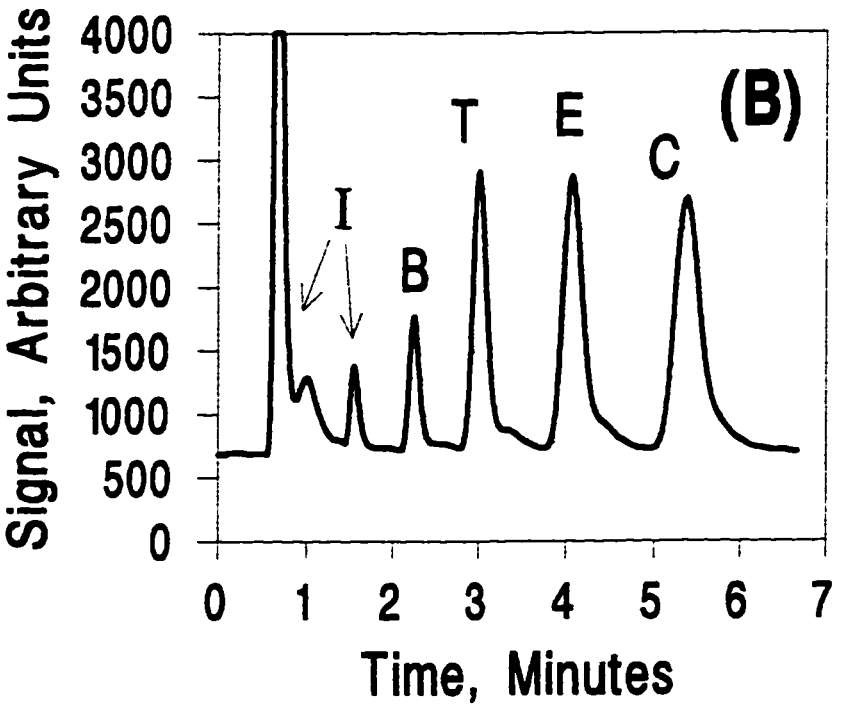
Signal, Arbitrary Units
4000
3500
3000
2500
2000
1500
1000
500
0
I
B
T
E
C
(B)
0
1
2
3
4
5
6
7
Time, Minutes

capacity factors shown by the WRP column is most easily describe by the decreased phase volume ratio of the WRP column. In general, for two columns utilizing the same stationary phase but with different phase volume ratios, which provide the same capacity factor for one of two similar components, a larger capacity difference will be provided by the column which has a smaller phase volume ratio. The reason for this is that for any single component and stationary phase, the capacity factor is linearly proportional to the phase volume ratio while the logarithm of the capacity factor is linearly related to the water content of the mobile phase. Additionally, for any two components, the slope of the logarithm of capacity factor versus fraction of water in the mobile phase is larger for the component having the higher capacity factor at a given mobile phase composition. Now consider the conditions needed to achieve equivalent capacity factors for a single component on columns of different phase volume ratio. A linear decrease in capacity factor brought about by a linear reduction in phase volume ratio can be compensated for by an exponential increase in the capacity factor achieved with a linear increase in the amount of water in the mobile phase. Since the difference in capacity factor between two components also increases exponentially with a linear increase in the fraction of water in the mobile phase there will be an increased range in capacity factor for the reduced phase volume column.

A more quantitative explanation can be arrived at by considering a simple model[32] for the retention behavior of alkyl benzenes on C18 as a function of the fraction of water in a methanol water mobile phase. Figure 4.4 demonstrates the linear relationship between the logarithm of the capacity factor and the fraction of water in the mobile phase for a homologous series of alkyl benzenes. Note that for any two components the slope is larger for the analyte which has the larger capacity factor at any given composition. This has been found to be true for RP-HPLC behavior of all analyes.[32] Now, to gain a quantitative understanding of the practical benefits achievable by the increase in capacity factor range, consider the lower and upper lines of Figure 4.4 which correspond to the retention behavior of benzene and propylbenzene on a porous C18 column. If we choose a fraction of water of 0.3 we find that the capacity

Figure 4.4 The linear relationship between the natural logarithm of the capacity factor and the percentage of water in a methanol mobile phase for this homologous series of alkyl aromatic compounds has been found to conform to the relationship shown here in Figure 4.4 as described in Reference 32. The behavior shown in for a traditional, porous C18 column. The identities of the components are supplied in the legend in Figure 4.4.

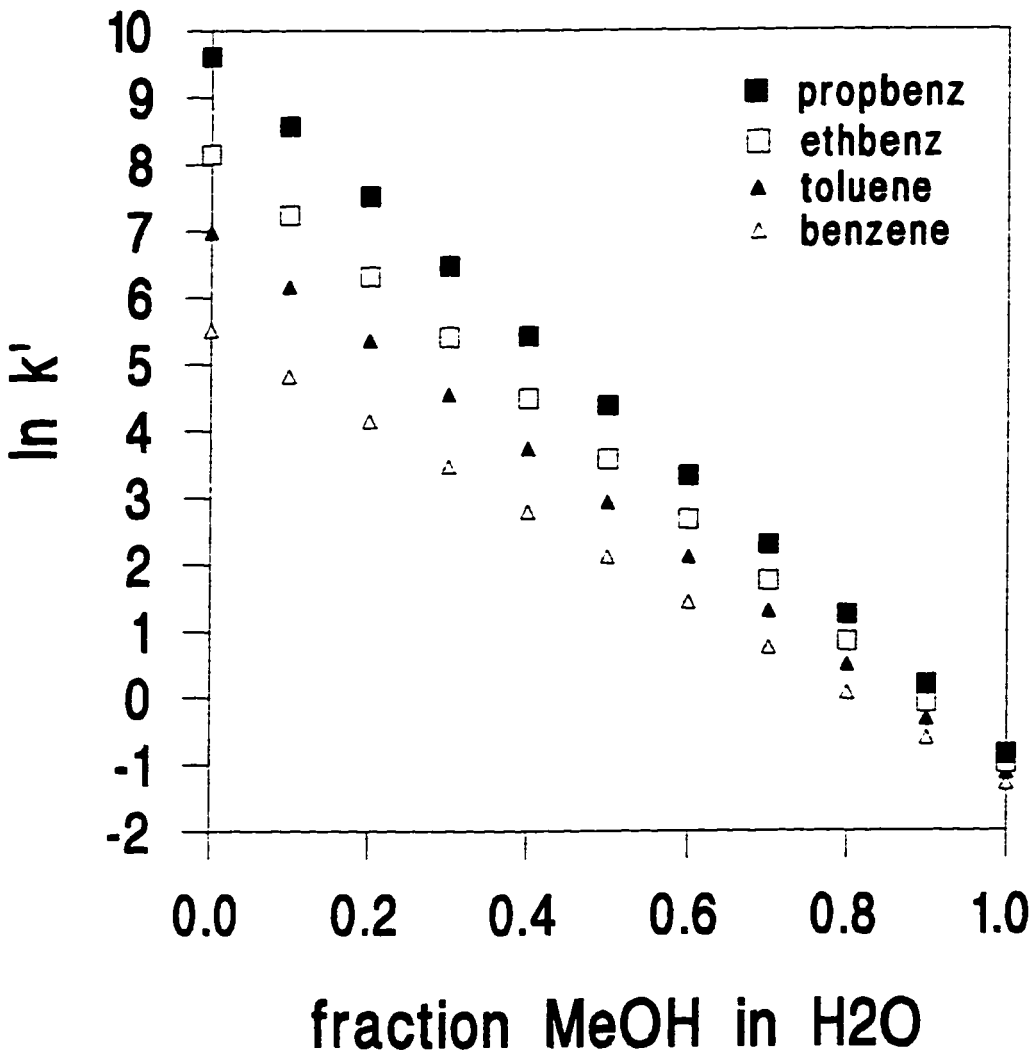
10
9
8
7
6
5
4
3
2
1
0
-1
-2
ln k'
propbenz
ethbenz
toluene
benzene
0.0
0.2
0.4
0.6
0.8
1.0
fraction MeOH in H2O

factors obtained are 2.1 and 10 respectively. By increasing the fraction of water to 0.74 we would obtain capacity factors of 42 and 1000. By reducing the phase volume ratio by a factor of 100, which is achievable by replacing the porous silica with a non-porous silica, we would obtain capacity factors of 0.42 and 10. This is an interesting and important result. By decreasing the phase volume ratio, we can not only decrease the amount of organic solvent required to elute components from the column, we also increase the capacity factor differences for any two similar components while maintaining the same maximum capacity factor. If this procedure is applied to two columns which provide the same number of plates we would expect an increase in peak capacity for the reduced phase volume column. The peak capacity refers to the maximum number of components which can be resolved with unit resolution in a given capacity factor range.[5] The peak capacity (n_c) is given by

$$n_c = 1 + (N^{1/2}/4) \ln (1 + k'_{max})/(1 + k'_{min}) \qquad (4)$$

where N is the number of plates for the column. Applying eq 4 to the two hypothetical columns described above with both columns achieving 10,000 plates we find that the nonporous C18 column provides a peak capacity of 53 components between benzene and propylbenzene and the typical porous column provides a peak capacity of 33 components between benzene and propylbenzene.

4.4.3 Comparison of Chromatographic Efficiency of WRP Columns and Traditional C18 Columns

The most striking difference between the WRP column separations and the separations on C18 columns is the vastly differing amounts of chromatographic space used for the separations. The peak widths on the WRP column can be seen to increase very rapidly with retention while the peak widths on the C18 column do not increase much at all with increasing retention. The chromatographic efficiency is an important figure of merit for chromatography. Due to a wide range of possible reasons, the efficiency for this WRP column was slightly worse than the commercial C18 column

and showed an almost linear decrease in plate count with increasing capacity factor. The efficiency of the WRP column for the three retained components of Figure 4.2(A) was determined at five different flow rates ranging from 0.1 mL/min to 1.6 mL/min. Figure 4.5(A) illustrates the flow rate effect on plate height for these three components. Note the large increase in plate height with increasing capacity factor and the relatively mild increase in plate height with increasing flow rate. This is in contrast to what is observed on traditional C18 columns. Typical behavior for a C18 column is demonstrated in Figure 4.5(B). Although the capacity factor ranges from 2.4 to 7.0 there is very little plate height dependence upon capacity factor. There is a large dependence upon linear flow velocity as commonly observed. The wide distribution of particle size for this packing material will contribute to a very large multi-path term for this column which may account for some of the excess band broadening. Another possibility for the poor efficiency at large capacity factor is that the polymeric stationary phase may be unevenly distributed over the glass beads leading to large, path dependent variations in capacity factor which is further aggravated by the large multipath term associated with the range of particle sizes for the glass beads. Another interesting possibility is that there may be a large resistance to mass transfer due to adsorption at the stationary phase/mobile phase boundary. There was considerable debate about the importance of adsorption effects in partition chromatography during the development of modern chromatographic theory. Band broadening due to adsorption in partition chromatography was considered to be insignificant for most forms whether they be LC or GC. WRP chromatography may finally show the effect of adsorption in partition chromatography due to the fact that the large decrease in phase volume ratio for WRP columns dictates a distribution constant which is two orders of magnitude larger than commonly encountered in previous types of partition chromatography. A discussion of the possible reasons for the excessive band broadening with increasing capacity factor is important, but will be saved for the end of this chapter so that discussion of some of the more general discussion of WRP LC can proceed.

Figure 4.5(A) Plate height as a function of linear flow velocity for WRP column #1 for the three most retained components of Figure 4.2(A), which were, butyrophenone (▲), benzene(□) and benzaldehyde(■). A linear flow velocity of 5.3 mm/sec corresponds to a volumetric flow rate of 1.6 mL/min. **4.5(B)** Plate height as a function of linear flow velocity for the separation shown in Figure 4.3(B)with a traditional porous C18 column (Keystone, 2.1 x 74 mm) and a mobile phase of 65% acetonitrile in water. Note that Figure 4.3(B) does not contain the same components as Figure 4.3(A) but is included to demonstrate that the performance of the C18 is relatively independent of the identity (or capacity factor) of the analyte. The porous C18 column was subject to very low back pressure so it was possible to obtain data for much higher linear flow velocities than the WRP column. Plate heights were determined from the measurement of the peak width at half height.

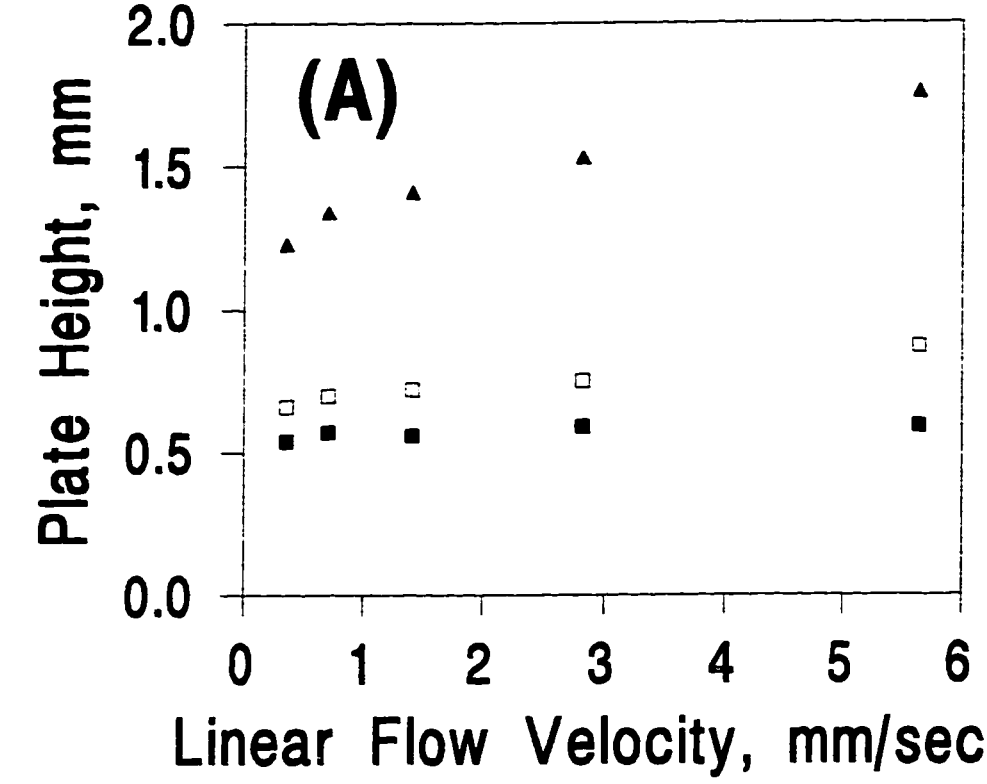
(A)
Plate Height, mm
2.0
1.5
1.0
0.5
0.0
0
1
2
3
4
5
6
Linear Flow Velocity, mm/sec

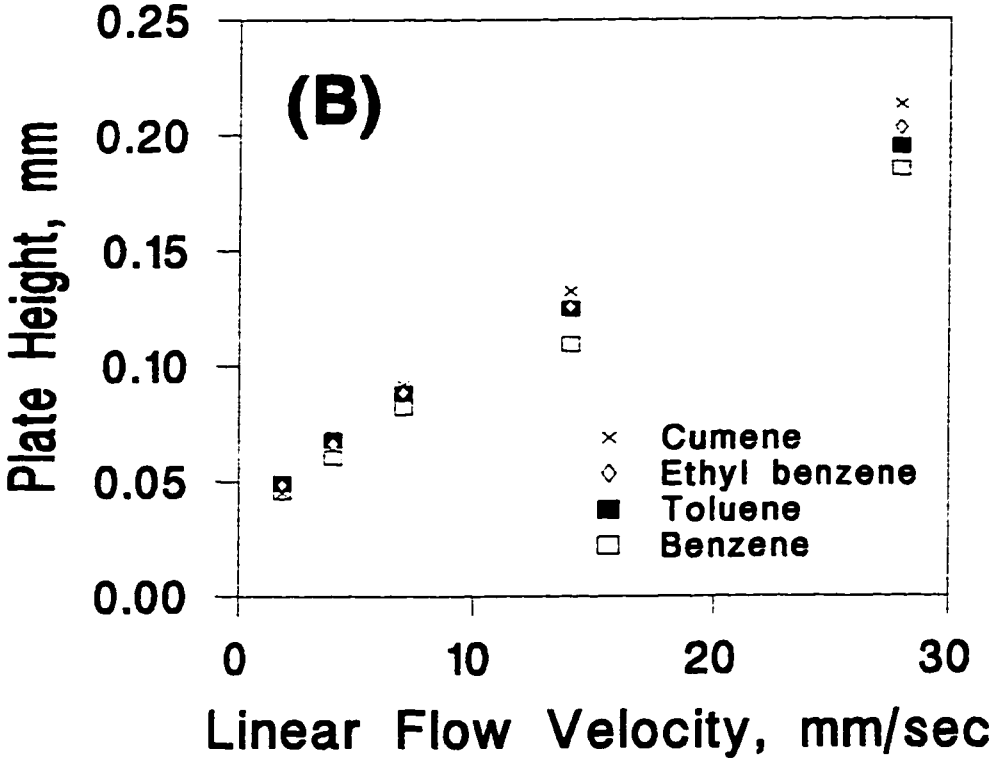
(B)
Plate Height, mm
0.25
0.20
0.15
0.10
0.05
0.00
0
10
20
30
Linear Flow Velocity, mm/sec
Cumene
Ethyl benzene
Toluene
Benzene

4.4.4 Demonstration of Reversed Phase Behavior; Capacity Factor Dependence Upon Mobile Phase Composition

The separation shown in Figures 4.2(A) and 4.3(A) demonstrates the analytical separation of components without the need for organic modifiers, but there are other techniques in LC that also make use of aqueous mobile phases without organic modifiers such as ion exchange chromatography[9] and hydrophobic interaction chromatography[10]. The novelty of this work is the demonstration of the utility of water-only mobile phase for separations of hydrophobic analytes by a reversed phase separation mechanism. To demonstrate that this separation operates by a reversed phase mechanism, the capacity factor of a retained component was measured in several different binary mobile phases made up of varying percentages of methanol in water. Perhaps the best known and most studied aspect of RP-HPLC is the approximately linear dependence of the logarithm of the capacity factor upon the percentage of water/organic in the mobile phase. This approximately linear behavior is demonstrated in Figure 4.6 for the logarithm of the capacity factor of butyrophenone in several methanol/water mobile phase compositions. Close examination of Figure 4.6 reveals a slight curvature of the line which suggests a slight quadratic behavior as reported by several authors[25,33-35] and which is consistent with eq 2. Fitting of the points in Figure 4.6 to a quadratic function provided an excellent fit with a correlation coefficient of 0.9997. Investigation of the behavior of the capacity factor with percentage of water has been extensive because the ability to predict the capacity factor of hydrophobic components in water (k'_w) on traditional columns is useful for the prediction of $\log P_0$ and $-\log X_0$ values. Due to the large phase volume ratio of traditional columns, large amounts of organic solvent are required to achieve reasonable capacity factors for very hydrophobic species. Extrapolation of capacity factors to a 100% water mobile phase has been reported, but there is often a large deviation from the quadratic model for mobile phases containing less than 10% organic modifier[11,25,36,37]. Many models have

Figure 4.6 An approximately linear relationship between log k' and the % water in the mobile phase is observed for the analyte butyrophenone in mobile phases from 40% methanol:60% water to 100 % water using WRP column #1. Close examination of the data indicates a very slight quadratic dependence upon the % water in the mobile phase.

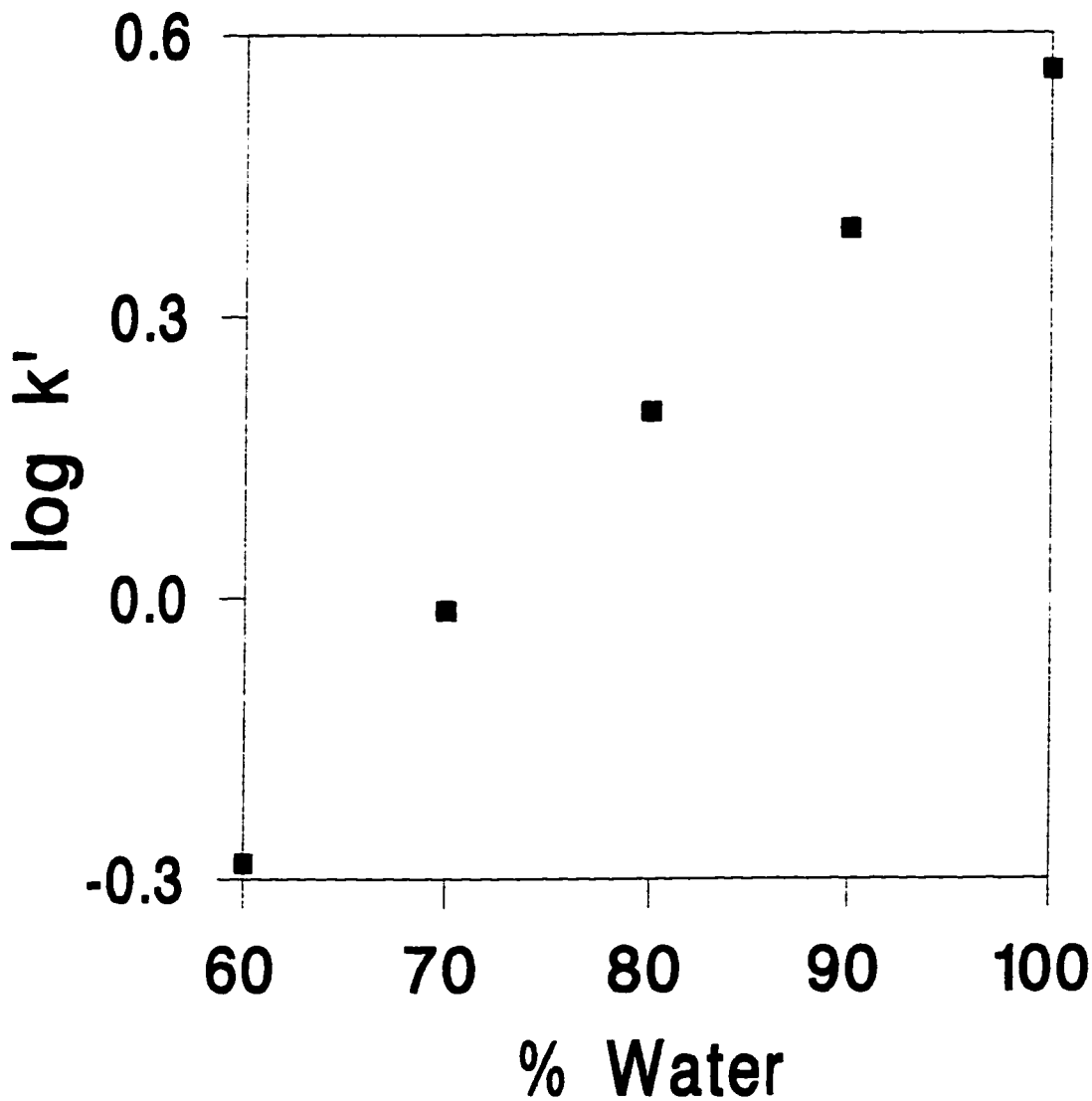
0.6
0.3
0.0
-0.3
log k'
60
70
80
90
100
% Water

been developed to predict k'_w from high organic content mobile phases, but an accurate model has not been produced. While these models lend support to a reversed phase mechanism for this separation technique, they also lend voice to the importance of directly measuring the capacity factor of these analytes in only water, as will be reported next.

4.4.5 Improved Prediction of Octanol/Water Partition Coefficients and Aqueous Solubility Using the WRP Columns

Predictions of aqueous solubility (X_0) and partitioning coefficients between octanol and water (P_0) for hydrophobic analytes are an ideal application of WRP-LC. There is a strong correlation between log P_0 and -log X_0 values and the capacity factor of the analyte in pure water. The difficulty in using traditional RP-HPLC columns to obtain the capacity factor is that the capacity factor in 100% water must be extrapolated from measurements in aqueous/organic mobile phases. A look at Figure 4.2(A) and 4.2(B) which show the separation of four components in a water-only mobile phase and also in a 70:30 methanol/water system, respectively, will illustrate the difficulty in making this extrapolation. Note that the selectivity changes drastically as the mobile phase system is changed so that the extrapolated prediction of the capacity factor in 100% water for any of these components using the C18 column as in Figure 4.2(B) would require measurements in several mobile phase compositions for each component and an extrapolation model for each component. The best approach to obtain capacity factors in 100% water is reduction in phase volume ratio and adjustment of stationary phase polarity to allow direct measurement of retention times for hydrophobic analytes in a water mobile phase as in Figures 4.2(A) and 4.3(A) Capacity factors for ten compounds were measured with WRP columns #1 and #2 in water and these values were compared to literature values for log P_0[38] and -log X_0.[39] The capacity factors for these ten compounds on columns #1 and #2 and also the reported log P_0 and -log X_0 values are tabulated in Table I in order of increasing

capacity factor. Note that the capacity factors are approximately twice as large for column #1 as for column #2 which is predicted by eq 1 since the phase volume ratio for column #1 is twice as large as for column #2. We can use the capacity factor and log P_0 values to infer the polarity of the TFPS phase relative to octanol. Since the phase volume ratio for column #2 was 0.01 and the capacity factor for cumene was 7.64, the distribution constant for cumene between the TFPS stationary phase and water is 764. For comparison, the distribution constant for cumene between octanol and water is calculated from the log P_0 value in Table I to be 4570. Since the distribution constant for octanol/water is larger than the distribution constant for TFPS/water and since the cumene is lower in polarity than either stationary phase material, we can surmise that the TFPS is more polar than octanol. Thus, determinations of capacity factors on non-porous polymer coated packing materials allows prediction of polymer properties as well as analyte properties. The plot of log k' versus log P_0 for column #2 is shown in Figure 4.7 and has a correlation coefficient of 0.998. The plot of log k' versus -log X_0 for column #2 is shown in Figure 4.8 and has a correlation coefficient of 0.998. These correlation coefficients compare quite well with values which have been achieved previously[17,18] but were obtained without the need to make several measurements and extrapolate to 100% water since the WRP column allows direct and rapid measurements in water. The correlations shown in Figure 4.7 and 4.8 are indeed a potentially useful application of the WRP column made with a TFPS stationary phase for a wide range of analyte hydrophobicity.

4.4.6 Sample Loading Capacity for WRP Columns

The loading capacity for an LC column is the maximum amount of material which can be injected onto the column without deteriorating chromatographic efficiency. The loading capacity for column #1 was tested by injecting increasing quantities of butyrophenone until the column efficiency began to deteriorate. Figure 4.9 shows a plot of peak width at half height versus the log of the mass of

Figure 4.7 Shown is a plot of log k' versus log P_0 for ten compounds as listed in Table I. Excellent correlation of experimental log k' to reported values of log P_0 is demonstrated with the WRP column #2. The experimental log k' values were obtained using the peak maximum as retention time for the analyte and dead time marker, which was sodium nitrate, in a water mobile phase on WRP columns #1 and #2. Typical determinations were made in less than two minutes. Log P_0 values were obtained from Reference 38.

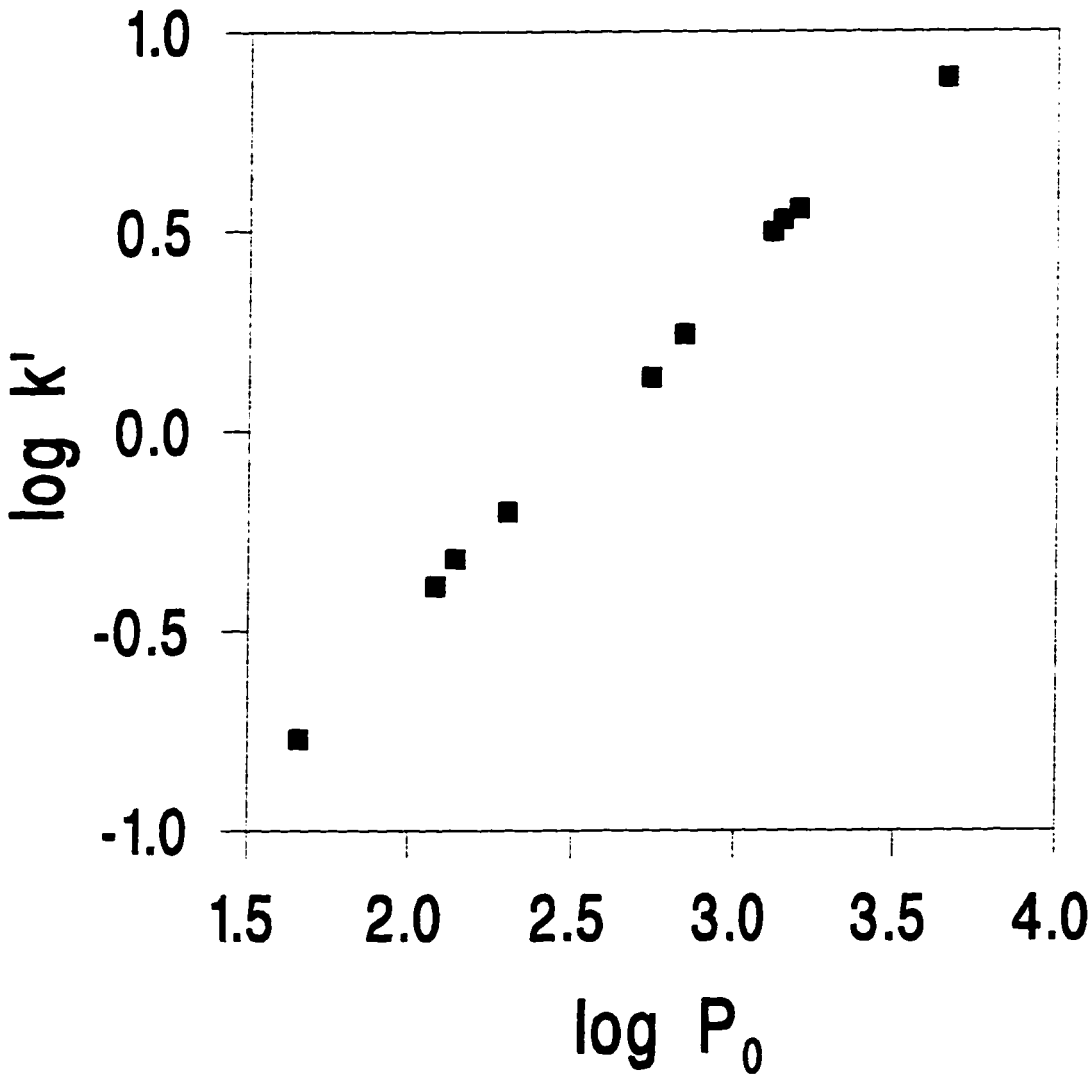
1.0
0.5
0.0
-0.5
-1.0
log k'
1.5
2.0
2.5
3.0
3.5
4.0
log P0

Figure 4.8 Similarly, experimentally determined capacity factors on a WRP column provide very good correlation to analyte solubility in water. Shown is a plot of log capacity factor determined on WRP column #2 versus the negative log of the aqueous solubility (-log X_0), as in Figure 4.7 and listed in Table I.

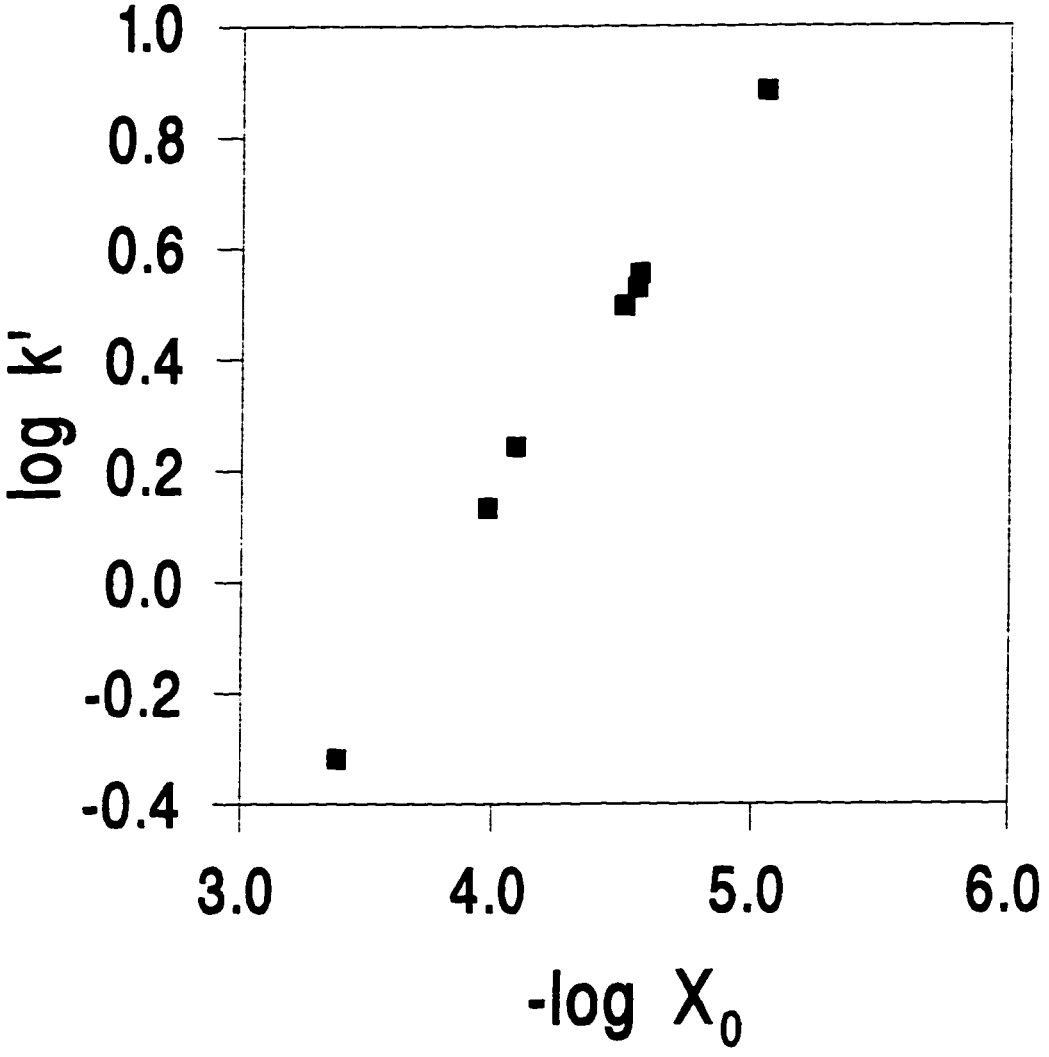
1.0
0.8
0.6
0.4
0.2
0.0
-0.2
-0.4
log k'
3.0
4.0
5.0
6.0
-log X0

Figure 4.9 The loading capacity for WRP column #1 is demonstrated in this plot of the peak width at half height (μL) versus the logarithm of the amount of analyte injected (ng). The analyte is butyrophenone and injections were made with a 20 μL injection loop for the six lower mass data points while a 1.0 μL injection disk was used for the three larger mass data points with butyrophenone concentrations of up to 10% by volume in methanol. The effect of column overloading is seen as a rapid increase in the peak width for loading of more than 20 μg.

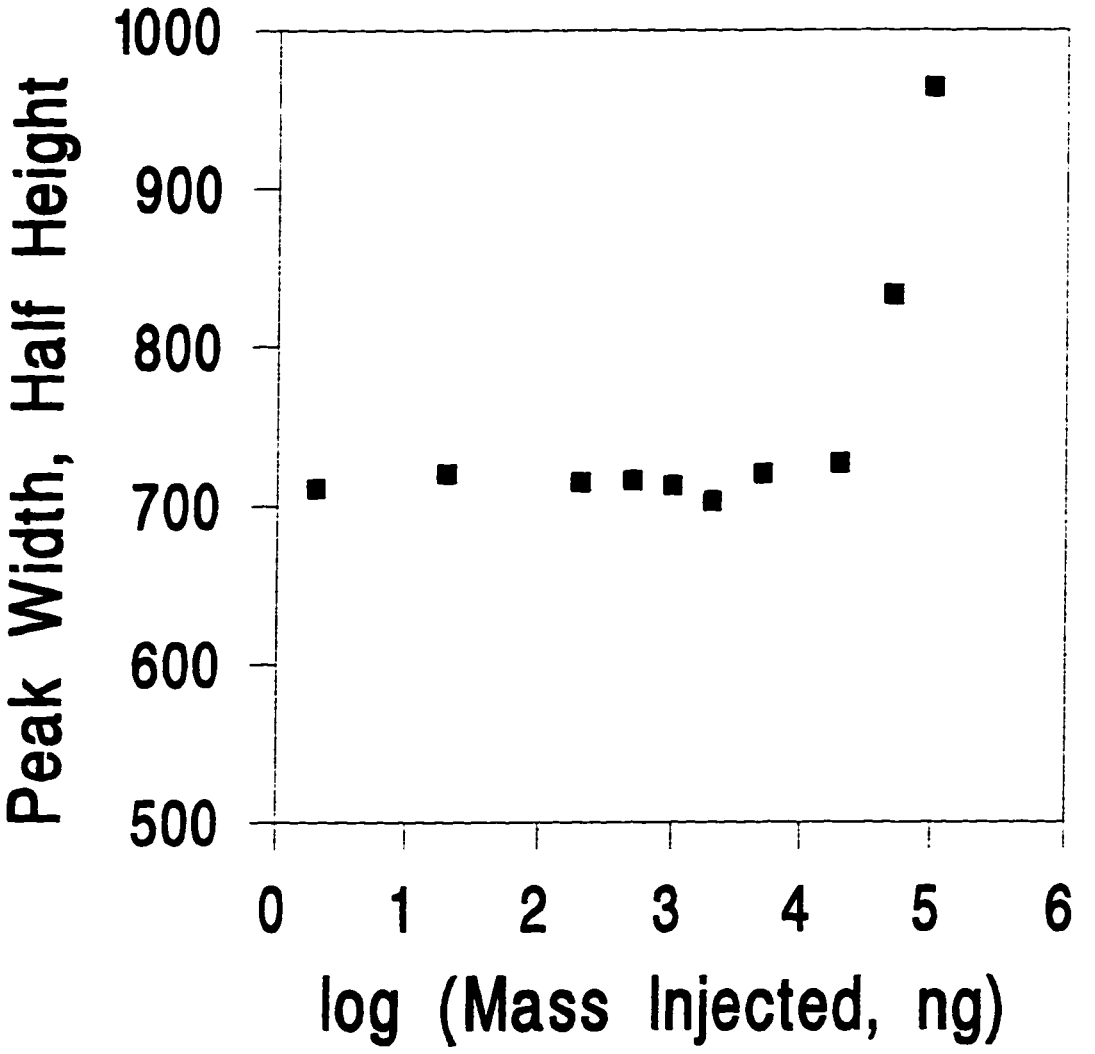
Peak Width, Half Height
1000
900
800
700
600
500
0
1
2
3
4
5
6
log (Mass Injected, ng)

butyrophenone injected. The peak width remains constant throughout most of the range, but injection of more than about 20 μg of butyrophenone causes the analyte zone to broaden with increasing mass injected as can be seen by the two data points at the far right in Figure 4.9. These two data points represent injections of 50 μg and 100 μg respectively. The effect upon capacity factor for the overloaded condition was interesting. As the peak width increased due to overloading the capacity factor actually began to increase slightly. This is probably due to an increase in phase volume ratio caused by swelling of the polymer and also possibly due to closer matching of the stationary phase polarity to the analyte polarity as the analyte began to contribute as significant fraction of the stationary phase volume. The data in Figure 4.9 suggest that the WRP column has suitable loading capacity for many chemical analysis applications.

4.4.7 Waste Water Monitoring Applications

The applicability for RP-HPLC separations with a water mobile phase extends to many types of chemical species and is well suited to environmental applications such as waste water monitoring of contaminated waters. As an example of the potential utility for such purposes, two very different type separations were performed with WRP column #1. Figure 4.10 shows the separation of the sodium salts of two surfactants, octyl sulfate (SOS) and dodecylsulfate (SDS). The small hump is very likely the 5% impurity in the octyl sulfate. Charged surfactants are usually separated by ion chromatography based on an ion exchange mechanism. The separation shown here is a reversed phase mechanism, with the SDS being more retained due to its larger hydrophobic tail. Unsuppressed conductivity detection was applied, and S/N was extremely high because the water mobile phase had an extremely low background conductance. A water mobile phase improves and simplifies conductivity detection[9]. The separation in Figure 4.11 is due to injection of water which was contaminated with gasoline. No effort was made to identify the peaks in the separation but they are likely due to various isomers of aromatic hydrocarbons having from six to eight carbons. The

Figure 4.10 Separation of a mixture containing one part per thousand (ppt) of sodium octyl sulfate (SOS) and two ppt of sodium dodecyl sulfate (SDS) on the WRP column #1. The 5 % impurity in SOS is labeled as I. Twenty microliters of the mixture was injected into a water mobile phase at a flow rate of 1 mL/min with unsuppressed conductivity detection.

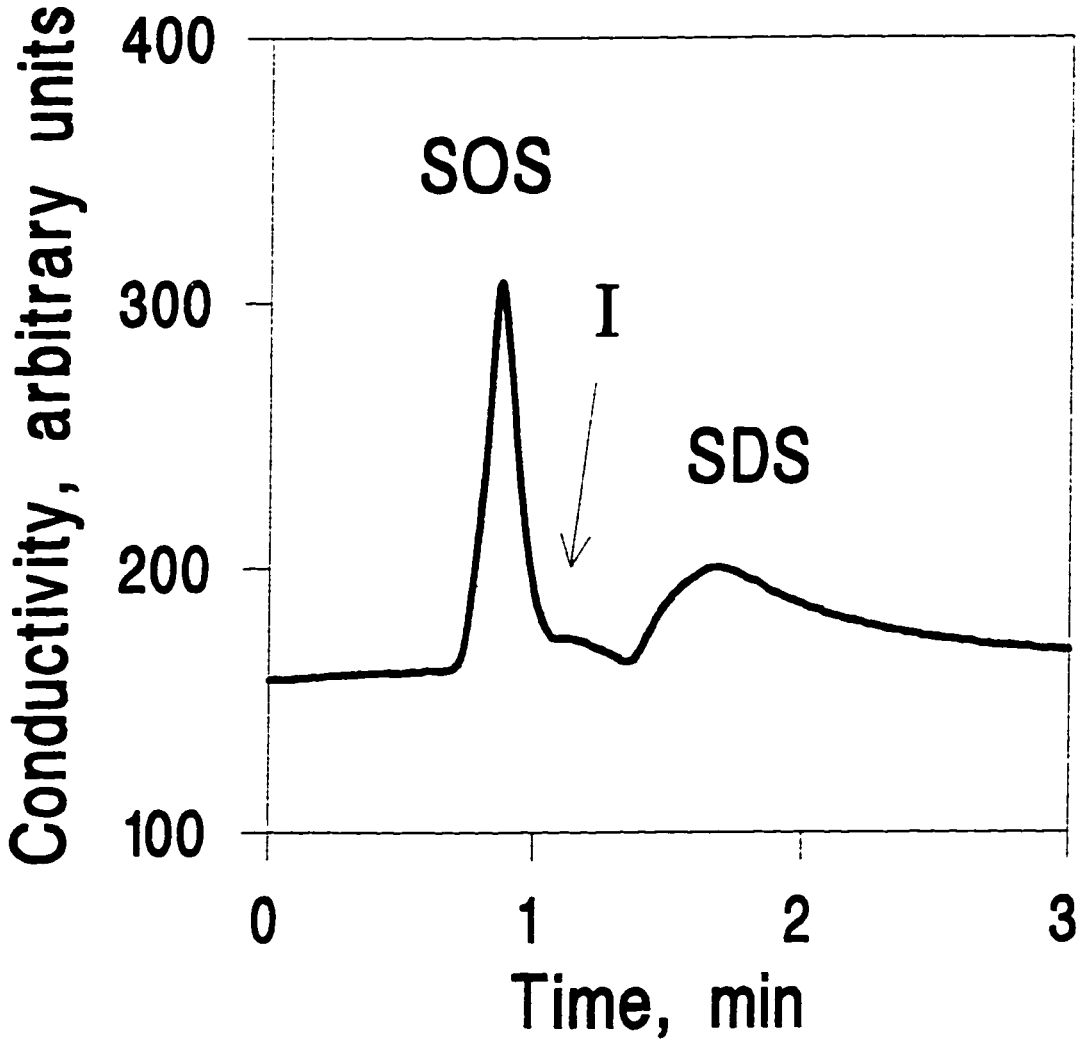
Conductivity, arbitrary units
400
300
200
100
SOS
I
SDS
0
1
2
3
Time, min

Figure 4.11 Separation of gasoline components in a contaminated water sample. Twenty microliters of a sample of water saturated with gasoline was injected onto WRP column #1. Flow rate of the water mobile phase was 0.8 mL/min. Components were monitored with UV/Vis absorbance detection at 260 nm.

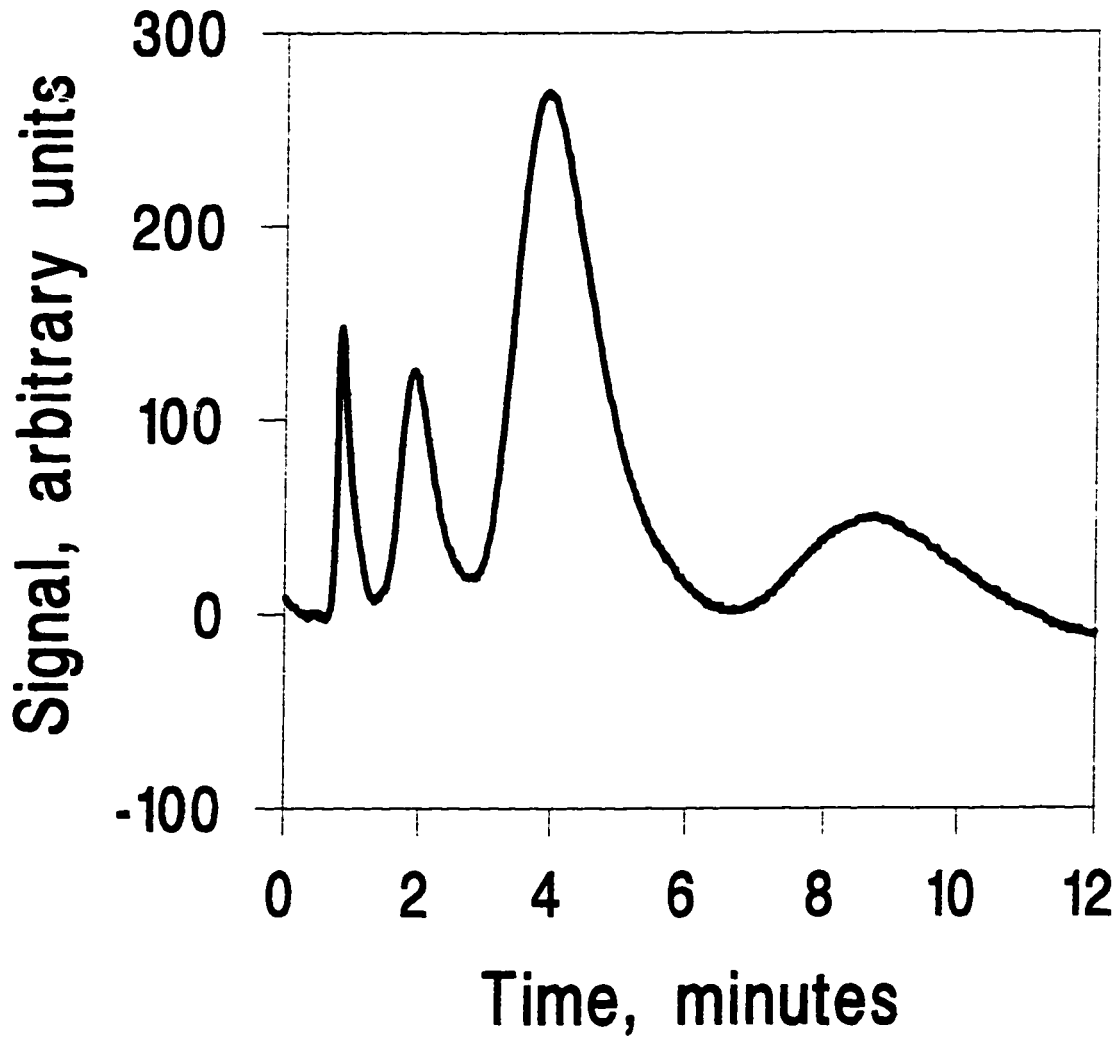
300
200
100
0
-100
Signal, arbitrary units
0
2
4
6
8
10
12
Time, minutes

beauty of the WRP system for gasoline monitoring is that the species which are of interest are the aromatic components which are selectively detected by the UV detector. For either of the two applications demonstrated here, the water mobile phase improves the detection limits for these compounds and will generally use no toxic chemicals such as organic solvents, and thus will generate very little waste. Operation of the waste water monitoring apparatus would be very straightforward. First, the instrument is centered around a specified WRP column that has been designed to provide the desired separation and chemical analysis of the analytes of interest using only water as the mobile phase. Sample introduction and mobile phase delivery is done in conventional way, with an injection valve. Second, the effluent from the WRP column is directed to a detector designed for liquid chromatography. Third, after passing through the detector, the effluent is passed through a mobile phase "clean-up" column, packed with a high capacity commercial C18, in order to extract out the small quantities of analytes that were previously separated on the analytical WRP column. Thus, the water mobile phase eluting from the clean-up column can be recirculated to serve as the mobile phase for future separations and chemical analyses. This instrument, as described, should function as a closed loop, coupled with introducing small volume samples using an automated injection valve and established sampling technology. Advantages for this instrument are many. Mobile phase preparation and cost is minimal, since pure water is used. Likewise, the closed loop design should require very little maintenance, with the clean-up column requiring replacement occasionally. Analyte breakthrough on the clean-up column will be easily diagnosed as an increase in the detected background, alerting the analyst to replace it. By using a clean-up column with a high capacity, the time between this maintenance should be long.

Alternatively, a continuously applied closed-loop design may not be the best implementation, especially if the detected effluent from the WRP column contains levels of analytes that are diluted enough in the water mobile phase to be returned directly to the original sample source, such as a waste water stream that is within

specifications. Likewise, if a small micellar mobile phase additive is used, then the mobile phase may be safe and legal to expel directly to the waste water stream being monitored. Since microbore columns operate at very low flow rates (2 μL/min typical for 0.25 mm i.d.), continuous operation without mobile phase recycling for a year can be obtained with a water reservoir of only one liter. For a 1 mm i.d. microbore column, at a flow rate of 40 μL/min, a mobile phase reservoir of only 20 L is required for continuous monitoring. In order to avoid reintroducing pollutants to the environment, the instrument should be designed with the in-line clean-up column as a microprocessor controlled option that is engaged in real-time whenever the detected separation indicates the presence of analyte pollutants that are above safe levels.

4.4.8 Improved UV/Vis Detection Using Water Only as the Mobile Phase

The detection advantage for an all water mobile phase for ion chromatography has been documented and will not be repeated here. The advantage of an all water mobile phase for UV detection should also be considerable and will be developed and shown in this section. UV detection is the most commonly used detection technique for HPLC for a number of reasons. A good UV detector will have a large dynamic range, with an approximately linear response over an absorbance range of perhaps four or more orders of magnitude. Many analytes of interest, such as any compound containing an aromatic system, have reasonably large molar absorptivities and so show good sensitivity for UV detection. Most commonly used mobile phases are mixtures of water and some simple organic solvent, and these mobile phases will have a very low absorbance as compared to the analyte of interest. Since the solvent has a low molar absorptivity and the analyte has a high molar absorptivity, the analyte signal can be measured against a low background so that a good signal to noise ratio is obtained. Fluorescence detection is also applied to HPLC and signal to noise ratios are commonly obtained which are much better than UV detection schemes. The advantage of fluorescence detection is that the signal due to the background is drastically reduced

so that the analyte signal is measured with respect to a very small amount of noise for in increase in signal to noise ratios. Unfortunately, very few analytes exhibit any significant fluorescence signal so that a derivatization step is generally required to convert a target analyte into a species which has a strong fluorescence signal. One of the large advantages which WRP column chromatography has for UV detection is that the molar absorptivity for water is smaller than for any other solvent. The way to capitalize on this advantage is to choose detection conditions such that the background absorbance of the mobile phase solvent is the dominant source of noise. There are two ways which the detection scheme could be altered to demonstrate the advantage of an all water mobile phase for HPLC detection. Signal to noise improvement could be demonstrated by either using a longer pathlength or also by switching to lower wavelength radiation. Switching to a longer pathlength will increase the amount of signal due to both analyte and solvent, since the absorbance is proportional to the pathlength. The analyte signal will increase with pathlength while the noise remains fairly constant for an increase in signal to noise ratios until the absorbance of the solvent becomes excessive and the increased noise due to stray light will mitigate the advantage of increasing path length. At a commonly used wavelength such as 260 nm, it is not known how long the pathlength would have to be in order to demonstrate the advantage of an all water mobile phase over a mixed aqueous organic mobile phase, but there it might be feasible to demonstrate a practical advantage for larger analytical columns where fairly long path lengths can be used without introducing additional band broadening due to the detector volume. A simpler demonstration of the advantage of an all water mobile phase is the use of very short wavelength radiation such as wavelengths below 200 nm. It is commonly known that the organic solvent will provide a fairly large background absorbance at very low wavelengths which at some point will begin to adversely affect the signal to noise ratio. Because of the significant absorbance of the solvent at very short wavelengths, a longer wavelength such as 260 nm is commonly chosen to avoid large background absorbance by the solvent. What is less commonly known is that the molar absorptivity for almost all species increases

rapidly with decreasing wavelength into the shorter UV region. Since water has an extremely low molar absorptivity even at 190 nm, the use of UV for detection of species in water around 190 nm should result in better detection limits than would be achieved in an aqueous/organic mobile phase. In order to demonstrate the effect of going to lower wavelengths while using an all water mobile phase, the separation of a mixture of sodium nitrate, benzene and toluene on WRP column #1 is shown using a UV detector at two different wavelengths. Figure 4.12(A) shows the separation at 260 nm and Figure 4.12(B) shows the separation at 200 nm. Both chromatograms show a peak to peak noise level of about 10^{-5} A.U. which is good performance for a UV detector. While the noise is similar for both chromatograms, the analyte signal is increased by nearly two orders of magnitude at 200 nm as opposed to 260 nm. The benefit of going to the lower wavelength can be easily quantified. The benzene peak had a signal to noise ratio of 25 at 260 nm and 1500 at 200 nm. The resulting detection limits are 65 ppb at 260 nm and approximately 1 ppb at 200 nm. This is a considerable difference. The question which might be asked at this point is whether or not the water mobile phase is even required to capitalize on the increased signal to noise ratios induced by the enhanced absorptivities at very short wavelengths. From the data obtained, it would appear that the all water mobile phase was crucial for realizing the improved signal to noise at shorter wavelengths. The UV signal at 190 nm was measured for a single, non-retained component eluted through WRP column #1 with pure water as shown in Figure 4.13(A) and in 70: 30 methanol/water as shown in Figure 2.14(B). The analyte was butyraldehyde which would normally not even be considered for UV detection without derivatization. Surprisingly, the butyraldehyde had a respectable detection limit of 4 ppm in the 70:30 methanol/water mobile phase at 190 nm and a detection limit of 0.35 ppm in the all water mobile phase. The enhanced signal to noise achievable by using an all water mobile phase at very short wavelengths not only improves the detection limits for analytes commonly analyzed with UV detection, but also opens the door for application of UV detection with reasonably

Figure 4.12 Separation on WRP column #1 of a mixture containing: 0.30 ng of sodium nitrate [S], 80 ng of benzene [B], and 140 ng of toluene [T]. The flow rate of the pure water mobile phase was 1.0 mL/min. **4.12(A)** UV/Vis detection of the separation monitored at 260 nm. **4.12(B)** UV/Vis detection of the same separation but at a wavelength of 200 nm. Due to the increase molar absorptivity at 200 nm and the extremely low background absorbance of the water mobile phase, the detection limit is improved by about two orders of magnitude as compared to Figure 4.12(A).

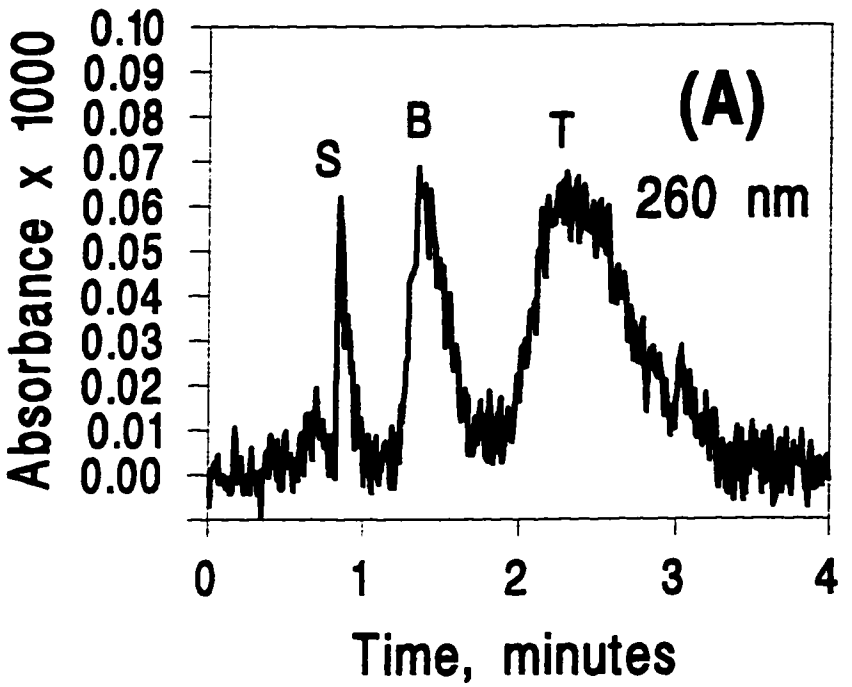
Absorbance x 1000
0.10
0.09
0.08
0.07
0.06
0.05
0.04
0.03
0.02
0.01
0.00
S
B
T
(A)
260 nm
0
1
2
3
4
Time, minutes

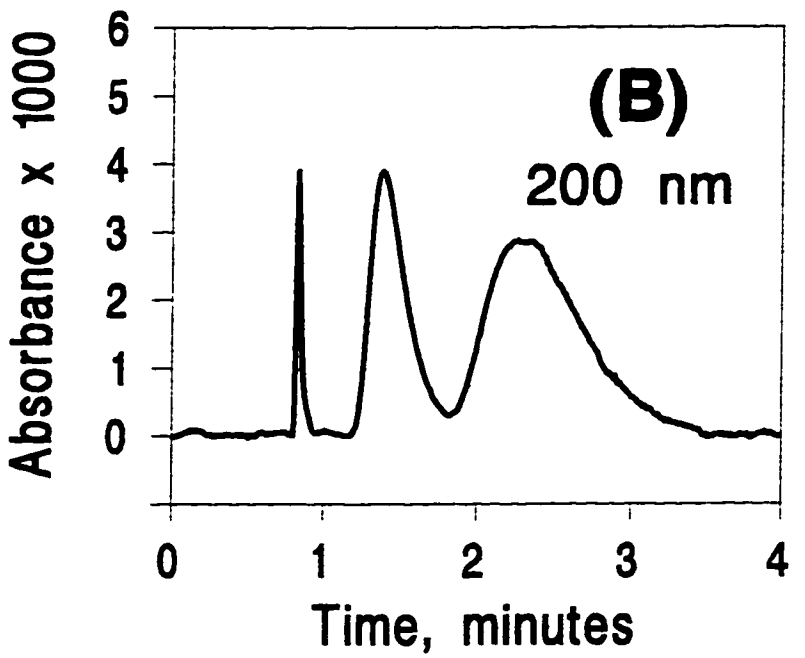
Absorbance x 1000
6
5
4
3
2
1
0
(B)
200 nm
0
1
2
3
4
Time, minutes

Figure 4.13 A demonstration of the improvement in UV/Vis detection by using water as the mobile phase rather than an organic solvent. The analyte is a total of 8 micrograms of butyraldehyde injected into WRP column #1 with detection at 190 nm and the mobile phase flow rate was 0.25 mL/min. **4.13(A)** UV/Vis detection with a 70:30 methanol/water mobile phase. **4.13(B)** Identical conditions to Figure 4.13(A) except the mobile phase is pure water.

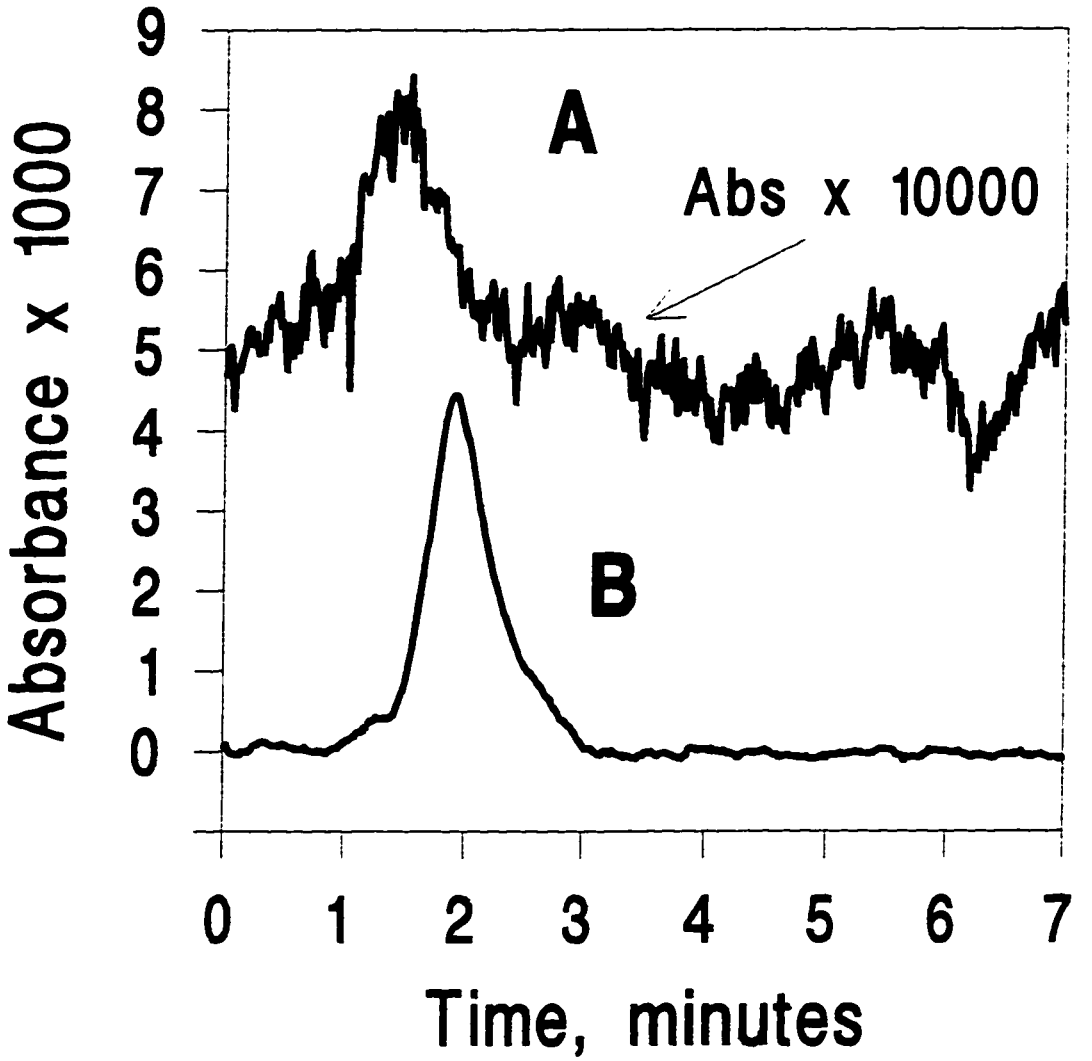
Absorbance x 1000
9
8
7
6
5
4
3
2
1
0
A
Abs x 10000
B
0
1
2
3
4
5
6
7
Time, minutes

good detection limits for analytes such as butyraldehyde which are very weak chromophores.

4.4.9 General Discussion of WRP Column Efficiency

As discussed in Section 4.4.3, the WRP columns developed do not perform as well as commercial C18 columns. In particular, the efficiency of the WRP column seems to decrease rapidly with increasing capacity factor. In contrast, the ratio of the peak width to retention time for peaks on the C18 columns is essentially constant and since the square of the ratio of retention time to peak width is equal to N, the number of plates for the column, it is equally accurate to state that N is also essentially constant with respect to retention for the C18 column, which is what is commonly observed with packed columns in HPLC. The efficiency of WRP column #1 and a C18 column was measured for the four retained components of Figures 4.3(A) and 4.3(B) and is shown versus the capacity factor for each component in Figure 4.14. As discussed above, the efficiency does not show any dependence upon capacity factor for the C18 column, but worsens with increasing capacity factor for the WRP column. Additionally, the non-retained component for the WRP column displays poorer efficiency than any of the peaks shown for the commercial C18 column. The increased capacity factor range for the reduced phase volume WRP column as discussed in Section 4.2 can also be seen in Figure 4.14. For a more complete look at the affect of capacity factor upon chromatographic efficiency, the plate height was measured for fourteen different compounds as shown in Figure 4.15. Figure 4.15 shows an decrease in efficiency with increasing capacity factor but suggests that the capacity factor dependence may begin to level off at very high capacity factor rather than increase without bound. The conclusions evident in the efficiency data for the WRP column so far is that the efficiency is a function of the capacity factor and decreases with capacity factor, although probably with less than the first power of the capacity factor, and that the efficiency of the non-retained component is not as good as it should be.

Figure 4.14 Plot of the plate height versus the analyte capacity factor for the aromatic hydrocarbon components separated on WRP column #1(■)as shown in Figure 4.3(A), and and on a commercial C18 column (□) as shown in Figure 4.3(B)

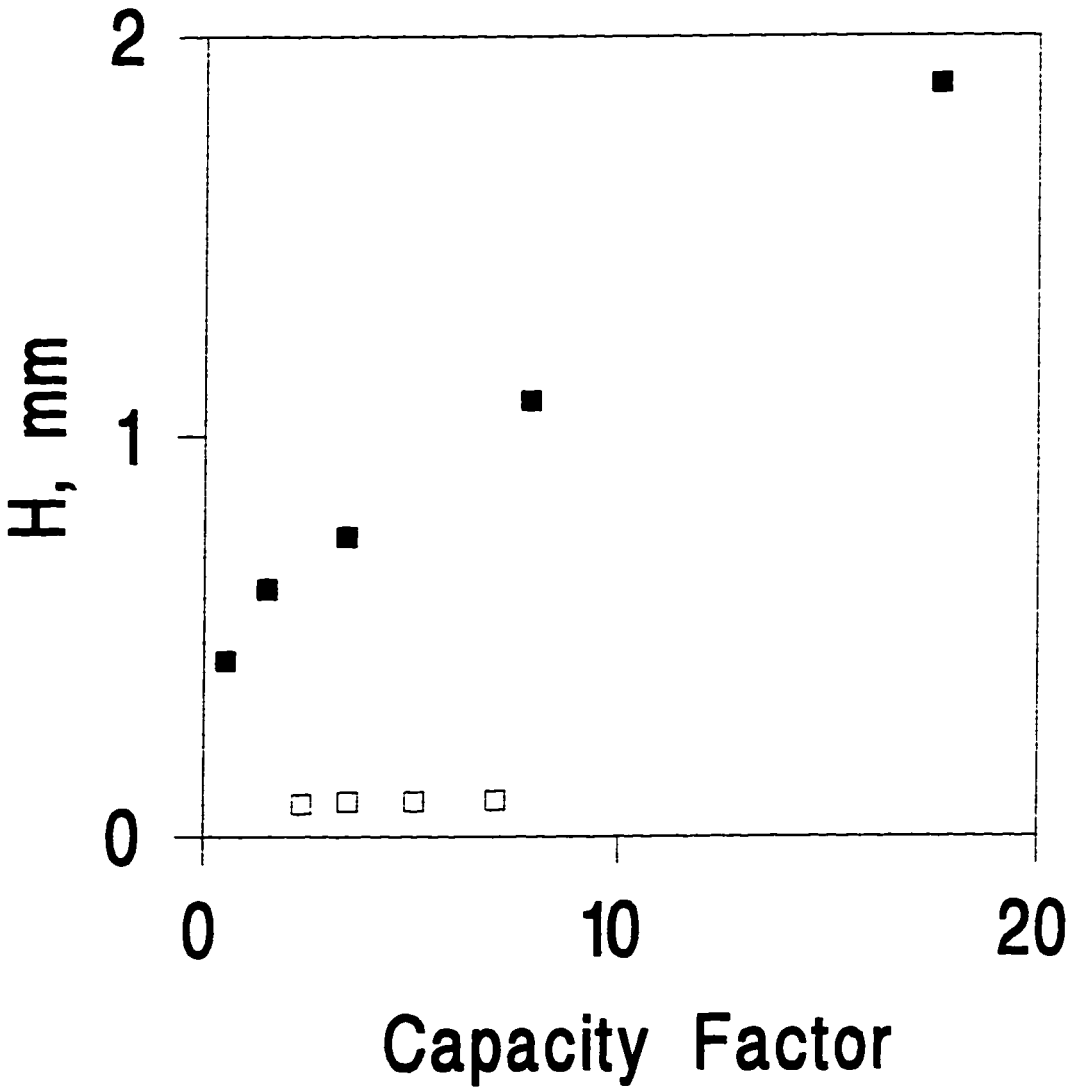
2
1
0
H, mm
0
10
20
Capacity Factor

Figure 4.15 Plot of the plate height versus the capacity factor for fourteen different components obtained from WRP column #1.

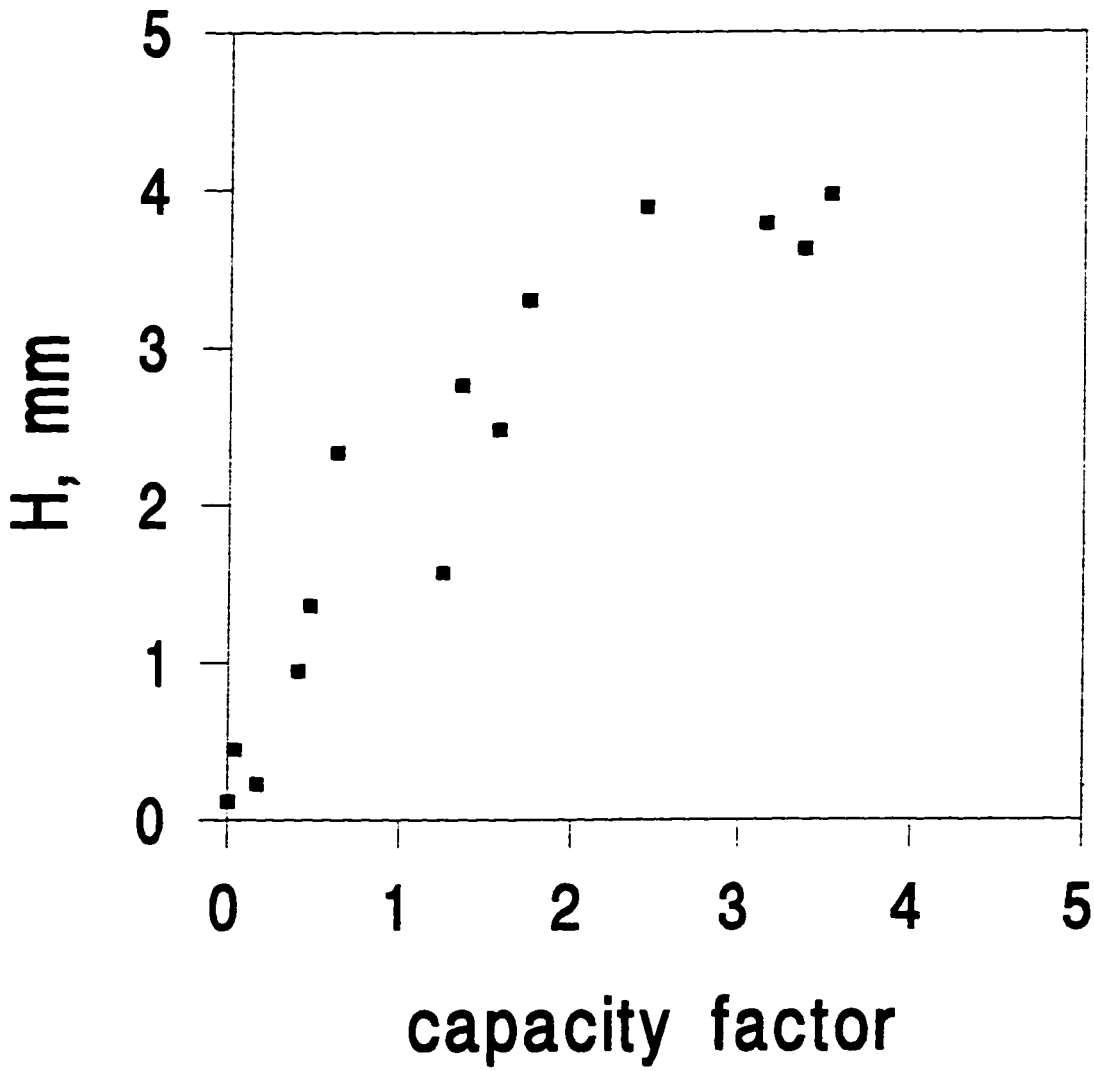
H, mm
0
1
2
3
4
5
0
1
2
3
4
5
capacity factor

To begin to understand the reasons for the poor efficiency of the WRP column the differences between the WRP column and commercial columns should be restated. Packing of the WRP columns was done without the use of a slurry packer. Since a slurry packer was unavailable, the WRP columns were packed with a standard high pressure chromatographic pump and an empty column as the slurry reservoir. The WRP column packing is composed of a wide size distribution silica which is widely stated by column manufacturers to be a source of band broadening. The WRP column stationary phase is an adsorbed polymer layer which may or may not be evenly coated on the silica surface. Uneven coating would lead to regions of higher and lower capacity factor which would result in increased broadening of peaks with capacity factor as is observed. Additionally, if regions of the silica are left uncoated, there could be band broadening due to adsorption to the silica surface for analytes having significant basicity. The mobile phase used is pure water which may be a source of band broadening due to kinetic effects such as slow mass transfer at the water/stationary phase interface due to poor wetting of the stationary phase caused by the high interfacial tension at the boundary.

The poor performance of the non-retained component on the WRP column is almost certainly due to either poor packing of the stationary phase or to the wide size distribution of the packing. To differentiate between these two sources of band broadening, a monodisperse silica was obtained and derivatized with a cyanopropyl silane and packed by the same procedure as the other WRP columns. The reduced plate height as a function of reduced flow velocity for an unretained component is shown in Figure 4.16. Since the reduced plate height goes to nearly theoretical efficiency, the packing techniques used must be sound and the source of band broadening for unretained components must be due to the wide size distribution of the packing material. A sample chromatogram from this column is displayed in Figure 17 for a volumetric flow rate of 16 microliters per minute. Unfortunately, the column packed for this experiment was ruined before the performance for retained components could be evaluated.

Figure 4.16 Reduced variable van Deemter plot for the cyanopropyl silane derivatized, 8 micron, nonporous, monodispersed WRP stationary phase. The column was 2.1 x 250 mm and the plate height was calculated from the width of the peak at half height. For calculation of the reduced flow velocity, the diffusion coefficient was taken to be 0.4 cm^2/sec.

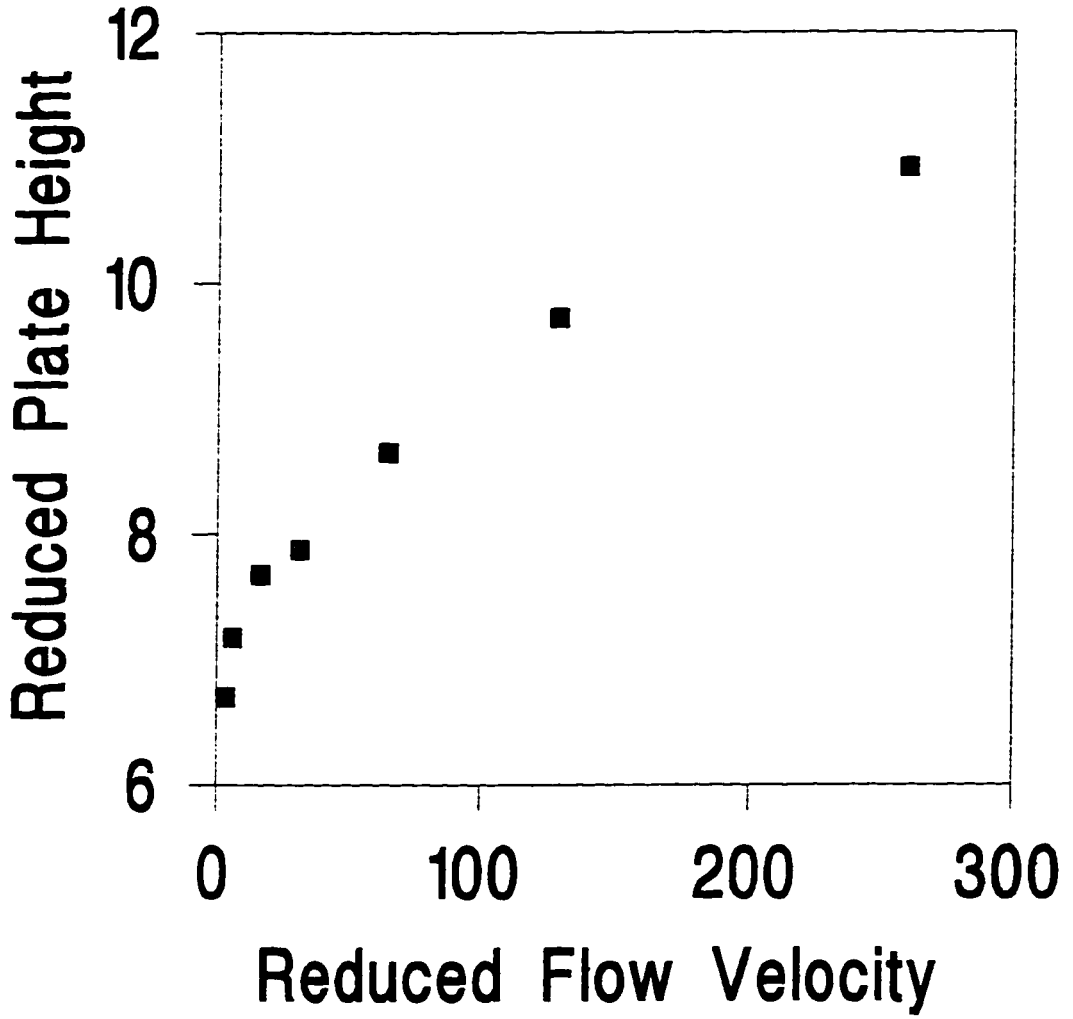
Reduced Plate Height
12
10
8
6
0
100
200
300
Reduced Flow Velocity

Figure 4.17 One of the better chromatograms from the data used for Figure 4.16. The analyte is sodium nitrate and the volumetric flow rate of the pure water mobile phase is 16 microliters per minute. UV/Vis detection at 260 nm was used.

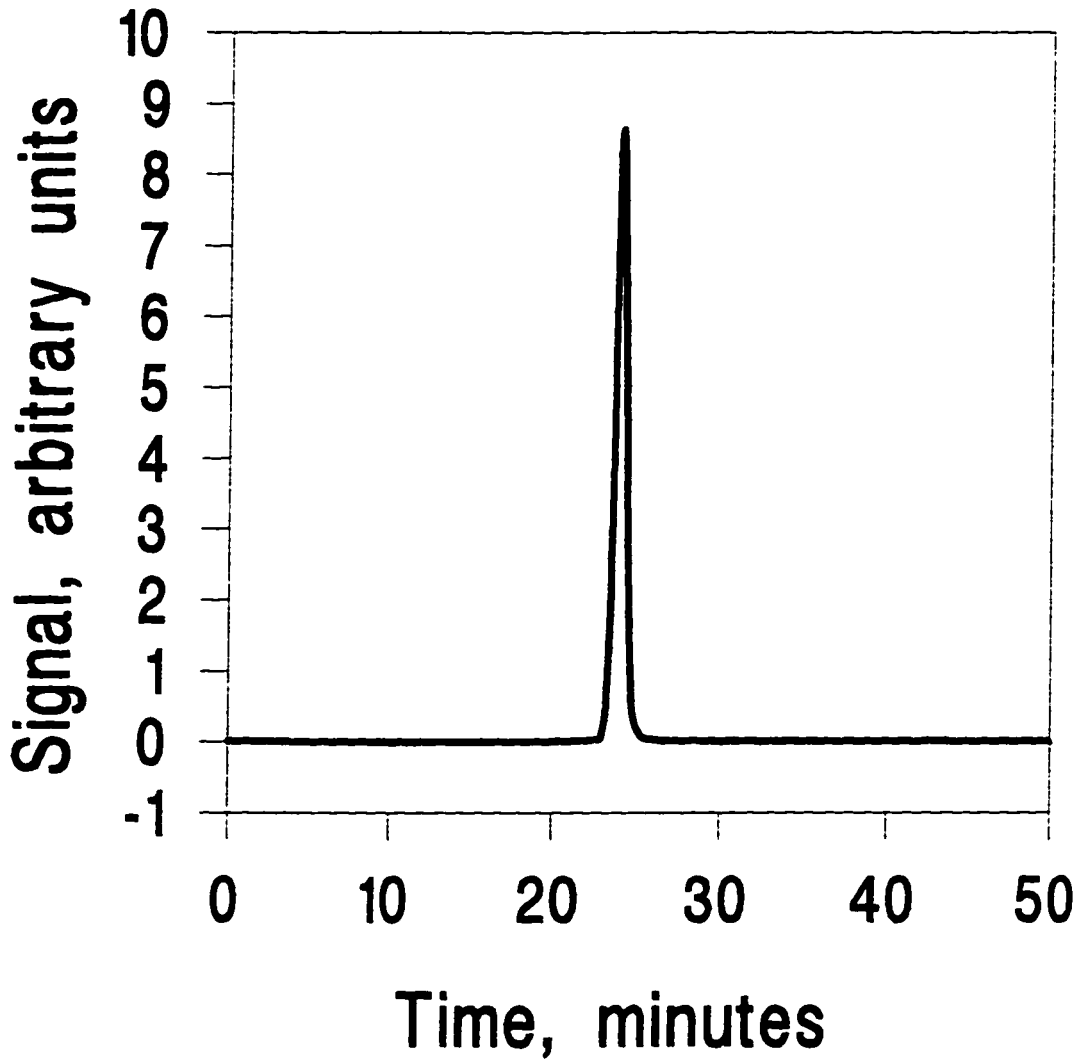
Signal, arbitrary units
10
9
8
7
6
5
4
3
2
1
0
-1
0
10
20
30
40
50
Time, minutes

The cause for increasing band broadening with capacity factor is more complex and it is helpful to first rule out some possible causes. Adsorption at exposed silica surfaces can be ruled out since the very basic species, aniline showed no more band broadening on WRP column #1 than benzene although they both had the same capacity factor.

A brief discussion of traditional band broadening theory is also instructive. Giddings 1965 book remains the most comprehensive discussion of band broadening theory.[40] Some general statements about band broadening terms can be made in reference to Giddings work. At very slow flow rates the contribution of longitudinal diffusion may become significant. Slow diffusion in the stationary phase contributes to band broadening at increases linearly with the flow rate. This term is usually not dominant and displays a maximum for components with a capacity factor of one and can be ruled out. At flow rates which are likely to be used with HPLC, the majority of band broadening is caused by flow rate inequalities in the mobile phase. On the smallest scale, there exist a range of velocities in the interstitial region between particles due to the laminar nature of liquid flow. This term has a large dependence on capacity factor and is the only flow rate inequality found in capillary columns which explains the efficiency dependence upon capacity factor displayed by capillary columns. For packed columns, there are additional flow rate inequalities which are attributable to the packing structure of the entire column. For instance, flow in one region of the channel will be faster than in a flow channel located a few particle distances away or at opposite edges of the column. The capacity factor dependence upon flow inequalities due to the packing structure is very mild or nonexistent and since these types of inequalities are dominant for most packed columns, little or no efficiency dependence upon capacity factor is observed for most packed columns. The conclusion to be drawn for the WRP column is that if flow rate inequalities are the dominant source of band broadening, as observed for most packed columns, then the largest flow inequality must exist in an interstitial regions between particles rather than at larger distances across the width of the column. This is entirely possible if the large and small particles tend to aggregate

into impermeable clumps leaving larger capillary like regions to carry the majority of the flow. The problem is easily eliminated by using a monodisperse packing material.

The most likely reason for the relatively poor performance of the WRP columns is local variations in capacity factor in the columns due to regions of differing phase volume ratio. If the polymer coating is not of uniform thickness there will be regions of differing phase volume ratio. Even if the polymer coating is of uniform thickness, there will still exist variations in phase volume ratio due to the non-uniform size of the packing material. The phase volume ratio will be larger in the vicinity of smaller particles since smaller particles have a larger surface to volume ratio. The observation of the effect of regions of varying phase volume ratio was made by Knox and Saleem in the study of packed columns in GC.[41] He observed that there often was a strong plate height dependence upon capacity factor which was not predicted in the theory advanced by Gidding for polymer coated particles in packed columns for GC. He attributed this to variations in phase volume ratio and derived an expression to account for the plate height dependence upon capacity factor due to variations in phase volume ratio. According to their theory[41], the plate height dependence upon capacity factor is

$$H \propto [\, k'/(1 + k')]^2 \qquad (5)$$

A plot of H versus capacity factor predicted by eq 5 and for the experimental results from the WRP column is shown in Figure 4.17. The dependence upon capacity factor predicted by eq 5 for variations in phase volume ratio is in excellent of the observed capacity factor dependence for the WRP column. Since the WRP columns must have some variation in phase volume ratio due to the size variation of the packing material, it is likely that this is the cause for the relatively poor chromatographic efficiency of the WRP columns.

One further issue which should be addressed is the possible contribution to band broadening due to adsorption at the water/stationary phase boundary. The band broadening contributions discussed thus far are easily fixed by using monodispersed particles and a uniform stationary phase. Adsorption might be a more difficult problem to address and has been previously attributed to significant band broadening in RP-

Figure 4.18 Overlay of the plate height versus capacity factor data obtained from the WRP column as in Figure 4.15 and the dependance of plate height on capacity factor due to variations in phase volume ratio predicted by reference 41.

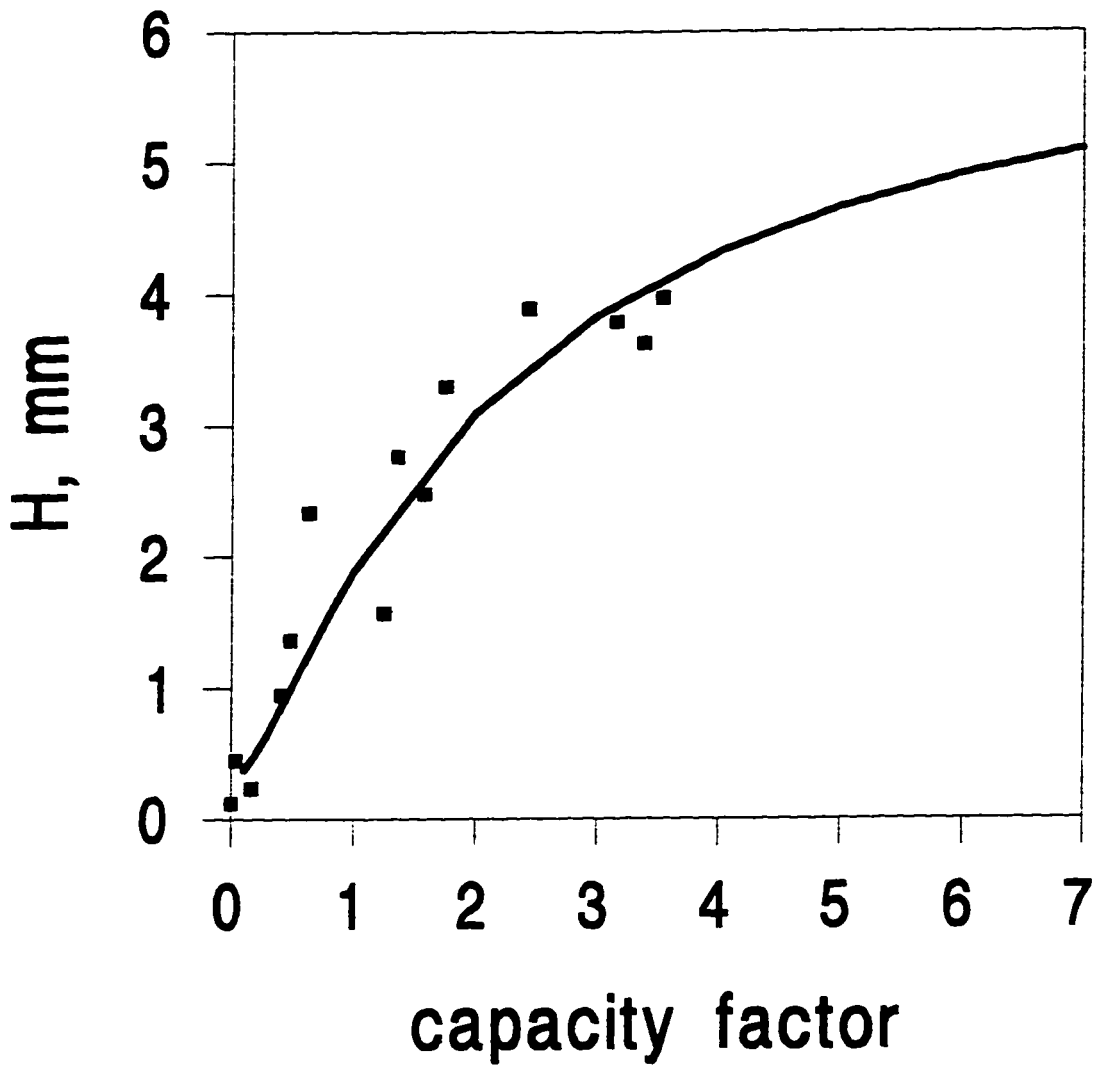
H, mm
0
1
2
3
4
5
6
0
1
2
3
4
5
6
7
capacity factor

HPLC with a water mobile phase. Horvath and Linn[42] developed a method for the evaluation of individual plate height contributions in the general plate height equation for HPLC. In one set of experiments they used a standard C18 column for the separation of organic acids in a buffered water mobile phase and attributed amount of the band broadening of the more retained components to adsorption at the water/stationary phase boundary. They suggested that the plate height dependence upon capacity factor due to adsorption at the water/stationary phase interface is given by

$$H \propto [\, k'/(1 + k')]^2 \qquad (6)$$

Note that this expression is identical to eq 5 describing the plate height dependence upon capacity factor due to variations in phase volume ratio. While it seems likely that the efficiency of the WRP columns developed were limited by phase volume ratio variations, adsorption effects can not be ruled out. Future research into the development of WRP columns should proceed by developing uniform phases on monodispersed particles. If the efficiency continues to display this type of capacity factor dependence then the role of adsorption will need to be addressed. Derivatization with a silane agent having a polar end group and would likely minimize any adsorption at the water/stationary phase interface.

4.5 Conclusions

The results of this research will most directly affect users that are interested in eliminating the generation of organic waste while performing RP-HPLC. WRP column chromatography is a chemical analysis methodology which will not produce any additional hazardous waste. Development of methodology by which organic modifiers can be reduced or eliminated from analysis by WRP-LC should have a real benefit to many laboratories that use RP-HPLC for analysis by reducing or possibly eliminating organic solvent consumption and disposal. The reduced solvent methodology developed should also be an excellent technique for waste water monitoring

applications. In addition to the reduction or elimination of hazardous waste caused by RP-HPLC, WRP columns have some distinct advantages over traditional C18 columns. The use of water as a mobile phase provides significant improvement for conductivity and UV detection and probably for fluorescence as well. The use of reduced phase volume ratio packing materials also offers the potential for increased peak capacity as opposed to standard porous based packing materials. In light of these benefits, the development of WRP methodology offers considerable benefit to the field of analytical chemistry

4.6 Notes to Chapter 4

1. Glajch, J. L.; Kirkland, J. J.; Snyder, L. R. *J. Chromatogr.* **1982**, 238, 269.
2. Fazio, S. D. et. al. *Anal. Chem.* **1985**, 57, 1559.
3. Grushka, E. in *Preparative-Scale Chromatography, Chromatogr. Sci. Series: Volume 46*, Marcel Dekker, 1989.
4. Karger, B. L.; Snyder, L. R.; Horvath, C. in *An Introduction to Separation Science*, Wiley-Interscience, New York, NY, 1973, Chapter 5.
5. Giddings, J. C. in *Unified Separation Science*, Wiley-Interscience, New York, NY, 1991, Chapters 10-12.
6. Moore, L. K.; Synovec, R. E. *Anal. Chem.* **1993**, 65, 2663-70.
7. Renn, C. N.; Synovec, R. E. *Anal. Chem.* **1991**, 63, 568-74.
8. Saito, M.; Hibi, K.; Ishii, D.; Takeuchi, T. in *Introduction to Microscale High-Performance Liquid Chromatography*, Ishii, D., ed. , VCH, 1988, Chapter 2.
9. Small, H.; Soderquist, M. E. Patent # 4,732,686 Weak Eluant Ion Chromatography March 22, 1988.
10. Horvath, C.; Haidacher, D. *Theoretical Advancement in Chromatography and Related Separation Techniques*; Dondi, F.; Guiochon, G. ed's., Kluwer Academic Publishers, Netherlands, 1992.
11. Jandera, P.; Kubat, J. *J. Chrom.* **1990**, 500, 281-99.
12. Hartwick, R. A.; Colwell, L. F. Jr. *J. High. Res. Chrom.* **1986**, 9,304-5.
13. Kronberg, B; Silveston, R. *J. Phys. Chem.* **1989**, 93, 6241-6.
14. Kronberg, B.; Silveston, R. *J. Chrom.* **1994**, 659, 43-56.
15. Giesche, H.; Unger, K. K.; Esser, U.; Eray, B.; Trudinger, U. *J. Chrom.* **1989**, 465, 39-57.
16. Foster, M. D.; Synovec, R. E. *Anal. Chem.* **1996**, 68, 1456-63.
17. Lambert, W. J. *J. Chrom.* **1993**, 656, 469-84.
18. Dorsey, J. G. *J. Chrom.* **1993**, 656, 485-99.
19. Kaliszan, R. *J. Chrom.* **1993**, 656, 417-36.
20. Hansch, C. H. *Sci. Tot. Environ.* **1991**, 109, 17-29.

21. Hildebrand, J. H.; Prausnitz, J. M.; Scott, R. L. *Regular and Related Solutions*, Van Nostrand-Reinhold, New York, 1970.
22. Karger, B. L.; Snyder, L. R.; C. Eon. *J. Chromatogr.* **1976**, 125, 71-88.
23. Tijssen, R.; Billiet, H. A. H.; Schoenmakers, P. J. *J. Chromatogr.* **1976**, 122, 185-203.
24. Hafkenscheid, T. L.; Tomlinson, E. *J. Chromatogr.* **1983**, 264, 47-62.
25. de Galan, L; Billiet, H. A. H.; Schoenmakers, P. J. *J. Chromatogr.* **1983**, 282, 107-121.
26. Govers, A. J. *J. Chem. Soc. Faraday Trans.* **1993**, 89(20), 3751-3759.
27. Hongwei, Z.; Hu, Z. *Chromatographia* **1992**, 33, 575-80.
28. Antle, P. E.; Goldberg, A. P.; Snyder, L. R. *J. Chromatogr.* **1985**, 321, 1-32.
29. Pietrogrande, M. C.; Dondi, F.; Blo, G.; Borea, P. A.; Bighi, C. *J. Liquid Chromatogr.* **1987**, 10(6), 1065-1075.
30. Xindu, G.; Carr, P. W., *J. Chromatogr.* **1983**, 269, 96-102.
31. Billiet, H. A. H.; Schoenmakers, P. J.; de Galan, L. *J. Chromatogr.* **1981**, 218, 443-454.
32. Tan, L. C.; Carr, P. W. *J. Chromatogr.* **1993**, 656, 521-535.
33. de Galan, L; Billiet, H. A. H.; Schoenmakers, P. J. *J. Chromatogr.* **1978**, 149, 519-37.
34. Dill, K. A. *J. Phys. Chem.* **1987**, 91, 1980.
35. Jandera, P.; Colin, H.; Guiochon, G. *Anal. Chem.* **1982**, 54, 435.
36. Scott, R. P. W.; Simpson, C. F. *J. Chromatogr.* **1980**, 197, 11-20.
37. Gilpin, R. K.; Gangoda, M. E.; *J. Chromatogr. Sci.* **1983**, 21, 352-361.
38. Hansch, C. H.; Leo, A. *Subtituent Constants for Correlation Analysis in Chemistry and Biology* John Wiley & Sons, Inc., New York, New York, 1979.
39. Hafkenscheid, T. L.; Tomlinson, E. *J. Chromatogr.* **1983**, 264, 47-62.
40. Giddings, J. C. *Dynamics of Chromatography* Marcel Dekker, Inc., New York, New York, 1965.
41. Knox, J. H.; Saleem, M. *J. Chromatogr. Sci.* **1972**, 10, 80-88.
42. Horvath, C.; Lin, H. J. *J Chromatogr.* **1978**, 149, 43-70.

Table I. Experimentally Determined Capacity Factors for Ten Hydrophobic Organic Species in Water and the Literature Values for log P_0 and -log X_0.

Analyte	*k' #1*[a]	*k' #2*[b]	*log P_0*[c]	*-log X_0*[d]
Acetophenone	0.26	0.17	1.66	-
Anisole	1.05	0.41	2.08	-
Benzene	1.25	0.48	2.14	3.35
N,N Dimethylaniline		0.63	2.30	-
Toluene	3.10	1.36	2.74	3.98
Chlorobenzene	4.42	1.75	2.84	4.09
O-Xylene		3.15	3.12	4.50
Ethyl Benzene		3.38	3.15	4.55
M-Xylene		3.59	3.20	4.56
Cumene		7.64	3.66	5.05

[a] capacity factor measured using column #1 (φ=0.02) with water mobile phase.

[b] capacity factor measured using column #2 (φ=0.01) with water mobile phase.

[c] ref. 38.

[d] ref. 39.

Bibliography

1. Antle, P. E.; Goldberg, A. P.; Snyder, L. R. J. Chromatogr. 1985, 321, 1-32.

2. Arnold, M. A. Anal. Chem. 1992, 64, 1015A-1025A.

3. Arthur, C. ; Pawliszyn, J. Anal Chem. 1990, 62, 2145-2148.

4. Bahowick, T. B.; Synovec, R. E. Anal. Chem. 1995, 67, 631-40.

5. Bender, W. J. H.; Dessy, R. E.; Miller, M. S.; Claus, R. O. Anal. Chem. 1994, 66, 963-967.

6. Billiet, H. A. H.; Schoenmakers, P. J.; de Galan, L. J. Chromatogr. 1981, 218, 443-454.

7. Bruno, A. E.; Bruin, G. J. M.; Krattiger, B. Anal. Chem. 1994, 66, 1-8.

8. Buchholz, K. D.; Pawliszyn, J. Anal. Chem. 1994, 66, 160-167.

9. Buffet, C. E.; Morris, M. D. Anal. Chem. 1982, 54, 1824-1825.

10. Callahan, M. S., Green, B. in Hazardous Solvent Source Reduction, McGraw-Hill, New York, NY, 1995.

11. Carey, W. P.; DeGrandpre, M. D.; Jorgenson, B. J. Anal. Chem. 1989, 61, 1674-1678.

12. Chemical and Engineering News, June 24, 1996, 40-46.

13. Colton, C. E., Skinner, P. N. in The Road to Love Canal, The University of Texas Press, Austin, TX, 1996.

14. Conversation with Layne Carlin, Seattle Office of the E.P.A.

15. de Galan, L; Billiet, H. A. H.; Schoenmakers, P. J. J. Chromatogr. 1983, 282, 107-121.

16. de Galan, L; Billiet, H. A. H.; Schoenmakers, P. J. J. Chromatogr. 1978, 149, 519-37.

17. DeGrandpre, M. D.; Burgess, L. W. Anal. Chem. 1988, 60, 2582-2586.

18. DeGrandpre, M. D.; Burgess, L. W.; White P. L.; Goldman, D. S. Anal. Chem. 1990, 62, 2012-2017.

19. Dietz, E. A.; Cortellucci, N. J.; Singley, K. F. J. Liquid Chromatogr. 1993, 16(15), 3331-3347.

20. Dill, K. A. J. Phys. Chem. 1987, 91, 1980.

21. Dorsey, J. G. J. Chrom. 1993, 656, 485-99.

22. Driss, M.R.; Hennion, M.-C.; Bouguerra, M. L. J. Chromatogr. 1993, 639, 352-358.

23. Egorov, O.; Ruzicka, J. Analyst 1995, 120, 1959-62.

24. Fazio, S. D. et. al. Anal. Chem. 1985, 57, 1559.

25. Fazio, S. D.; Tomellini, S. A.; Shih-Hsien, H.; Crowther, J. B.; Raglione, T. V.; Floyd, T. R.; Hartwick, R. A. Anal. Chem. 1985, 57, 1559.

26. Fiehn, O.; Reemtsma, T.; Jekel, M. Anal. Chimica Acta 1994, 295, 297-305.

27. Foster, M. D., Synovec, R. E. Anal. Chem. 1996, 68, 1456-1463.

28. Fuh, M. S.; Burgess, L. W. Anal Chem. 1987, 59, 1780-1783.

29. Fujita, I.; Nishiyama, K.; Nagano, K.; Nakayama, M.; Sugii, A. Intern. J. Environ. Anal. Chem. 1994, 56, 57-62.

30. Fujiwara, K.; Fuwa, K. Anal. Chem. 1985, 57, 1012-1016.

31. Giddings, J. C. Dynamics of Chromatography Marcel Dekker, Inc., New York, New York, 1965.

32. Giddings, J. C. in Unified Separation Science, Wiley-Interscience, New York, NY, 1991, Chapters 10-12.

33. Giddings, J. C.; Chang, J. P.; Myers, M. N.; Davis, J. M.; Caldwell, K. D. J. Chromatogr., 1983, 255, 359-369.

34. Giesche, H.; Unger, K. K.; Esser, U.; Eray, B.; Trudinger, U. J. Chromatogr. 1989, 465, 39-57.

35. Gilpin, R. K.; Gangoda, M. E.; J. Chromatogr. Sci. 1983, 21, 352-361.

36. Giuliani, J. F.; Jarvis, N. L. J. Chem. Phys. 1985, 82, 1021-1024.

37. Giuliani, J. F.; Jarvis, N. L. Sensors and Actuators 1984, 6, 107-112.

38. Glajch, J. L.; Kirkland, J. J.; Snyder, L. R. J. Chromatogr. 1982, 238, 269.

39. Golay, M. J. E. in Gas Chromatography, 1958; Desty, D. H. ed., Academic Press, New York, N.Y., 1958.

40. Govers, A. J. J. Chem. Soc. Faraday Trans. 1993, 89(20), 3751-3759.

41. Grushka, E. in Preparative-Scale Chromatography, Chromatogr. Sci. Series: Volume 46, Marcel Dekker, 1989.

42. Hafkenschied, T. L.; Tomlinson, E. J. Chromatogr. 1983, 264, 47-62.

43. Hansch, C. H. Sci. Tot. Environ. 1991, 109, 17-29.

44. Hansch, C. H.; Leo, A. Subtituent Constants for Correlation Analysis in Chemistry and Biology John Wiley & Sons, Inc., New York, New York, 1979.

45. Harris, F.W.; Seymour, R.B. Structure-Solubility Relationships in Polymers Academic Press, New York, New York, 1977.

46. Hartwick, R. A.; Colwell, L. F., Jr. J. High. Res. Chrom. 1986, 9, 304-5.

47. Hildebrand, J. H.; Prausnitz, J. M.; Scott, R. L. Regular and Related Solutions, Van Nostrand-Reinhold, New York, 1970.

48. Hongwei, Z.; Hu, Z. Chromatographia 1992, 33, 575-80.

49. Horvath, C.; Haidacher, D. Theoretical Advancement in Chromatography and Related Separation Techniques; Dondi, F.; Guiochon, G. ed's., Kluwer Academic Publishers, Netherlands, 1992.

50. Horvath, C.; Lin, H. J. J Chromatogr. 1978, 149, 43-70.

51. Horvath, C.; Melander, W.; Molnar, I. J. Chromatogr. 1976, 125, 129-156.

52. Husain, S.; Narsimha, R.; Alvi, S. N.; Rao, R. N. J. High Res. Chrom. 1993, 16, 381-383.

53. Jandera, P.; Colin, H.; Guiochon, G. Anal. Chem. 1982, 54, 435.

54. Jandera, P.; Kubat, J. J. Chromatogr. 1990, 500, 281-99.

55. Joseph, M.; Kagdiyal, V.; Tuli, D. K.; Rai, M. M.; Jain, S. K.; Srivastava, S. P.; Bhatnagar, A. K. Chromatographia 1993, 35(3/4), 173-176.

56. Kaliszan, R. J. Chromatogr. 1993, 656, 417-436.

57. Karger, B. L.; Snyder, L. R.; Eon, C. J. Chromatogr. 1976, 125, 71-88.

58. Karger, B. L.; Snyder, L. R.; Horvath, C. in An Introduction to Separation Science, Wiley-Interscience, New York, NY, 1973, Chapter 5.

59. Kawahara, F. K.; Fiutem, R. A.; Silvus, H. S.; Newman, F. M.; Frazar, J. H. Anal. Chim. Acta 1983, 151, 315-327.

60. Khaledi, M. G.; Dorsey, J. G. J. Chromatogr. 1993, 656, 485-99.

61. Klainer, S. M.; Thomas, J. R.; Dandge, D. K.; Frank, C. A.; Butler, M. S.; Arman, H.; Goswami, K. SPIE Environmental Sensing and Combustion Diagnostics 1991, Vol. 1434, pp. 119-126.

62. Knox, J. H.; Saleem, M. J. Chromatogr. Sci. 1972, 10, 80-88.

63. Kronberg, B.; Silveston, R. J. Chromatogr. 1994, 659, 43-56.

64. Kronberg, B; Silveston, R. J. Phys. Chem. 1989, 93, 6241-6.

65. Lambert, W. J. J. Chromatogr. 1993, 656, 469-84.

66. Lawton, L. A.; Edwards, C.; Codd, G. A. Analyst 1994, 119, 1525.

67. Lehotay, J.; Baloghova, M.; Hatrik, S. J. Liquid Chromatogr. 1993, 16(5), 999-1006.

68. Levine, A. G. in Love Canal: Science, Politics and People, D.C. Heath and Company, Lexington, MA, 1982.

69. Linn, Z.; Booksh, K. S.; Burgess, L. W.; Kowalski, B. R.; Anal. Chem. 1994, 66,2552-60.

70. Linn, Z.; Burgess, L. W.; Anal. Chem. 1994, 66, 2544-51.

71. Lundgren, J. S.; Bekos, E. J.; Wang, R.; Bright, F. V. Anal. Chem. 1994, 66, 2433-2440.

72. Luo, Y.; Al-Othman, R.; Ruzicka, J.; Christian, G. D. Analyst 1996, 121, 601-606.

73. Marcus, M. A.; Hartog, A. H.; Purdum, C. F.; Leach, A. P. SPIE Chemical, Biochemical, and Environmental Sensors 1989, Vol. 1172, pp. 194-201.

74. Melcher, R. G.; Bakke, D. W.; Hughes, G. H. Anal. Chem. 1992, 64, 2258-2262.

75. Moore, L. K.; Synovec, R. E. Anal. Chem. 1993, 65, 2663-70.

76. Motohashi, N; Meyer, R.; Molnar, J.; Parkanyi, C.; Fang, X. J. Chromatogr. 1995, 710, 117-128.

77. Murugaiah, V.; Synovec, R. E. Anal. Chem. 1992, 64, 2130-2137.

78. Novotny, M. Anal. Chem. 1988, 60, 500A-510A.

79. Novotny, M.; Blomberg, L.; Bartle, K. D. J. Chromatgr. Sci. 1970, 8, 390-393.

80. Pietrogrande, M. C.; Dondi, F.; Blo, G.; Borea, P. A.; Bighi, C. J. Liquid Chromatogr. 1987, 10(6), 1065-1075.

81. Piraud, C.; Mwarania, E.; Wylangowski, G.; Wilkinson, J.; O'Dwyer, K.; Schiffrin, D. J. Anal. Chem. 1992, 64, 651-655.

82. Renn, C. N.; Synovec, R. E. Anal. Chem. 1991, 63, 568-574.

83. Richmond, E. W.; Dessy, R. E. Anal. Chem. 1992, 64, 1379-1382.

84. Saito, M.; Hibi, K.; Ishii, D.; Takeuchi, T. in Introduction to Microscale High-Performance Liquid Chromatography, Ishii, D., ed. , VCH, 1988, Chapter 2.

85. Saito, M.; Hibi, K.; Ishii, D.; Takeuchi, T. in Introduction to Microscale High-Performance Liquid Chromatography, Ishii, D., ed. , VCH, 1988, Chapter 2.

86. Schoenmakers, P. J.; Billiet, H. A. H.; de Galan, L. J. Chromatogr. 1983, 282, 107-121.

87. Scott, R. P. W.; Simpson, C. F. J. Chromatogr. 1980, 197, 11-20.

88. Selg, R. A. in Hazardous Waste Control, Marcel Dekker, Inc., New York, NY, 1993.

89. Skogerboe, K. J.; Yeung, E. S. Anal. Chem. 1987, 59, 1812-1815.

90. Small, H.; Soderquist, M. E. Patent # 4,732,686 Weak Eluant Ion Chromatography March 22, 1988.

91. Sun, Z. L.; Liu, M. C.; Hu, Z. D. Chromatographia 1994, 38, 599-608.

92. Synovec, R. E.; Bruckner, C. A.; Burgess, L. W.; Foster, M. D. SPIE Chemical, Biochemical and Environmental Sensors; SPIE: Bellingham, WA., 1994; Vol. 2293, pp167-177.

93. Synovec, R. E.; Sulya, A. W.; Burgess, L. W.; Foster, M. D.; Bruckner, C. A. Anal. Chem. 1995, 67,473-481.

94. Synovec, R. E.; Yeung, E. S. Anal. Chem. 1985, 57, 2162-2167.

95. Tan, L. C.; Carr, P. W. J. Chromatogr. 1993, 656, 521-535.

96. Thomas, S. T. in Facility Manager's Guide to Pollution Prevention and Waste Minimization, BNA Books, Washington, D.C.,1995.

97. Tijssen, R.; Billiet, H. A. H.; Schoenmakers, P. J. J. Chromatogr. 1976, 122, 185-203.

98. U. S. Environmental Protection Agency in Solvent Waste Reduction, Noyes Data Corporation, Park Ridge, NJ, 1990.

99. Van De Merbel, N. C.; Lagerwerf, F. M.; Lingeman, H.; Brinkman, U. A. TH. Intern. J. Environ. Anal. Chem. 1994, 54, 105-118.

100. Vera-Avila, L. E.; Covarrubias, R. Intern. J. Environ. Anal. Chem.. 1994, 56, 33-47.

101. Virkki, L.; Knuutinen, J.; Hyotylainen, J. Intern. J. Environ. Anal. Chem. 1994, 56, 133-147.

102. Vreeken, R. J.; Van Dongen, W. D.; Ghijsen, R. T.; Brinkman, U. A. TH. Intern. J. Environ. Anal. Chem. 1994, 54, 119-145.

103. Williams, R.; Meares, J.; Brooks, L.; Watts, R.; Lemieus, R. Intern. J. Environ. Anal. Chem. 1994, 54, 299-314.

104. Xi, X.; Yeung, E. S. Anal. Chem. 1990, 62, 1580-1585.Chromatogr., 1983, 255, 359-369.

105. Xindu, G.; Carr, P. W., J. Chromatogr. 1983, 269, 96-102.

106. Yang, L.; Saavedra, S. Anal. Chem. 1995, 67, 1307-1314.

107. Yokoyama, Y.; Kondo, M.; Sato, H. J Chromatogr. 1993, 643, 169-172.

Vita

Marc Douglas Foster was born on November 30th, 1963 in Placerville, California to Robert and Dorothy Foster. He has two sisters, Laura and Suzanne Foster. Marc was raised on a ranch in the foothills of California where he developed a strong appreciation for the rural life and activities such as hiking, fishing and canoeing. In January of 1988, Marc earned his Bachelor of Science degree in Chemistry from California State University Sacramento and began working as a chemist at Progressive Circuit Products. In 1991, Marc came to the University of Washington to earn his PhD in Analytical Chemistry. Marc will begin a career developing instrumentation at a small company called Anatel which is located in Boulder, Colorado